Danish Meteorological Institute
Ministry of Climate and Energy

Danish Climate Centre Report 09-08

Assessment of the temperature, precipitation and snow in the RCM HIRHAM4 at 25 km resolution

Guðfinna Aðalgeirsdóttir, Martin Stendel, Jens Hesselbjerg Christensen, John Cappelen, Flemming Vejen, Helle Astrid Kjær, Ruth Mottram and Philippe Lucas-Picher

Colophone

Serial title:
Danish Climate Centre Report 09-08

Title:
Assessment of the temperature, precipitation and snow in the RCM HIRHAM4 at 25 km resolution

Subtitle:

Authors:
Guðfinna Aðalgeirsdóttir, Martin Stendel, Jens Hesselbjerg Christensen, John Cappelen, Flemming Vejen, Helle Astrid Kjær, Ruth Mottram and Philippe Lucas-Picher

Other Contributers:

Responsible Institution:
Danish Meteorological Institute

Language:
English

Keywords:
Regional Climate model, weather station data

Url:
www.dmi.dk/dmi/dkc09-08

ISSN:
1399-1957

ISBN:
978-87-7478-584-2

Version:

Website:
www.dmi.dk

Contents

Colophone . . . 2
1 Dansk resumé **4**
2 Abstract **5**
3 Introduction **6**
4 Temperature and precipitation data **6**
4.1 DMI weather station data . . . 6
4.1.1 Temperature . . . 6
4.1.2 Precipitation . . . 7
4.2 GC-Net weather station data . . . 10
5 Regional Climate Model HIRHAM4 **11**
6 Validation of the output from HIRHAM4 **12**
6.1 Temperature point measurements . . . 12
6.2 Precipitation point measurements . . . 31
6.3 Temperature distribution over ice sheet . . . 43
6.4 Precipitation, Evaporation and Snow fields . . . 45
6.4.1 Precipitation and Evaporation distributions . . . 46
6.4.2 Snow . . . 47
7 Conclusion **76**
Previous reports . . . 80

1. Dansk resumé

Vi har anvendt den regionale klimamodel HIRHAM4 for et område der dækker Grønland og det omkringliggende hav i en opsætning med en horisontal gitterafstand på 25 km. Eksperimentet dækker perioden 1950-2080. Regional modellen modtager løbende atmosfærisk information på randen og havtemperaturer fra et eksperiment med den globale klimamdeol ECHAM5/MPI-OM med T63 opløsning. Temperaturer, nedbør, fordampning og sne fra HIRHAM4 er sammenlignet med data fra DMI vejrstationer på kysten af Grønland og automatiske vejrstationer fra GC-Net på iskappen. Temperatur og nedbørsfelter er også sammenlignet med en simpel parametereseringsmodel til kortgenerering for overfladetemperatur og nedbør. Klimaet over Grønlands Indlandsis er i store træk godt simuleret med HIRHAM4. Både år til år variationer og variationen hen over året vise god overensstemmelse mellem model og observationer. Der er anvendt en ny metode til at korrigere nedbørsmålingerne på Grønland. Korrektions faktorerne er beregnet fra et statistisk model som kræver information om vindhastighed, temperatur og nedbørs intensitet samt relativ sne mængde. Længst mod nord i Grønland kan korrektionerne betyde mere end en fordobling i forhold til den målte nedbør om vinteren. De validerede felter fra HIRHAM4 er efterfølgende brugt til at forcere iskappemodel. Dette studie dokumenterer det første skridt i udviklingen af et koblet iskappe- klima modelsystem som skal bruges til at forudsige hvor meget og hvor hurtig indlandsisen reagerer på forudsagte klimaændringer i de næste to århundreder.

2. Abstract

The Regional Climate Model (RCM) HIRHAM4 has been run for the period 1950-2080 at 25 km resolution covering Greenland ice sheet and the surrounding seas. The RCM is forced by the general circulation model (GCM) ECHAM5/MPI-OM at T63 resolution on the boundaries and for sea surface temperature (SST). RCM generated temperature, precipitation, evaporation and snow fields are compared to available data from weather stations (DMI station on the coast and GC-Net AWS on the ice sheet), to a previously used temperature parameterisation and to compilations of temperature and precipitation measurements. HIRHAM4 simulates the large scale characteristics of the climate over the Greenland Ice Sheet well. The inter annual variability in both temperature and precipitation is very similar in the model and the observations. The seasonal variation in precipitation along the coast is well captured and the seasonal temperature variation is also well simulated with the coldest and warmest months at the right time. A new set of monthly and annual correction factors for precipitation measurements in Greenland are presented and these are used to correct the measurements. The monthly correction values are dependent on winds peed, temperature, precipitation intensity and relative amount of snow. At the stations furthest north the magnitude of deficit can amount to more than half of the true precipitation in the winter months. These output fields are used to force the ice sheet model SICOPOLIS in a separate ice sheet model study as the first steps towards a fully coupled climate-ice sheet model system.

3. Introduction

The Regional Climate Model (RCM) HIRHAM4 has been run for the period 1950-2080 at 25 km resolution covering Greenland ice sheet and the surrounding seas. This model run was done within the project "Regionale klimaændringer for Grønland og omkringliggende hav" funded by the Danish Ministry of the Environment, Environmental Protection Agency (http://klimagroenland.dmi.dk, (*Stendel et al.*, 2008a))

The RCM is forced by the general circulation model (GCM) ECHAM5/MPI-OM at T63 resolution on the boundaries (*May*, 2008) and for sea surface temperature (SST). Radiative forcing is according to observations until 2000 and the SRES scenario A1B thereafter. (CO_2 concentration in 2100 of 700 ppm and global temperature increase of 3.5°C) (*Stendel et al.*, 2008a,b). In this report the model output (temperature, precipitation, evaporation and snow) from the model run is assessed and compared to available measurements on the coast from the DMI weather stations network (*Cappelen et al.*, 2008) and from automatic weather stations (AWS) on the ice cap (GC-NET, *Steffen and Box* (2001)). 30 year mean fields of the same variables (1961–1990) from the RCM are also compared with the temperature parameterisation that has been widely used for ice sheet modelling purpose (*Ritz et al.*, 1997) and accumulation maps, both the one based on the work of *Ohmura and Reeh* (1991) and provided on digital from by *Calanca et al.* (2000) and the PARCA accumulation maps (*Bales et al.*, 2001, 2009).

This report is a supporting document to a publication on the first steps towards a coupled regional climate - ice sheet model system (*Aðalgeirsdóttir et al.*, 2009). Detailed comparison for all the stations is presented here, in the publication a subset of this data set is presented, as well as the monthly means of the precipitation fields across the ice cap at 3 cross sections, in the publication the annual means are presented.

4. Temperature and precipitation data

4.1 DMI weather station data

The Danish Meteorological Institute (DMI) operates a number of weather stations around the coast of Greenland. The very first systematic observations in Greenland started in 1760s and official instrumental records date back to 1873. These stations measure temperature and precipitation, among other climate parameters. A full description of the instruments and the measured parameters, the monthly mean values and the annual data are published in technical reports (*Cappelen et al.*, 2001, 2008), that are available on DMI's website (www.dmi.dk).

4.1.1 Temperature

Temperature is measured every hour or every 3 hours, depending on the location. The thermometers are placed inside a so called "radiation screen" 2 m above the ground. The screen could be a white painted slat, allowing ventilation, or a white metal screen in the case of the new types of sensors. Inhomogeneities occur in the time series due to changes of one or more factors during the observation period. These can be changes in the instrumentation set-up, introduction of automatic equipment, relocation of a stations etc. The time series presented here have been subject to close visual scrutiny and compared with the time series of related climate elements from same station, resulting in a homogenised time series which is the best available from these stations (*Cappelen et al.*, 2001).

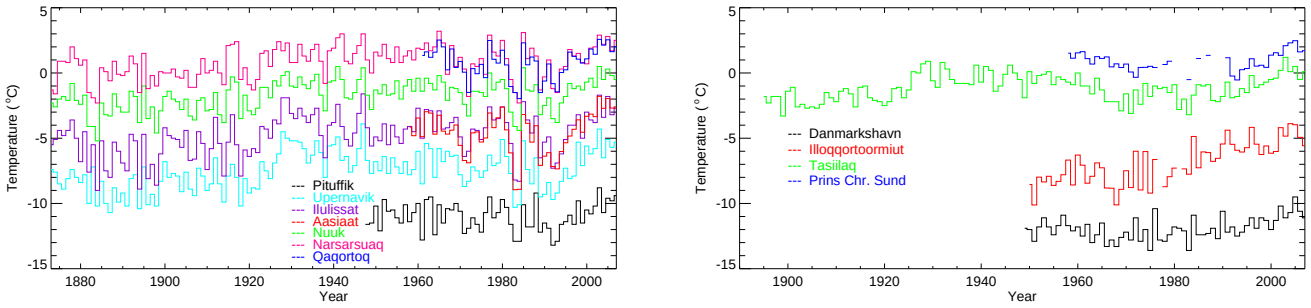

Figure 4.1: Mean annual temperature from the DMI weather stations on Greenland. (A) West coast stations (B) East coast stations.

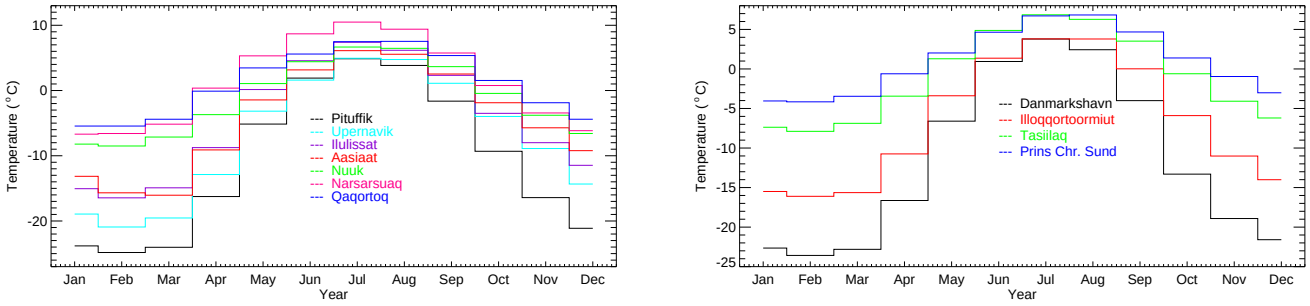

Figure 4.2: Mean monthly temperature from the DMI weather stations on Greenland. (A) East coast stations (B) West coast stations.

The time series of the mean annual temperature of selected stations on the west and the east coast of Greenland are shown in Figure 4.1. There is a clear north-south gradient in the time series, coldest in northern Greenland. The stations on the west coast show relatively cold temperatures in the late 1800 and early 1900, warmer temperatures in the 1930s and gradual warming since 1990 with cold years 1981-1982 at all stations and again in early 1990s. On the east coast there is only one long time series that shows the generally warmer temperatures in the 1930s, cooler in 1970s and the three continuous stations show gradual warming since 1980. There is smaller inter annual variability on the east coast, compared to the west coast stations. All stations show temperature increase during the last 2-3 decades, but the temperature at present is not significantly warmer than in the earlier warm periods during the observation period.

The monthly mean values are computed as a mean of all days in the month, each day containing 8 or 24 temperature readings per day. The average of the monthly means for each stations during the period 1961-1990 is shown in Figure 4.2. The seasonality is similar at all stations with July-August the warmest months and February the coldest. The largest amplitude of the annual temperature cycle is at the northern most stations, decreasing towards south.

4.1.2 Precipitation

Precipitation is measured with a Hellmann gauge of 200 cm^2 orifice placed 2.5 m above ground surface to prevent accumulation from drifting snow. Further, a Nipher shield is positioned on top of the measure stations at Greenland to damp the influence of wind (*Allerup et al.*, 2000).

Precipitation is extremely difficult to measure, in particular under strong wind conditions. Both because not all of the precipitation may be caught in the measuring device and because the collected

Table 4.1: Precipitation correction coefficients from *Allerup et al.* (2000). The station name, number, position and period of measurements, α is the fraction of solid precipitation (%), and K is the precipitation correction coefficient.

Station	Number	Latitude	Longitude	Height(m)	Period	α(%)	K
Danmarkshavn	4320	76°45' N	18°40' W	11	1949-2006	78	1.97
Aasiaat	4220	68°42' N	52°45' W	43	1958-1999	58	1.59
Illoqqortoormiut	4339	70°29' N	21°57' W	65	1950-2006	70	1.57
Qaqortoq	4272	60°43' N	46°03' W	32	1961-1999	27	1.31
Nuuk	4250	64°10' N	51°45' W	80	1890-2006	48	1.62
Prins Chr. Sund	4390	60°03' N	43°10' W	88	1959-2006	37	1.48
Tasiilaq	4360	65°36' N	37°38' W	50	1898-2006	49	1.21
Pituffik	4202	76°32' N	68°45' W	77	1961-1999	72	1.94

amount might get lost before data collection. Particularly solid precipitation is influenced by the wind. Only a fraction of the precipitation that falls as snow will fall in the gauge when strong winds make the precipitation fall at an angle from the vertical into the measurement bucket. The amount of collected precipitation will therefore decline with the wind. The aerodynamics of the snowflakes will make them move turbulently. This means that not only is the measured precipitation affected by wind speed, but also by the temperature which defines the shape of the snowflake. In the case of wet precipitation, the temperature is not as important, but the intensity of the shower is important since small water drops are easier caught by the wind. Further loss occurs while the precipitation is in the gauge. Snow can be blown up from the gauge, the gauge can be filled if not emptied frequently enough, and most important a wetting loss due to evaporation and adhesion takes place. The evaporation loss is in this case the part that has actually fallen to the bottom of the gauge, and from here evaporates, while the adhesion loss is the part of the precipitation that sticks to the side of the gauge, and therefore does not add to the total measured precipitation.

A comprehensive model for correcting annual precipitation measurements has been developed (*Allerup et al.*, 1997) and applied to data from eight climate stations in Greenland for the period 1994–1998 (*Allerup et al.*, 2000, Table 4.1). Only observations from synoptic weather stations were considered because data of wind speed, temperature and precipitation type every 3-hour is needed for the correction model. The results show that correction of the precipitation increase the gauge-measured precipitation by 30-95% on a yearly basis. These corrections are mainly due to fraction of solid precipitation, which in southern part of Greenland amounts to about 50% of the total precipitation and in the northern regions can be close to 100%. This leads to a yearly correction value of up 95% in the stations furthest north and 20-60% further south.

These correction factors have now been revisited and the model has been applied on data from 8 weather stations in Greenland for the period 1994–2008. Only observations from synoptic weather stations were considered because data on wind speed, temperature and precipitation type every 3 hours is needed for the correction model. Data were scrutinised and validated and then used to compute new yearly correction factors as well as monthly correction factors shown in Table 4.2.

The model that is used to compute these correction factors is a combination of two statistical correction models for solid and liquid precipitation where the percentage of snow, α, is used to weigh between the two models

$$K(\alpha) = \alpha e^{\beta_0+\beta_1 V+\beta_2 T+\beta_3 VT} + (1-\alpha)e^{\gamma_0+\gamma_1 V+\gamma_2 \log I+\gamma_3 V \log I}. \quad (4.1)$$

Table 4.2: Monthly and Yearly correction factors and fraction of solid precipitation for 8 weather stations in Greenland.

Station	PI	AA	NU	PH	QA	DH	TA	PC
Number	04202	04220	04250	04260	04272	4320	4360	4390
Latitude	76^{o}32' N	68^{o}42' N	64^{o}10' N	62^{o}00' N	60^{o}43' N	76^{o}45' N	65^{o}36' N	60^{o}03' N
Longitude	68^{o}45' W	52^{o}45' W	51^{o}45' W	49^{o}43' W	46^{o}03' W	18^{o}40' W	37^{o}38' W	43^{o}10' W
Elevation (m)	77	43	80	16	32	11	50	88
Jan K	2.55	2.01	2.56	1.56	1.67	2.27	1.32	1.80
Jan $\alpha(\%)$	*100*	*93*	*91*	*87*	*71*	*100*	*65*	*79*
Feb K	2.48	2.03	2.54	1.35	1.75	2.42	1.42	2.11
Feb $\alpha(\%)$	*100*	*96*	*82*	*87*	*79*	*100*	*85*	*83*
Mar K	2.88	2.03	2.55	1.53	1.70	2.45	1.30	2.06
Mar $\alpha(\%)$	*100*	*97*	*84*	*92*	*79*	*100*	*79*	*83*
Apr K	2.11	1.88	2.23	1.48	1.33	2.28	1.22	1.74
Apr $\alpha(\%)$	*98*	*89*	*68*	*59*	*45*	*97*	*66*	*68*
May K	1.82	1.53	1.49	1.11	1.13	2.29	1.12	1.57
May $\alpha(\%)$	*91*	*70*	*35*	*26*	*17*	*94*	*38*	*30*
Jun K	1.44	1.24	1.38	1.10	1.11	2.02	1.12	1.32
Jun $\alpha(\%)$	*35*	*12*	*13*	*8*	*1*	*56*	*2*	*8*
Jul K	1.25	1.23	1.32	1.09	1.09	1.27	1.09	1.28
Jul $\alpha(\%)$	*12*	*2*	*4*	*2*	*0*	*7*	*0*	*1*
Aug K	1.37	1.17	1.32	1.11	1.10	1.29	1.08	1.23
Aug $\alpha(\%)$	*26*	*2*	*3*	*0*	*1*	*21*	*0*	*1*
Sep K	1.60	1.23	1.33	1.09	1.12	1.56	1.09	1.31
Sep $\alpha(\%)$	*66*	*19*	*15*	*2*	*2*	*85*	*10*	*8*
Oct K	1.94	1.48	1.66	1.13	1.22	2.15	1.13	1.54
Oct $\alpha(\%)$	*98*	*73*	*57*	*41*	*21*	*98*	*43*	*36*
Nov K	2.20	1.83	2.10	1.34	1.36	2.42	1.28	1.64
Nov $\alpha(\%)$	*100*	*91*	*69*	*76*	*43*	*100*	*68*	*53*
Dec K	2.15	1.97	2.61	1.35	1.76	2.28	1.34	1.76
Dec $\alpha(\%)$	*100*	*96*	*86*	*79*	*70*	*100*	*67*	*73*
Year K	1.83	1.59	1.92	1.29	1.33	2.07	1.23	1.58
Year $\alpha(\%)$	*77*	*62*	*50*	*45*	*36*	*80*	*43*	*43*

PI=Pituffik, AA=Aasiaat, NU=Nuuk, PH=Paamiut Heliport, QA=Qaqortoq, DH=Danmarkshavn, TA=Tasiilaq, PC=Prins Christians Sund

K is the correction factor, the ratio between the true and measured precipitation, V the wind speed (m s^{-1}) at gauge level during precipitation, T temperature (^{0}C) during precipitation, I is the rain intensity (mm hour^{-1}) and β and γ are parameters dependent on the gauge type. Both models are based on bi-linear empirical structure found in the data and represents a simple first order approximation, a property not found when introducing squared wind speed, which has little or no physical justification.

The results show that the correction of the precipitation increases the gauge-measured precipitation by 23-100% on a yearly basis. These corrections are mainly due to the fraction of solid precipitation which, in the southern part of Greenland, amounts to about 50% of the total precipitation and in the northern regions can be close to 100%. The monthly correction values are clearly dependent on temperature and the relative amount of snow. At the stations furthest north the magnitude of deficit can amount to more than half of the true precipitation in the winter months.

Figure 4.3 shows the mean annual precipitation on the western and eastern coastal stations (note the different length of the time series and the different vertical scale). These values have been corrected for wind effects (temperature and intensity) with the factors in Table 4.2 and it assumed that these do not change over the period of measurement. The earlier part of the precipitation data series from

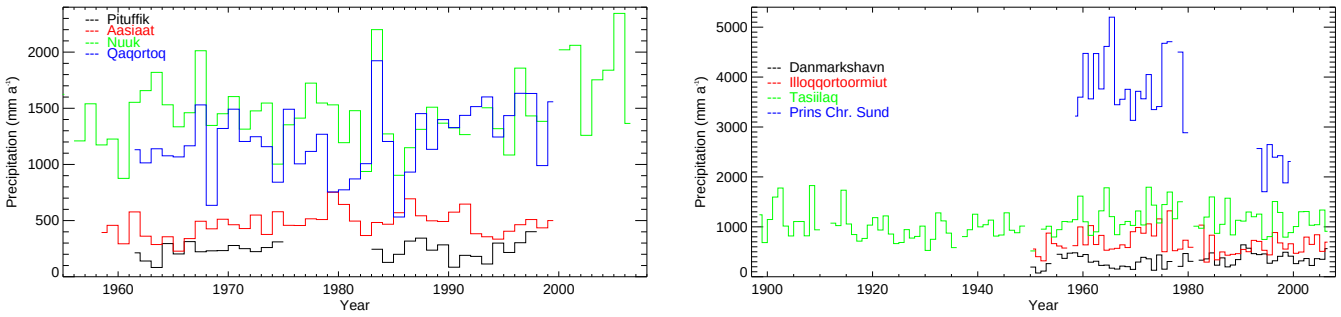

Figure 4.3: Mean annual precipitation from the DMI weather stations on Greenland. (A) West coast stations (B) East coast stations. These values are corrected for wind induced errors and wetting losses using model for correction of liquid as well as solid precipitation (see text).

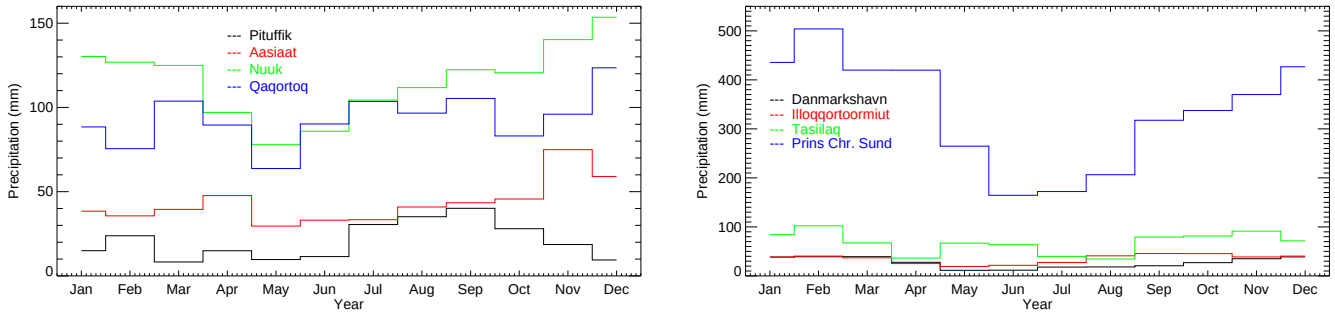

Figure 4.4: Mean monthly precipitation from the DMI weather stations on Greenland. (A) West coast stations (B) East coast stations. Note that the averages are over different time periods. (NB These values are corrected for wind induced errors and wetting losses using model for correction of liquid as well as solid precipitation).

Nuuk is not necessarily homogeneous and therefore only the latter part, since 1957 is shown. The only long time series is therefore from Tasiilaq on the east coast. There is a clear north-south trend in the data on both the east and west coasts, the precipitation decreases towards north. Also, there is a larger annual variability in the southern stations. The station with the highest precipitation is Prins Christians Sund on the southern tip of Greenland, receiving precipitation from weather systems on both east and west coasts. There is no clear trend in the time series, it appears that there is higher precipitation in the 1970s in Illoqqortoormiut and Tasiilaq, while there is higher values in the 1990s in Danmarkshavn. This variation could be due to changes in the weather systems. On the western side the stations Qaqortoq and Nuuk have similar amount of precipitation and the correlation between those two stations is higher than any other pair, indicating that these two places are subject to the same circulation pattern. The precipitation increases at these two stations, starting in the 1990s, but it is not a significant increase.

The monthly mean values for the period of measurements are shown in Figure 4.4 for the eastern and western coasts. These measurements have also been corrected, with the monthly correction factors shown in Table 4.2. The seasonal variability is clearly observed, reflecting the different source of precipitation on the east and west coasts. There is a minimum in precipitation during summer months on the east coast, except at Tasiilaq, where there is additional increase in May an June. The onshore wind in the southeast is strongest during wintertime. On the northwest coast (Pituffik) on the other hand there is peak in precipitation during the summer months, when most of the precipitation falls as rain and the ocean is not covered with sea ice, increasing the humidity of the air.

4.2 GC-Net weather station data

During the 1990s a network of 18 Automatic Weather Stations (AWS) was established on the Greenland Ice Sheet (*Steffen et al.*, 1996; *Steffen and Box*, 2001), distributed in order to give a good coverage of regional differences in the climate of the northern, eastern, and western sectors of the ice sheet, as well as the area along the ice sheet crest (for information about the Greenland Climate Network (GC-Net) and location of the stations see http://cires.colorado.edu/science/groups/steffen/gcnet/). The objectives of this network of AWS are to measure daily, annual, and inter annual variability in accumulation rate, surface climatology, and surface energy balance at selected locations on the ice sheet. A total of 32 parameters are transmitted hourly via a satellite link. We compare the published monthly mean values of temperature at these stations (*Steffen and Box*, 2001) to the 30 year mean temperatures of the HIRHAM4 model.

5. Regional Climate Model HIRHAM4

The regional model HIRHAM4 (*Christensen et al.*, 1996) is based on the adiabatic part of the HIRLAM (High-Resolution Limited Area Model) short-range weather forecast model (*Källén*, 1996) that was jointly developed by a number of European weather services. For climate modelling purposes, the standard physical parameterisation of HIRLAM was replaced by that of the global climate model ECHAM4 (the predecessor of ECHAM5 (*Roeckner et al.*, 2003)), so that HIRHAM4 can be thought of as a high resolution limited area version of ECHAM4. HIRHAM4 uses a rotated latitude-longitude coordinate system, where the rotated South Pole is positioned at the intersection of equator and Greenwich Meridian. Forcing fields as well as sea surface temperatures, sea ice cover and the time-dependent concentrations of greenhouse gases for this Greenland simulation are taken from a transient simulation of ECHAM5-MPI/OM1 at a comparably high horizontal resolution of T63 (approximately 1.8° by 1.8°) (*May*, 2008). This global model has been shown to perform well over Greenland and the Arctic when compared with other global models (*Walsh et al.*, 2008). The forcing from the global model is updated every six hours in a region 10 grid points wide with a simple relaxation of all prognostic variables. The model output is therefore not directly comparable with measurements during observation period as the atmosphere is not forced by the observed SSTs and sea ice concentrations, but rather by the modelled ones. This implies that in order to obtain meaningful statements on variability and change projected by the model the compared periods need to be long enough due to large internal variability, particularly in the Arctic. The regional model was run at a 25 km resolution with 19 vertical levels for the period 1950–2080.

The model output has been assessed and compared to the ECMWF (European Centre for Medium-Range Weather Forecast) reanalysis data set (ERA40), which is generally regarded to be of high quality in the Arctic (*Uppala and others*, 2005). The comparison concluded that the HIRHAM4 model realistically simulates present-day large- and regional scale climate over the Greenland Ice Sheet (*Stendel et al.*, 2008a,b). The ERA40 reanalysis is generally colder over the north-western part of the ice sheet, while temperatures over the sea ice are similar. The large scale distribution of precipitation over Greenland is well captured by the HIRHAM4 model, the model simulates, however, larger amount of precipitation with greater detail on the south-east coast compared to the re-analysis. The distribution of sea level pressure shows well known quasi-permanent features such as the Icelandic Low and high pressure over the interior of the ice sheet. The pressure gradient in the HIRHAM4 model is always larger than the ERA40, presumably due to the higher resolution (*Stendel et al.*, 2008a).

After the simulation was finished it was noted that there was a minor error in the generation of the 25 km resolution elevation model from the original high resolution (1 km) digital elevation model

(DEM), leading to offsets in elevation in some locations on the order of ±100-200 m (with two areas in north west and north east with differences up to 500 m) (*Stendel et al.*, 2008a). In the comparison of the HIRHAM4 model output with other temperature data and parameterisation described below, a lapse-rate correction based on the elevation difference between the model DEM and the elevation of the weather station for the temperature has been applied, but no correction of the precipitation has been made as the elevation error would only cause small changes in the general precipitation pattern of the model.

6. Validation of the output from HIRHAM4

The RCM model is run for the period 1950-2080 with forcing from the global model ECHAM4 at the boundary. It is therefore not expected that the model output compares directly to the data from the same period. However, in order to assess the model performance, a comparison with the available data of precipitation and temperature from the DMI coastal stations and the data from the GC-Net stations is done. In addition to the point measurements from the weather stations, there are available distributed estimates of both present day temperature and precipitation that the output of HIRHAM4 can be compared to. The temperature over Greenland Ice sheet has been parameterised using elevation and latitude as independent variables for ice sheet modelling purpose (*Ritz et al.*, 1997) and this parameterisation has been updated by including more input data and longitude as a third variable (*Fausto et al.*, 2009). Two estimates for the present day accumulation were used to assess the precipitation of HIRHAM4, the one based on the work of *Ohmura and Reeh* (1991) and provided on digital from by *Calanca et al.* (2000) and the accumulation maps from the PARCA project (*Bales et al.*, 2001, 2009). The mean annual temperature and precipitation fields for the period 1961-1990 is computed from the RCM output and compared with these estimates.

6.1 Temperature point measurements

The temperature measurements from the DMI coastal stations and the GC-NET Automatic Weather Stations can be used to validate the output from HIRHAM4 against point measurements. It should be emphasised that the HIRHAM4 has not been forced with assimilated data at the boundary, but rather a GCM output, as discussed above, and it can therefore not be expected that the model output accurately resembles the measured time series. It is nevertheless useful to compare the annual and seasonal variation to assess the capability of HIRHAM4 to simulate the temperature in Greenland.

The model temperature with HIRHAM4 is remarkably similar to the measurements and the model prediction of warming temperatures during the 21st century around the coast is clearly visible in the figure. HIRHAM4 simulates about 1-2°C colder temperatures on the west coast stations Upernavik, Ilulissat, Aasiaat and Nuuk for the measurement period and 3-5°C increase in temperature until 2080 with decreasing temperature increase towards south. The comparison is similar on the east coast stations, the RCM simulates about 1-3°C colder temperature at Danmarkshavn, Tasiilaq and Narsarsuaq, but the modelled temperature is similar as the measured at Prins Christian Sund. The temperature increase until 2080 is 3-7°C, largest at Danmarkshavn, the farthest north station and decreasing temperature increase towards south. The standard deviation of the modelled temperature during the observation period and the observations (see labels on Figures 6.5- 6.8) are remarkably similar for all stations. That indicates that HIRHAM4 simulates well the inter annual variability in temperature around the coast of Greenland.

The seasonality in the RCM is well simulated, the warmest and coldest periods are in the same months as measured. However, the model simulates higher summer temperatures and lower winter temperatures compared to the measurements at the coastal stations. At the west coast stations, the

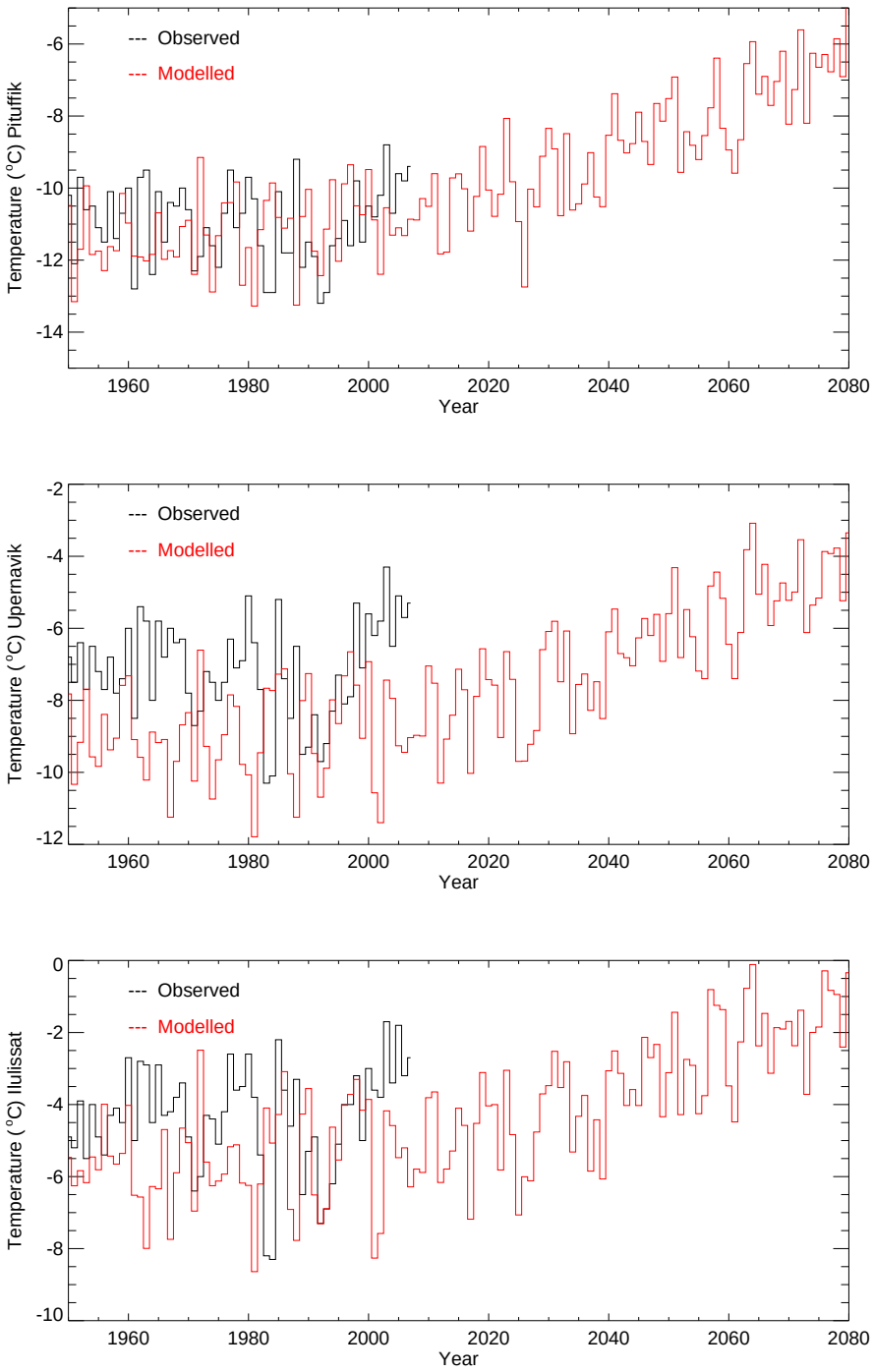

Figure 6.1: The mean annual temperature from the DMI weather stations compared with the temperature of the closest land grid point from the HIRHAM4 output.

summers are simulated about 5°C warmer and the winter temperatures are 5-10°C colder than measurements during the same period. There is a somewhat smaller difference at the east coast stations, with the summer temperatures about 1-4°C warmer and winter temperatures 4-6°C colder than measurements, resulting in mean annual temperatures along the coast that are too cold as can bee seen in Figure 6.32. All the west coast stations and the two northern most stations on the east coast (Danmarkshavn and Illoqqortoormiut) have warm bias in the spring and cold bias in the autumn. The three stations in the south (Qaqortoq, Narsarsuaq and Prins Christian Sund) have a cold bias in both spring and autumn.

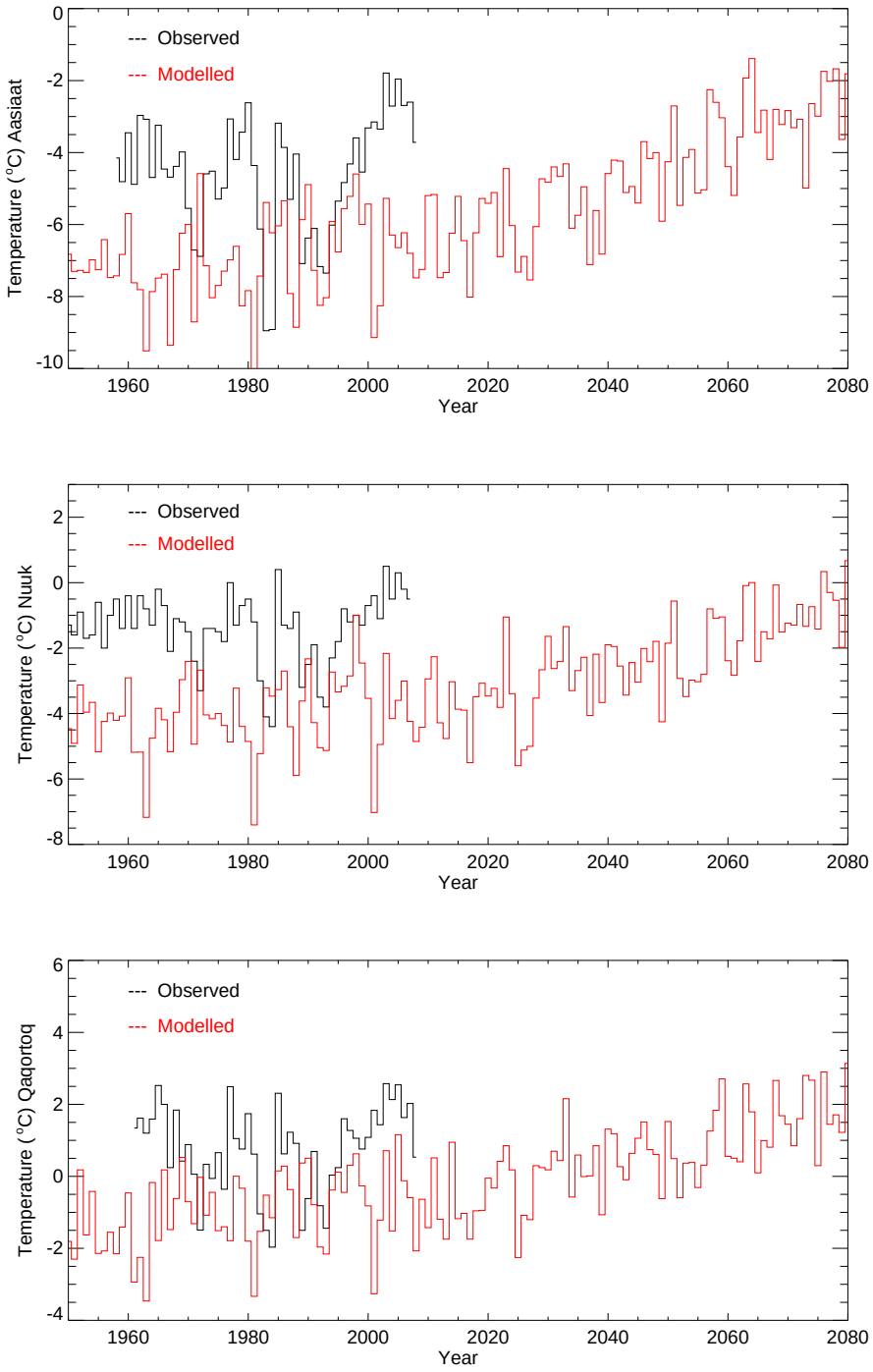

Figure 6.2: The mean annual temperature from the DMI weather stations compared with the temperature of the closest land grid point from the HIRHAM4 output.

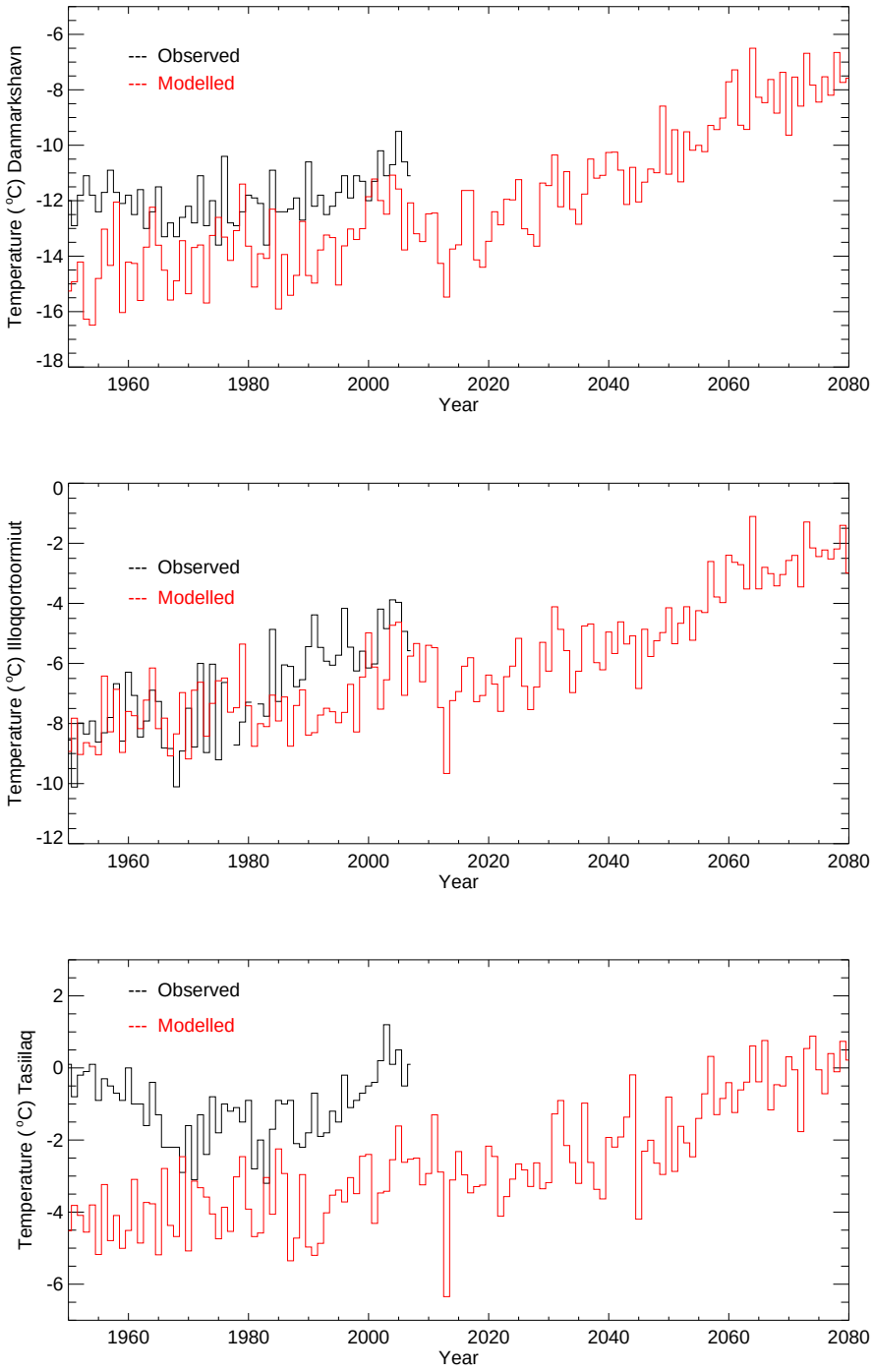

Figure 6.3: The mean annual temperature from the DMI weather stations compared with the temperature of the closest land grid point from the HIRHAM4 output.

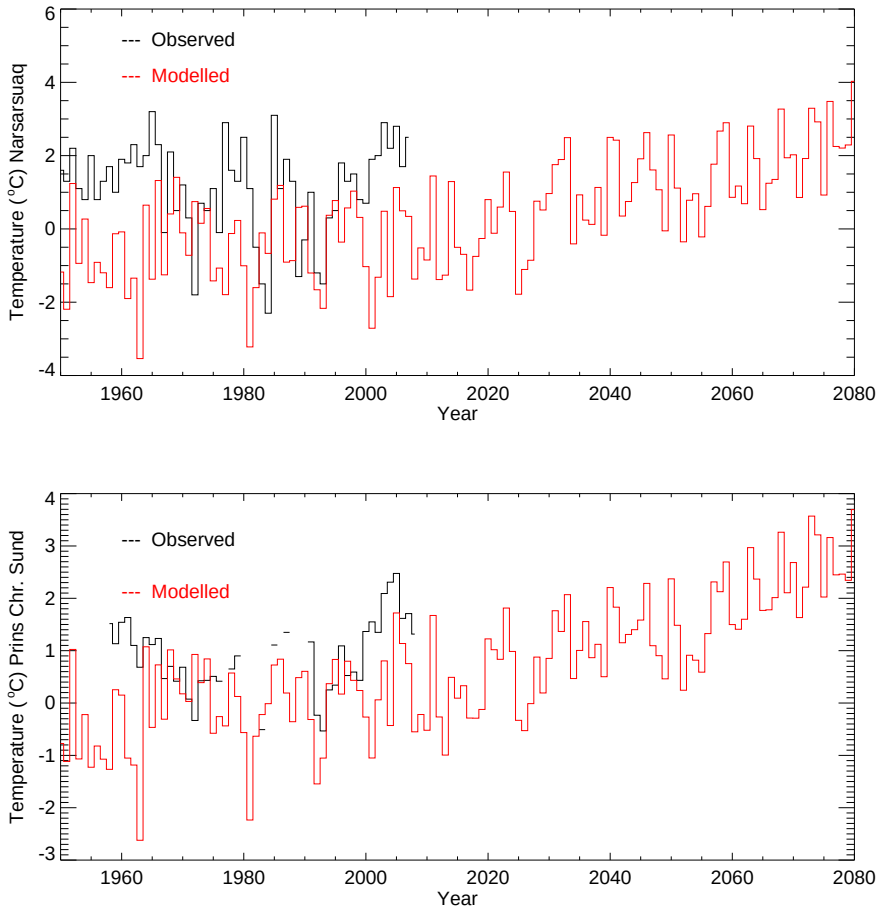

Figure 6.4: The mean annual temperature from the DMI weather stations compared with the temperature of the closest land grid point from the HIRHAM4 output.

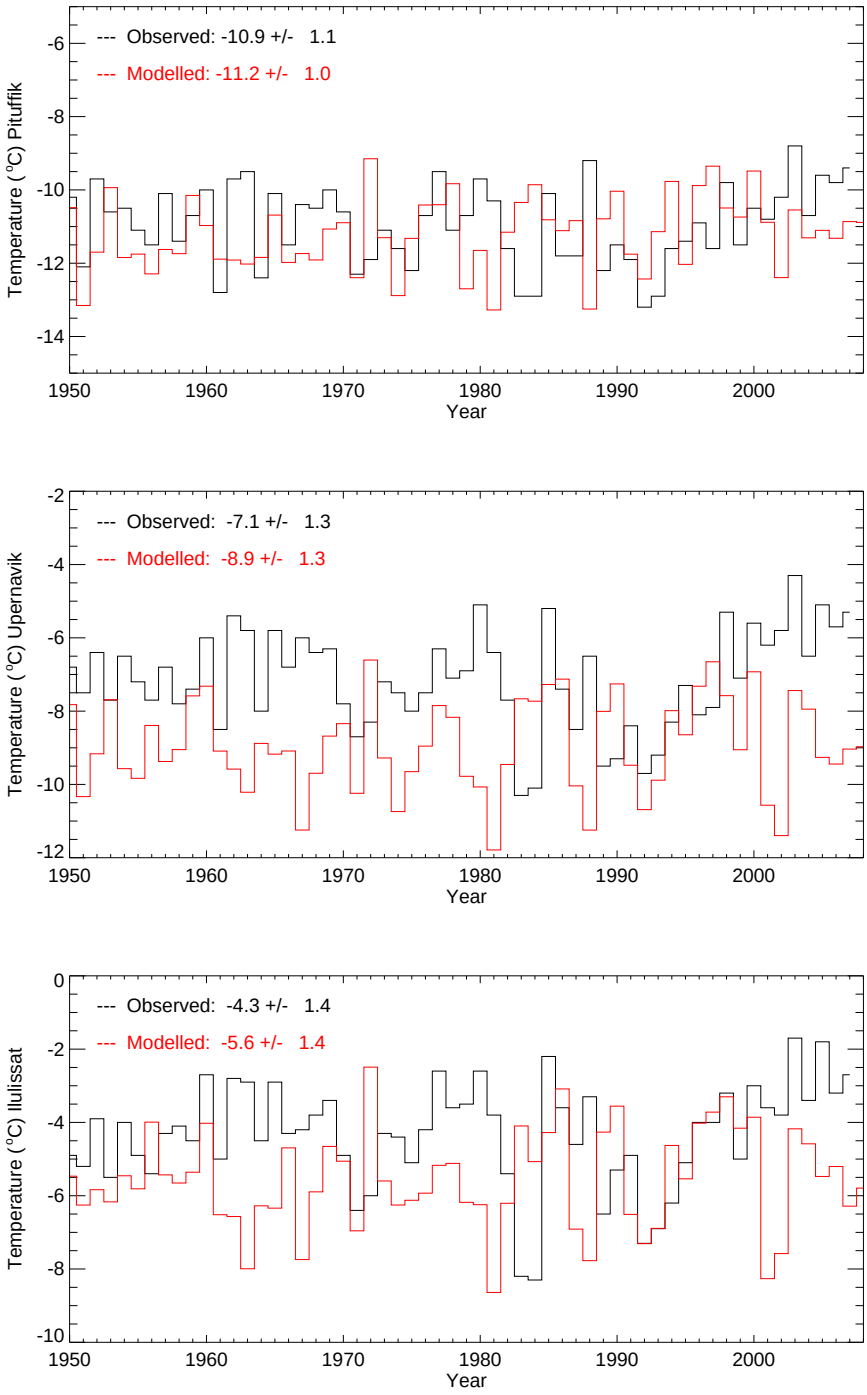

Figure 6.5: The mean annual temperature from the DMI weather stations and the closest land grid point from the HIRHAM4 output. Only the period of available measurements is shown as well as the mean and standard deviation of both the observations and model output.

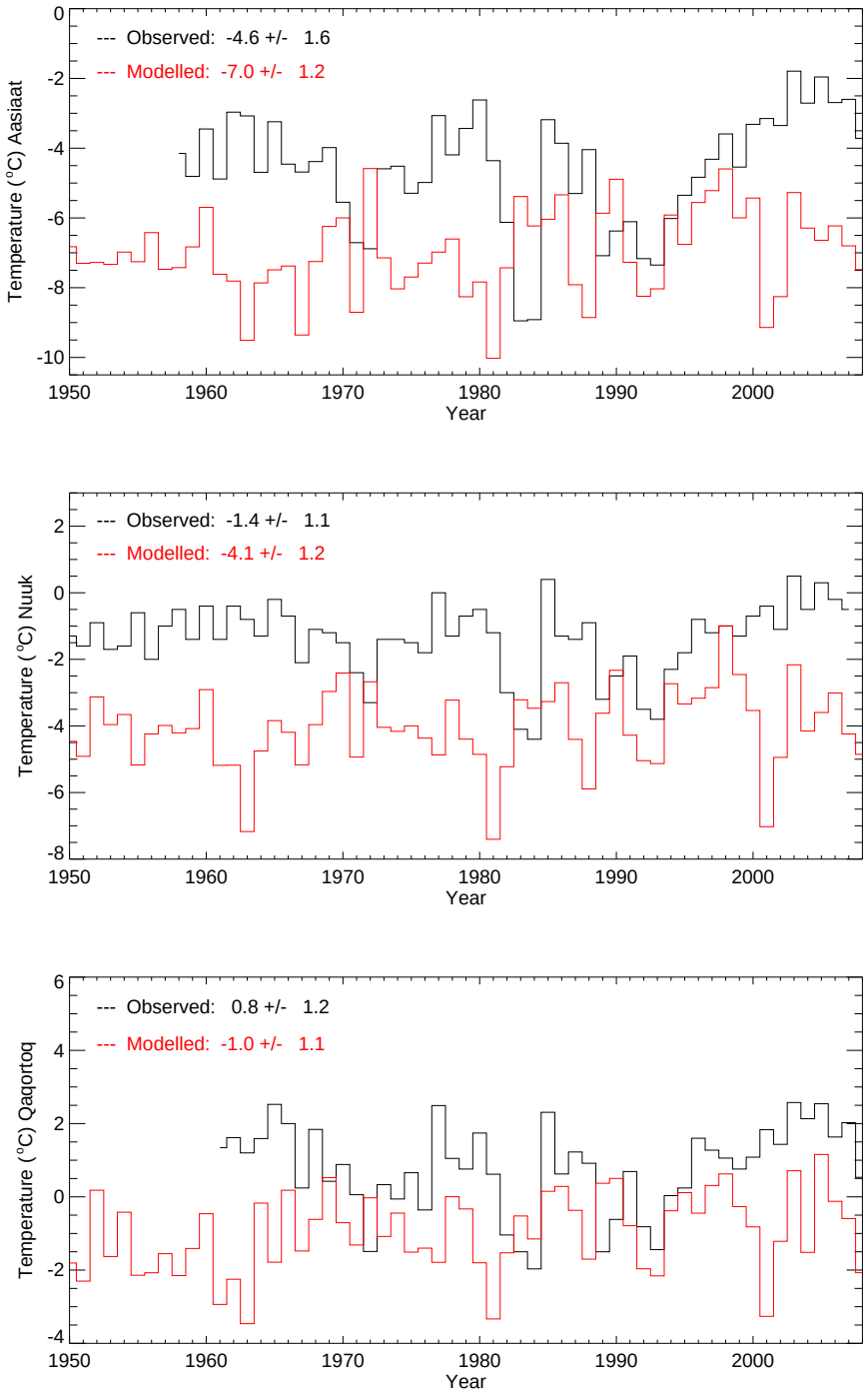

Figure 6.6: The mean annual temperature from the DMI weather stations and the closest land grid point from the HIRHAM4 output. Only the period of available measurements is shown as well as the mean and standard deviation of both the observations and model output.

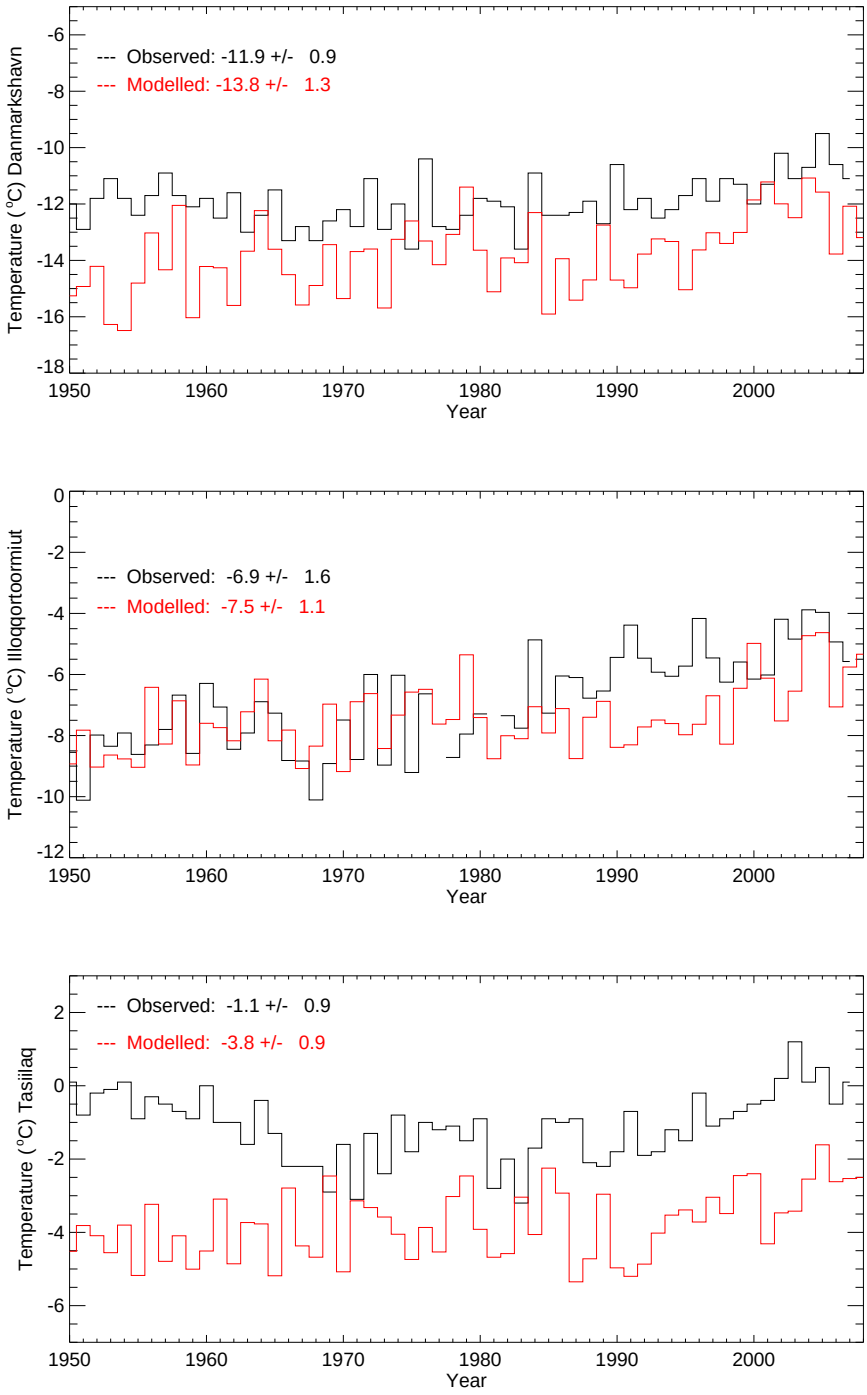

Figure 6.7: The mean annual temperature from the DMI weather stations and the closest land grid point from the HIRHAM4 output. Only the period of available measurements is shown as well as the mean and standard deviation of both the observations and model output.

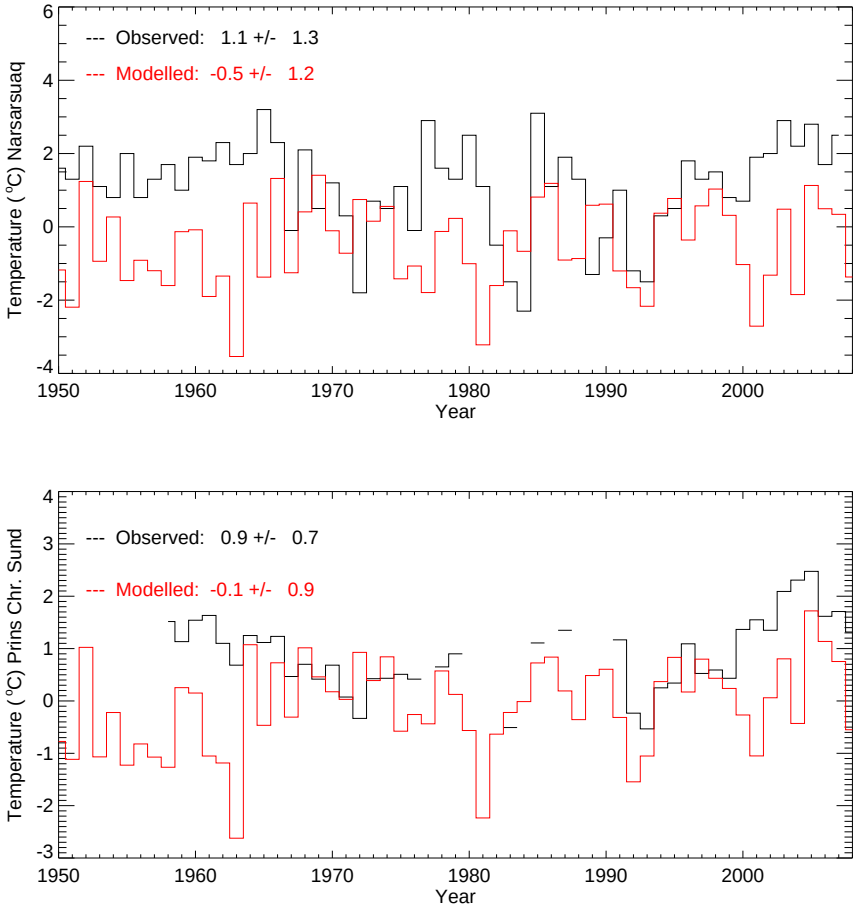

Figure 6.8: The mean annual temperature from the DMI weather stations and the closest land grid point from the HIRHAM4 output. Only the period of available measurements is shown as well as the mean and standard deviation of both the observations and model output.

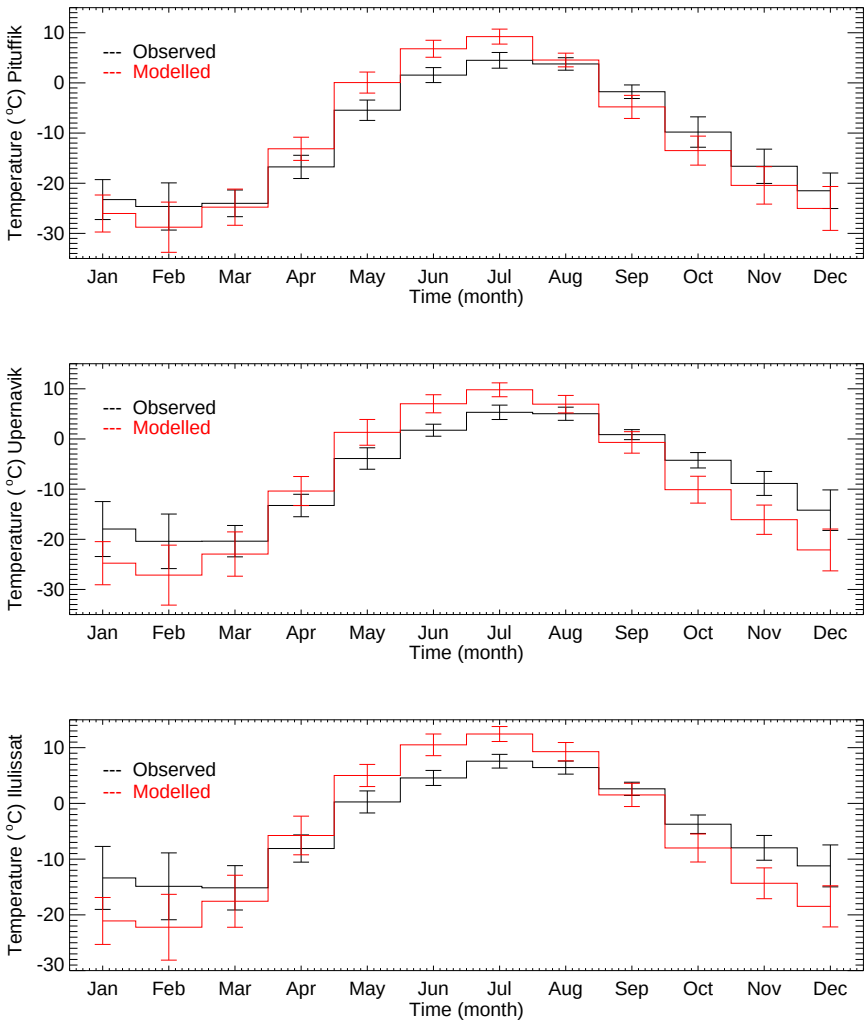

Figure 6.9: Monthly mean temperature from the DMI weather stations and the closest land grid point from HIRHAM4. The bars indicated the standard deviation of observations/model output during the 30 year period.

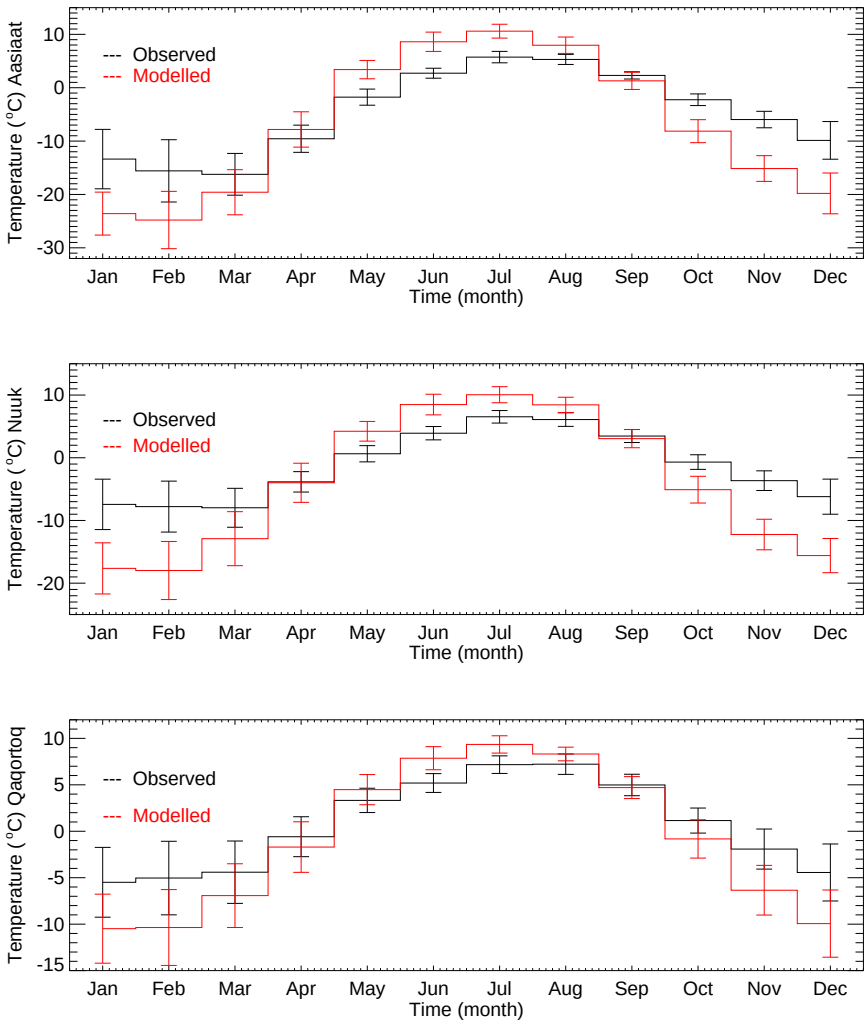

Figure 6.10: Monthly mean temperature from the DMI weather stations and the closest land grid point from HIRHAM4. The bars indicated the standard deviation observations/model output during the 30 year period.

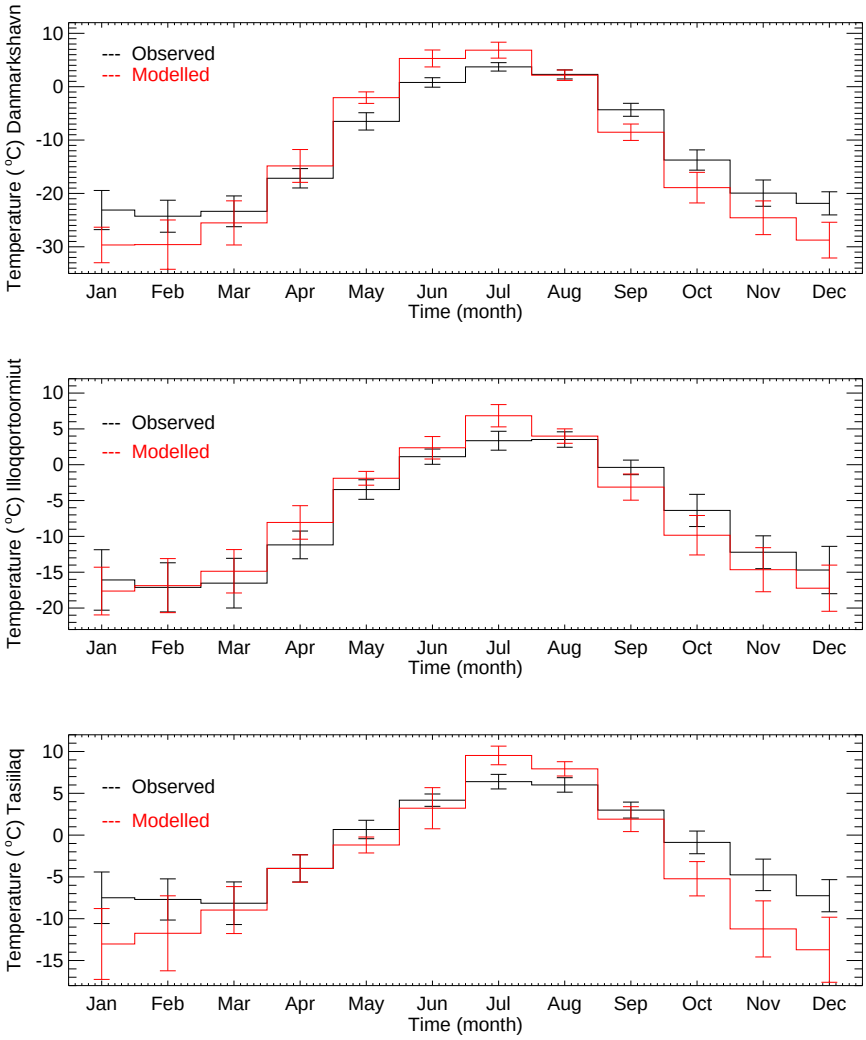

Figure 6.11: Monthly mean temperature from the DMI weather stations and the closest land grid point from HIRHAM4. The bars indicated the standard deviation observations/model output during the 30 year period.

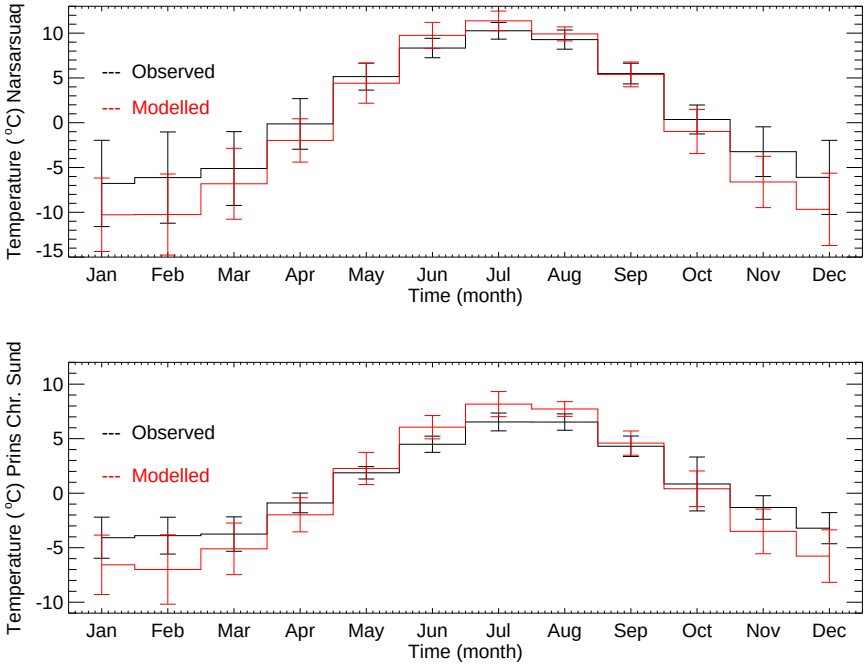

Figure 6.12: Monthly mean temperature from the DMI weather stations and the closest land grid point from HIRHAM4. The bars indicated the standard deviation observations/model output during the 30 year period.

The comparison with the GC-Net weather stations (*Steffen and Box*, 2001), reveals that the seasonal difference between the HIRHAM4 output and the measurements is in the opposite direction over the main ice sheet. The winter temperatures are warmer than measured but the summer temperatures are close to the observations, they can be either too cold or too warm. This results in smaller annual temperature range in the RCM series than measured. In figures 6.13- 6.18 comparison between the measured temperature at the GC-Net stations and the RCM modelled temperature (red line) is shown. The parameterised temperature (blue line) that has been used to force large scale ice sheet models and the temperature distribution from *Calanca et al.* (2000) (green line) are also shown. It should be kept in mind that the parameterisation is an altitude and latitude dependent function and the yearly variation is parameterised with a sinusoidal function between the mean annual and July temperature distributions (*Ritz et al.*, 1997), the temperature grids are based on observations over a long period (*Calanca et al.*, 2000; *Ohmura*, 1987), the RCM model output is averaged over the period 1961–1990, and the available measurements are from the period 1995–1999 (*Steffen and Box*, 2001). The figures show the smaller temperature range from the RCM output discussed above, but also that the temperature range simulated with the sinusoidal curve results in too large range, with a cold bias in the winter temperatures.

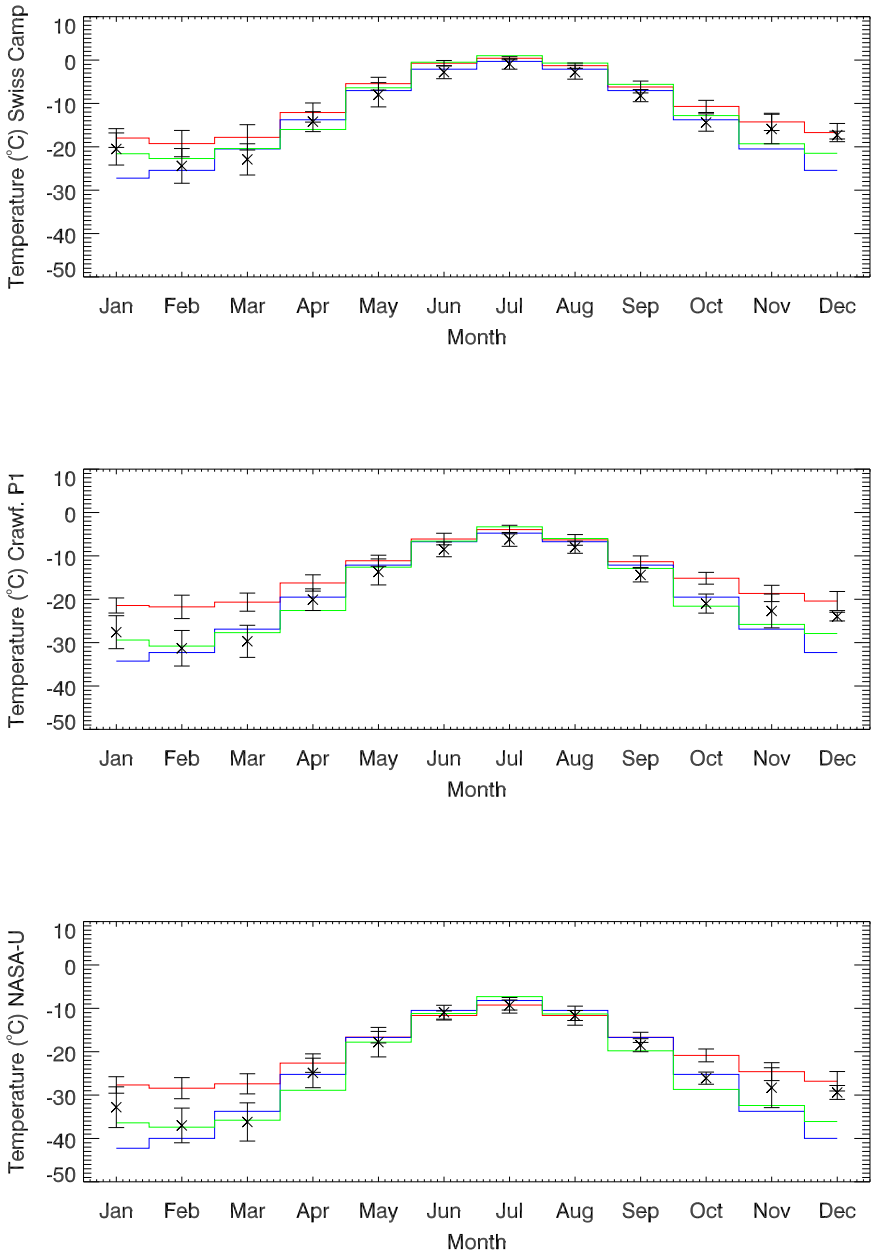

Figure 6.13: Monthly mean temperature from the GC-Net weather stations and the closest grid point from HIRHAM4 (red line). The blue and green lines show the temperature parameterisation (*Ritz et al.*, 1997) and temperature distribution from *Calanca et al.* (2000) at the same point, respectively.

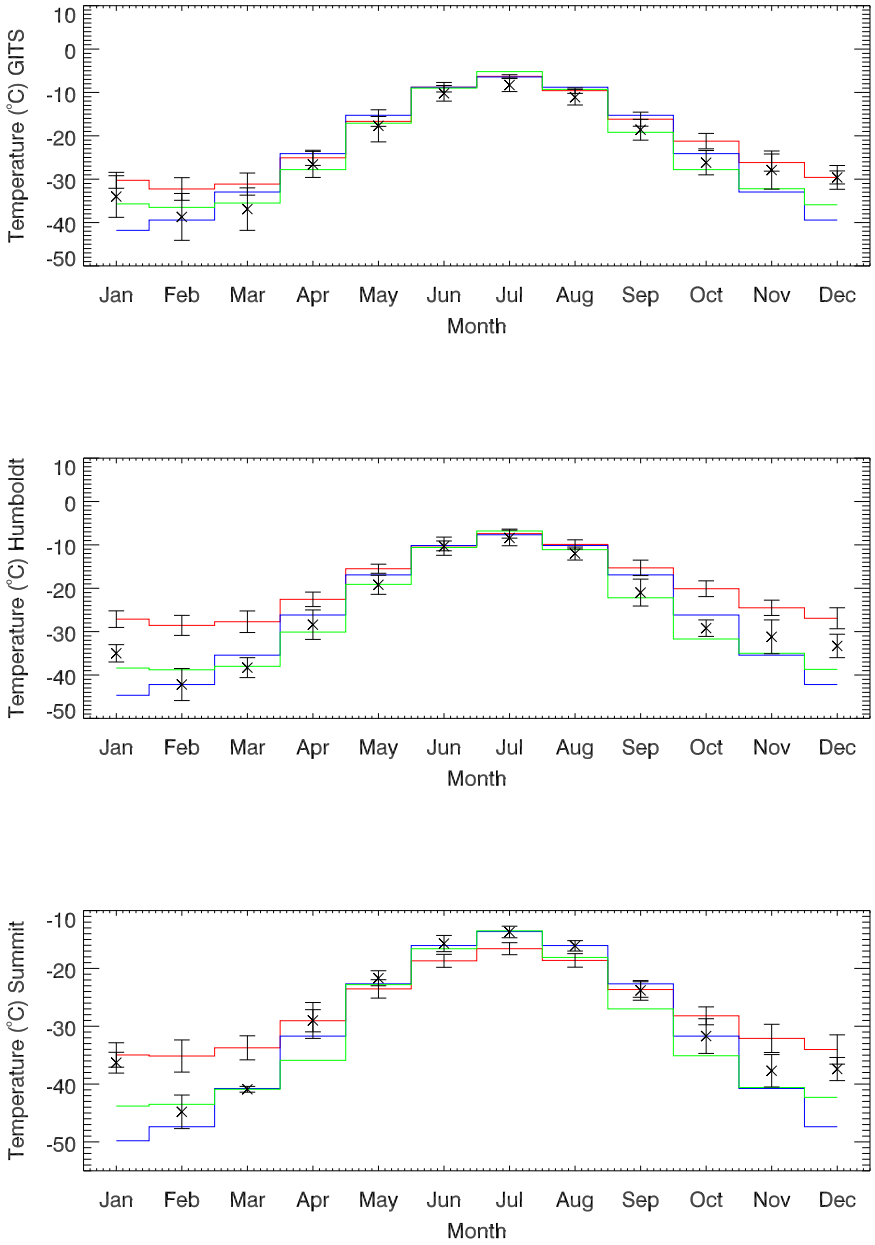

Figure 6.14: Monthly mean temperature from the GC-Net weather stations and the closest grid point from HIRHAM4 (red line). The blue and green lines show the temperature parameterisation (*Ritz et al.*, 1997) and temperature distribution from *Calanca et al.* (2000) at the same point, respectively.

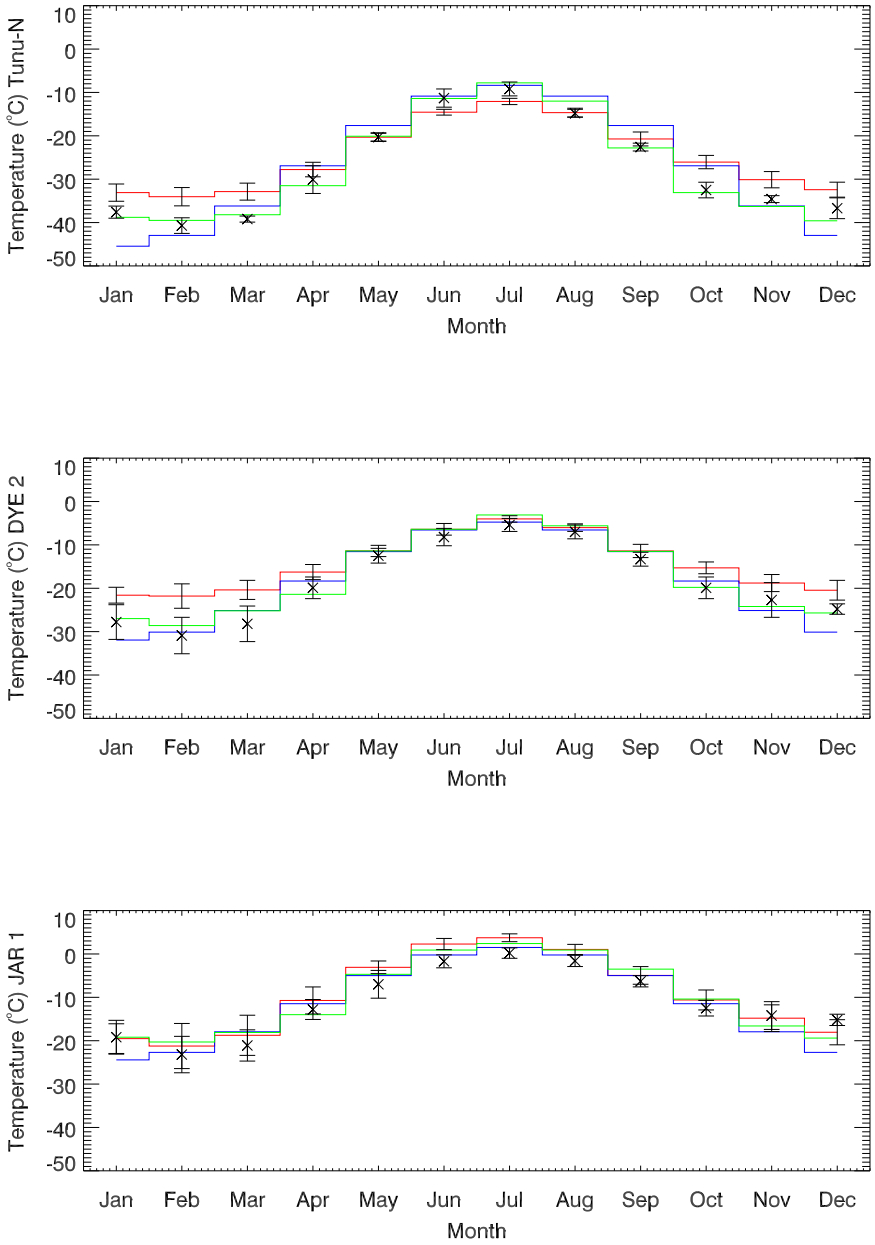

Figure 6.15: Monthly mean temperature from the GC-Net weather stations and the closest grid point from HIRHAM4 (red line). The blue and green lines show the temperature parameterisation (*Ritz et al.*, 1997) and temperature distribution from *Calanca et al.* (2000) at the same point, respectively.

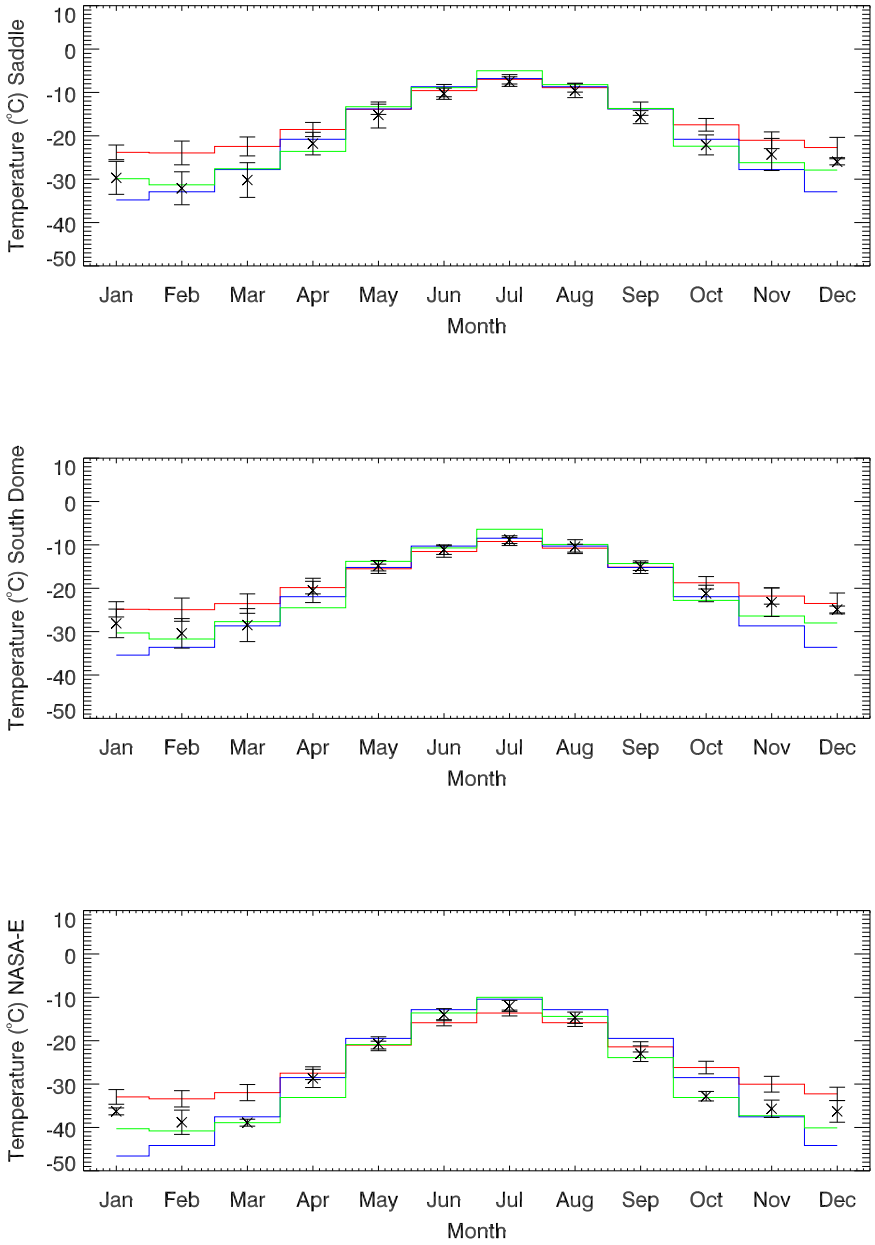

Figure 6.16: Monthly mean temperature from the GC-Net weather stations and the closest grid point from HIRHAM4 (red line). The blue and green lines show the temperature parameterisation (*Ritz et al.*, 1997) and temperature distribution from *Calanca et al.* (2000) at the same point, respectively.

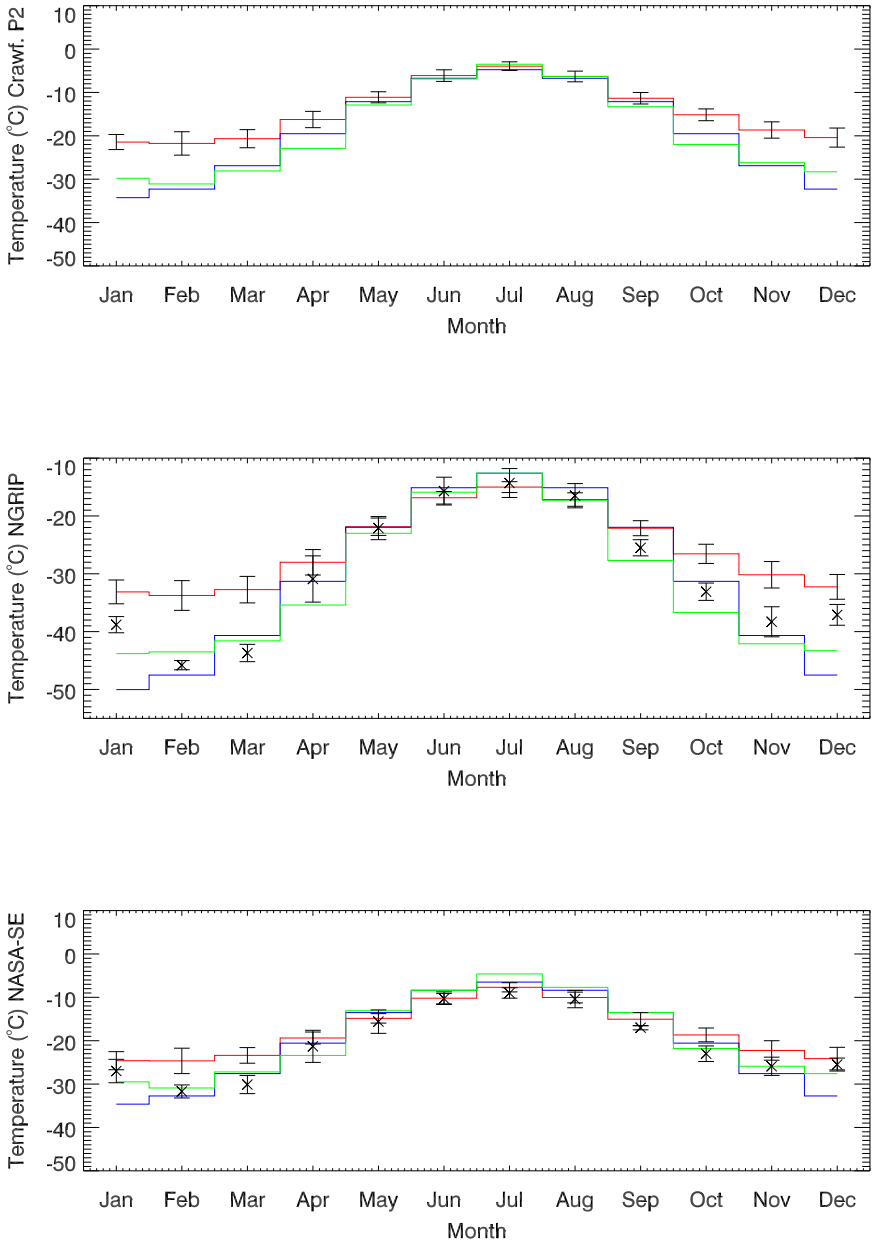

Figure 6.17: Monthly mean temperature from the GC-Net weather stations and the closest grid point from HIRHAM4 (red line). The blue and green lines show the temperature parameterisation (*Ritz et al.*, 1997) and temperature distribution from *Calanca et al.* (2000) at the same point, respectively.

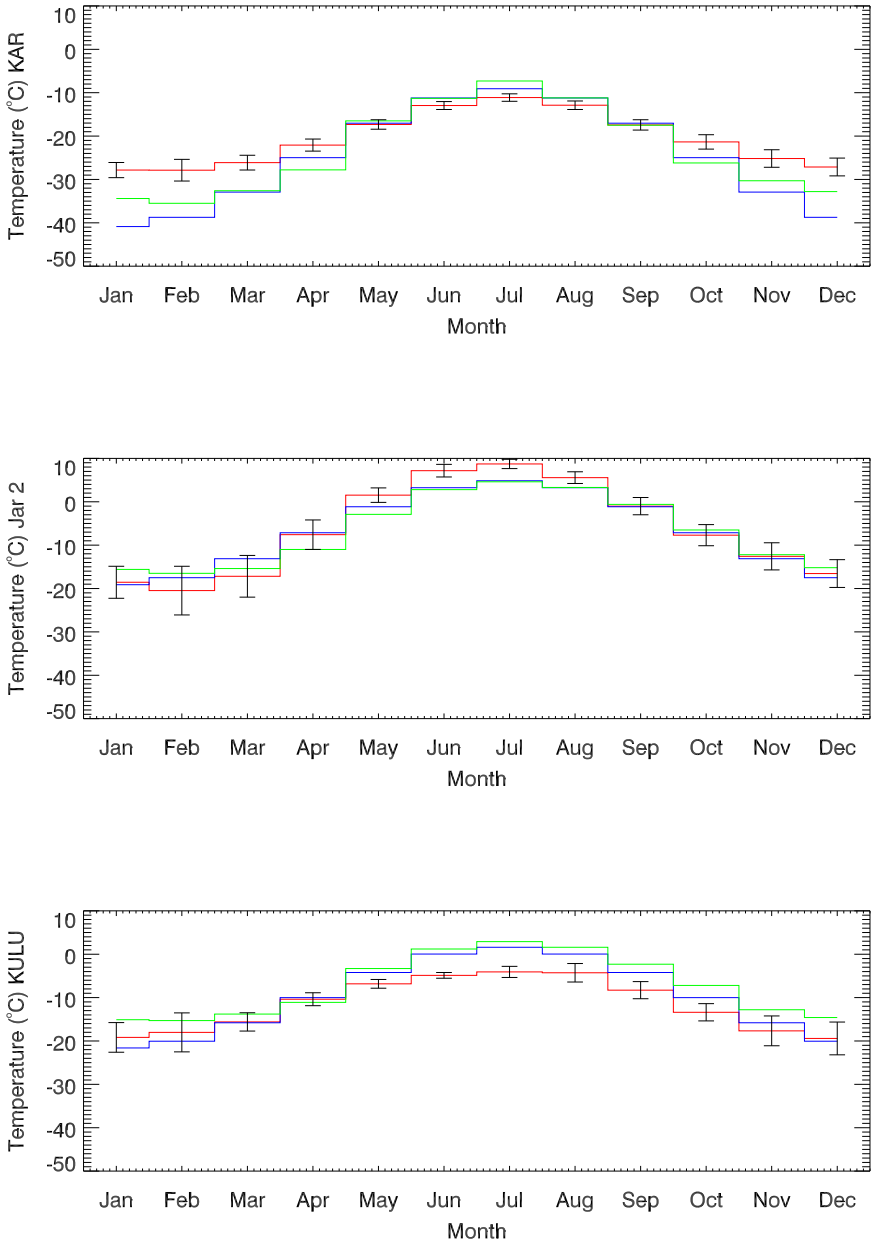

Figure 6.18: Monthly mean temperature from the GC-Net weather stations and the closest grid point from HIRHAM4 (red line). The blue and green lines show the temperature parameterisation (*Ritz et al.*, 1997) and temperature distribution from *Calanca et al.* (2000) at the same point, respectively.

Comparison of the parameterised temperature that has been used in large scale ice sheet models reveals that the simple parameterisation compares remarkably well with the measurements on the ice cap. For the 18 GC-Net stations the temperature range is too large at 9 locations and reasonably good at 5. The summer temperature is too warm at 8 locations but reasonably good at 6 locations. The winter minimum in the measurements is at all measured locations in February, not in December as the simple parameterisation assumes, which causes cold bias in December and January. The most important temperatures for the amount of melt in the model are the summer and autumn temperatures (July-September). These are 2-5° too warm at the stations on the northern part of the ice cap (GITS, Humboldt, Tunu-N, NGRIP, NASA-E, NASA-U) and on the west coast points

(Crawford Point 1, JAR1) and in NASA-SE, but close to measured temperature on Summit and the southern stations (DYE2, Saddle and South Dome).

Comparison of the HIRHAM4 temperatures and the GC-Net measurements indicates that the range in temperature in the RCM is too small over the ice cap. The range is too small in 13 out of 14 locations, it is only at station JAR1 that the range is similar to the measurements. This is mainly due to warm bias in winter, all stations have about 5°C, up to 10°C too high temperatures in the winter. The most probable reason for this warm bias is that the vertical resolution of the model is not sufficient to capture the inversion over the ice sheet. The observed winter minimum in February is well simulated with the RCM. The summer temperatures are not as much different, out of 14 stations there are 5 where the summer temperatures compare well with the measurements, 3 where they are 2-3° too cold and 6 where the temperatures are 1-3° too warm. The stations that summer temperatures compare well with measurements are at the South Dome and Saddle and at higher elevations in the north west (Humboldt, N-GRIP and NASA-U), the ones that are too cold are on the highest and north east side (Summit, Tunu-N, and NASA-E) and the stations where the RCM output is too warm are on the west coast (GITS, JAR1, Swiss Camp, Crawford Point1, Dye 2 and NASA-SE). The mean annual temperature at all locations is generally higher in the RCM output than measured at the GC-Net stations.

6.2 Precipitation point measurements

As discussed above, we do not expect the year-to-year model results to exactly represent the available measurements because the RCM simulation is forced at the boundary with a GCM simulation and not a reanalysis product. It should also be kept in mind that the spatial variability in precipitation is large and therefore it cannot be expected that point observations are well represented by a grid point of 25x25 km size. It is however, useful to compare the modelled precipitation with available measurements from the coastal stations to assess the model performance particularly with regard to the inter-annual and seasonal variability. Note that the measurements have been corrected with the factors given in Table 4.2. The mean annual precipitation from the weather stations and the nearest land grid point from the HIRHAM4 output is shown in Figures 6.19- 6.22 for the whole model period and in Figures 6.23- 6.26 for the period 1950–2008. The mean and standard deviation from the observations and the model is shown on the figures.

The amount of precipitation in the model is somewhat higher than the observations at the stations on the northern and eastern coasts, but at the stations on the west coast, Upernavik, Ilulissat, Aasiaat and Nuuk the modelled precipitation is similar to measurements. The standard deviation over this period is similar for all the stations, indicating that the model simulates the inter annual variability well.

The monthly mean values for the period 1961–1990 are shown in Figures 6.27- 6.30. There is a large variability in the monthly means from the model, the standard deviation of the monthly mean values for the period is shown with bars on the figure the variability in the observations is of similar magnitude, but not shown. The seasonality in the precipitation is well simulated in the model. The maximum precipitation during the summer months on the west coast, as well as the minimum in summer and maximum during spring and autumn months (Prins Christians Sund and Tasiilaq) or winter (Danmarkshavn and Illoqqortoormiut) is relatively well simulated in the RCM.

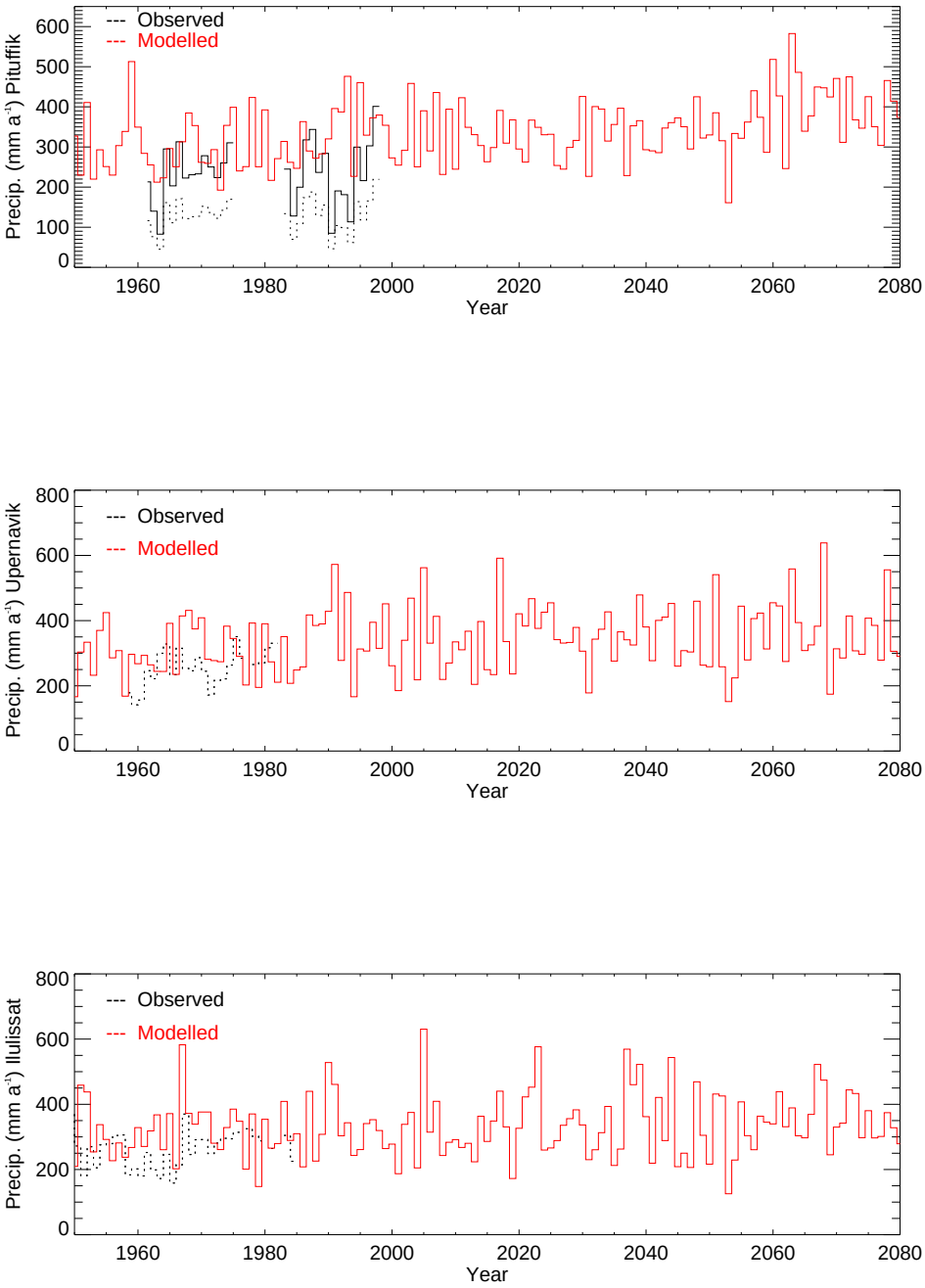

Figure 6.19: Mean annual precipitation from the DMI weather stations and the closest grid point from HIRHAM4. Measurements are corrected with a factor (Table 4.1) for each location. The uncorrected annual time series is shown with a dotted line.

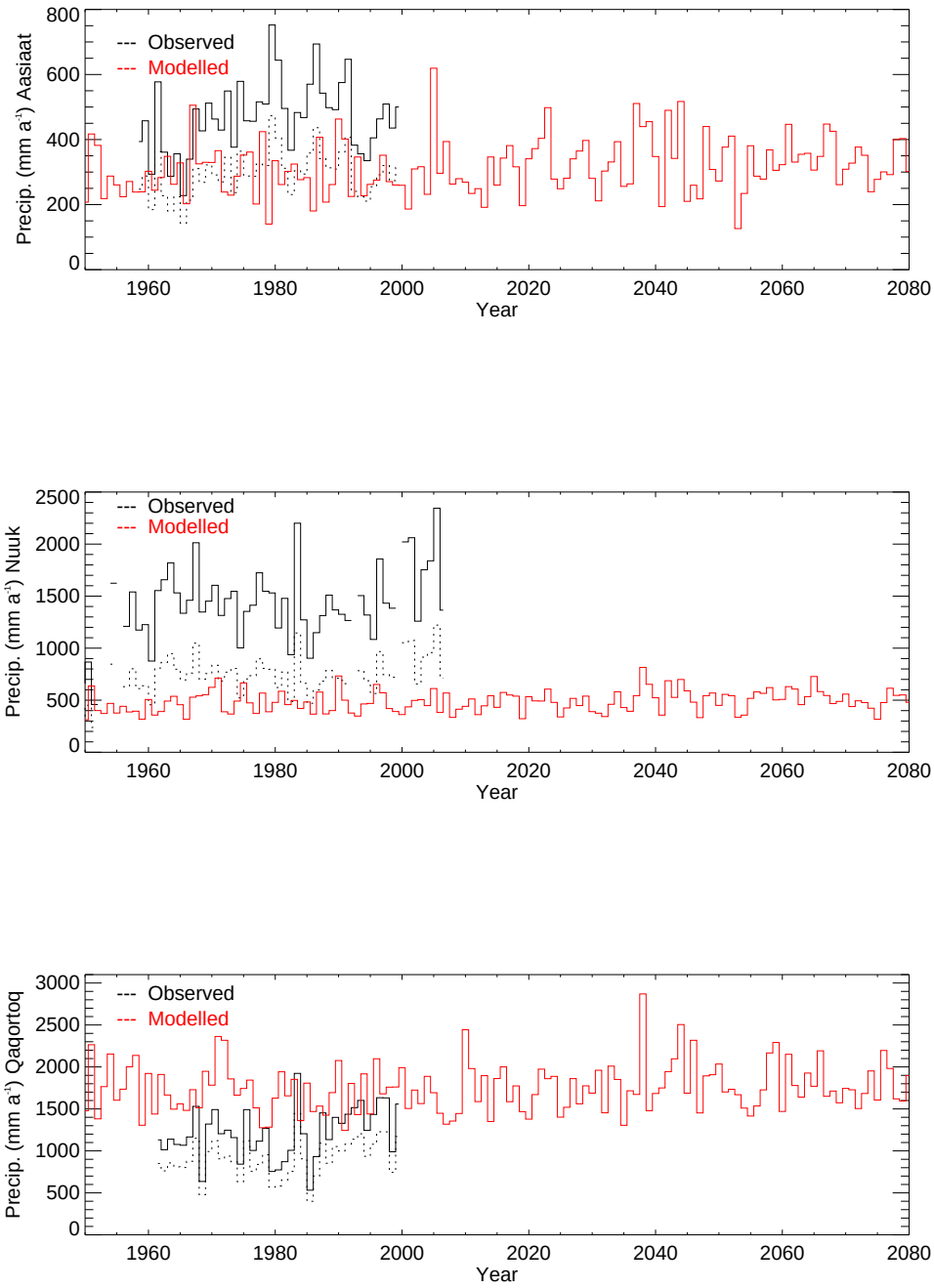

Figure 6.20: Mean annual precipitation from the DMI weather stations and the closest grid point from HIRHAM4. Measurements are corrected with a factor (Table 4.1) for each location. The uncorrected annual time series is shown with a dotted line.

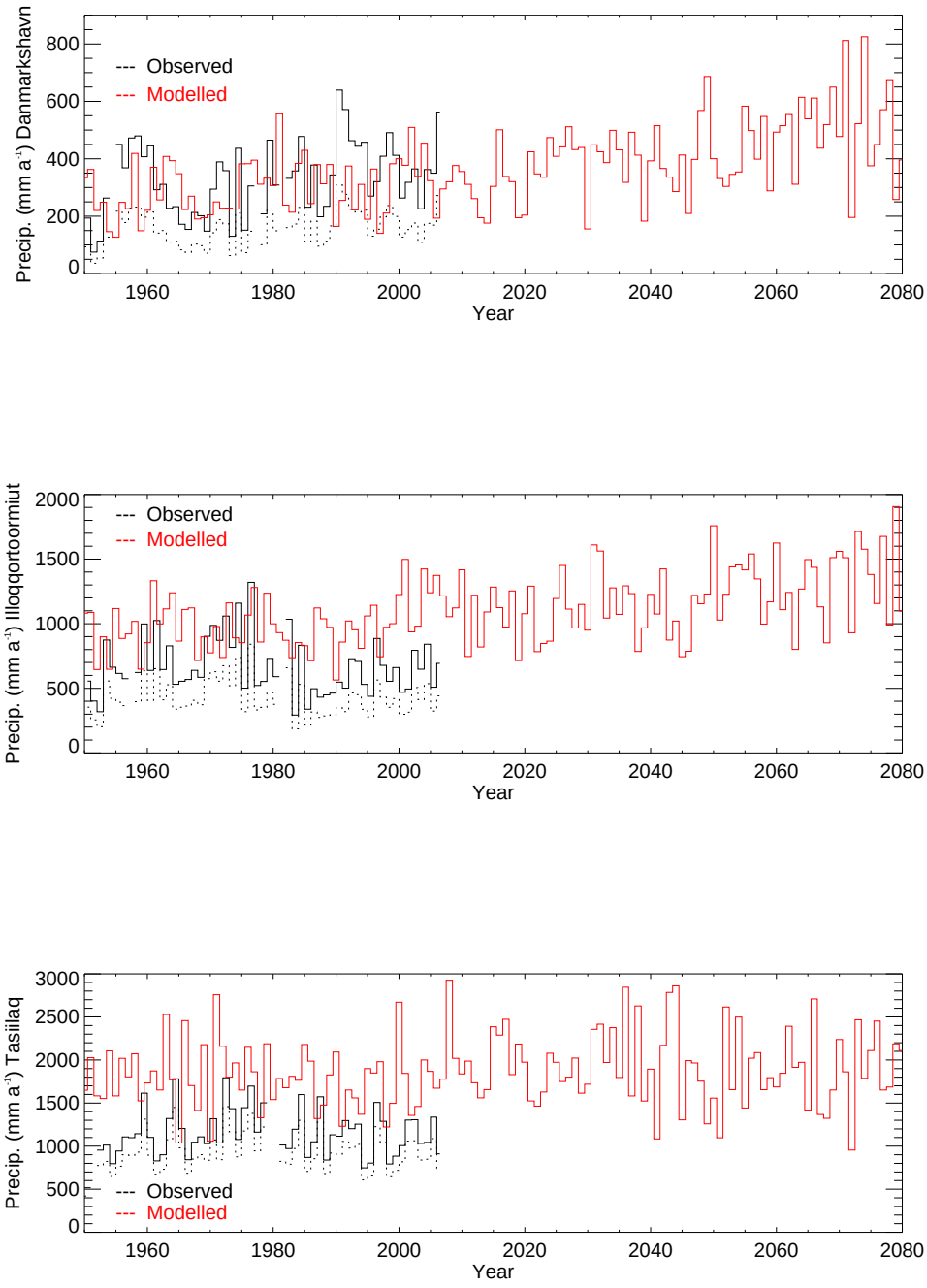

Figure 6.21: Mean annual precipitation from the DMI weather stations and the closest grid point from HIRHAM4. Measurements are corrected with a factor (Table 4.1) for each location (correction for Illoqqortoormiut is from *Allerup et al.* (2000)). The uncorrected annual time series is shown with a dotted line.

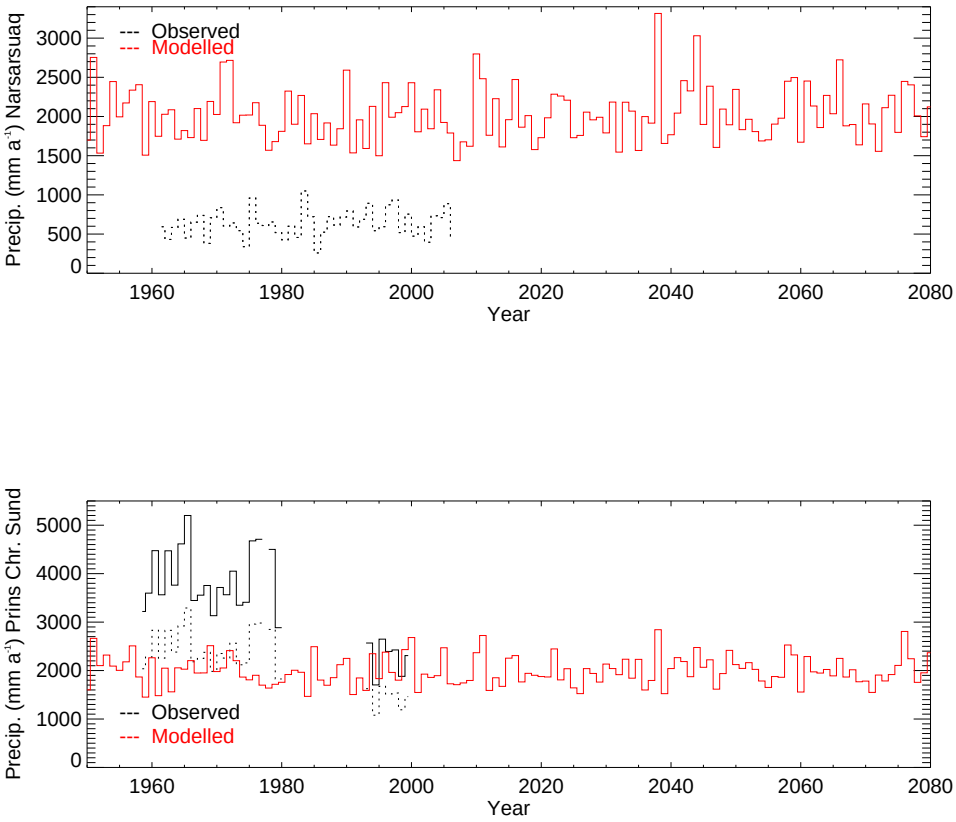

Figure 6.22: Mean annual precipitation from the DMI weather stations and the closest grid point from HIRHAM4. Measurements are corrected with a factor (Table 4.1) for each location. The uncorrected annual time series is shown with a dotted line.

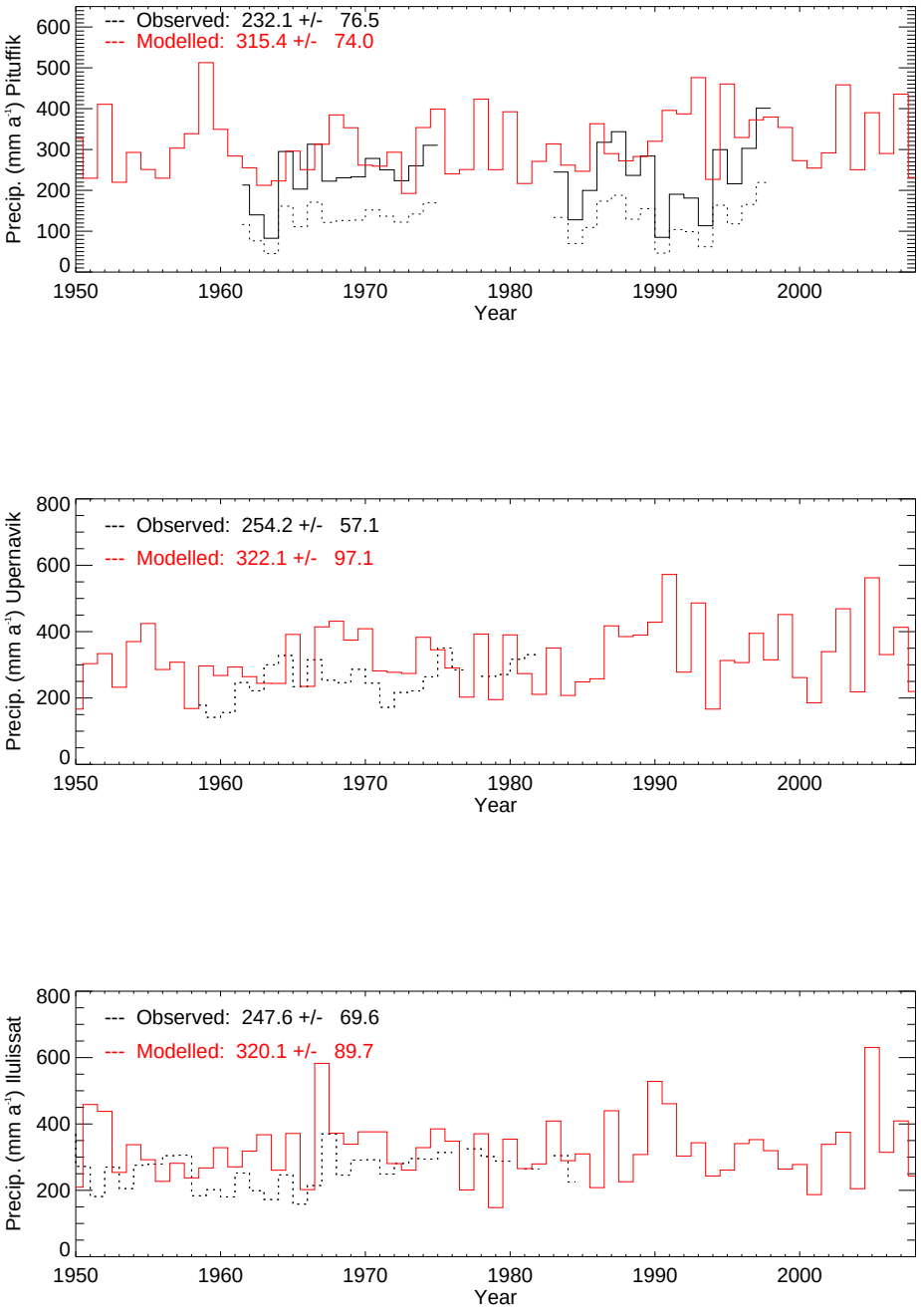

Figure 6.23: Mean annual precipitation from the DMI weather stations and the closest grid point from HIRHAM4 for the period 1950-2008. The mean value and standard deviation for this period is shown. Measurements are corrected with a factor (Table 4.1) for each location. The uncorrected annual time series is shown with a dotted line.

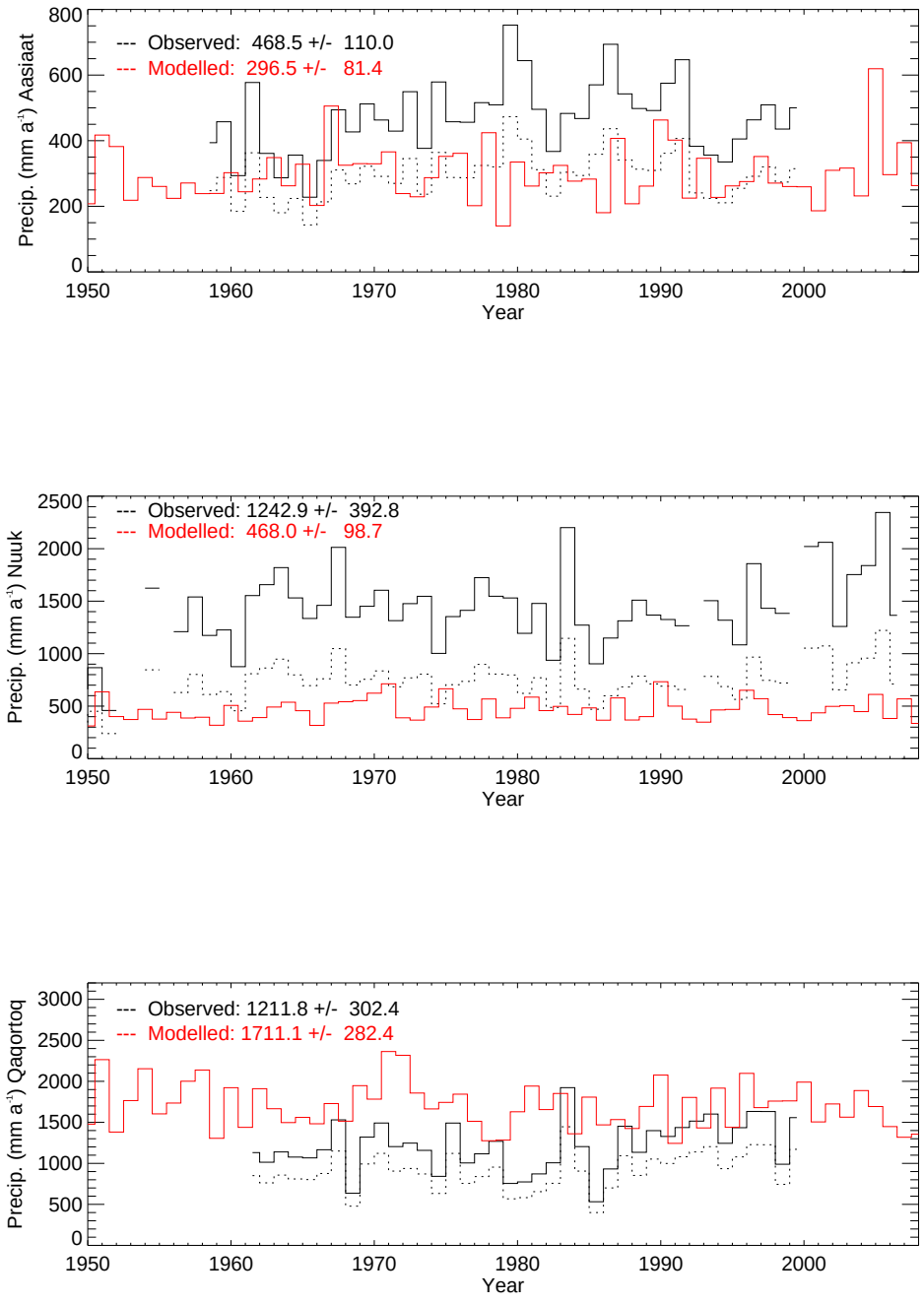

Figure 6.24: Mean annual precipitation from the DMI weather stations and the closest grid point from HIRHAM4 for the period 1950-2008. The mean value and standard deviation for this period is shown. Measurements are corrected with a factor (Table 4.1) for each location. The uncorrected annual time series is shown with a dotted line.

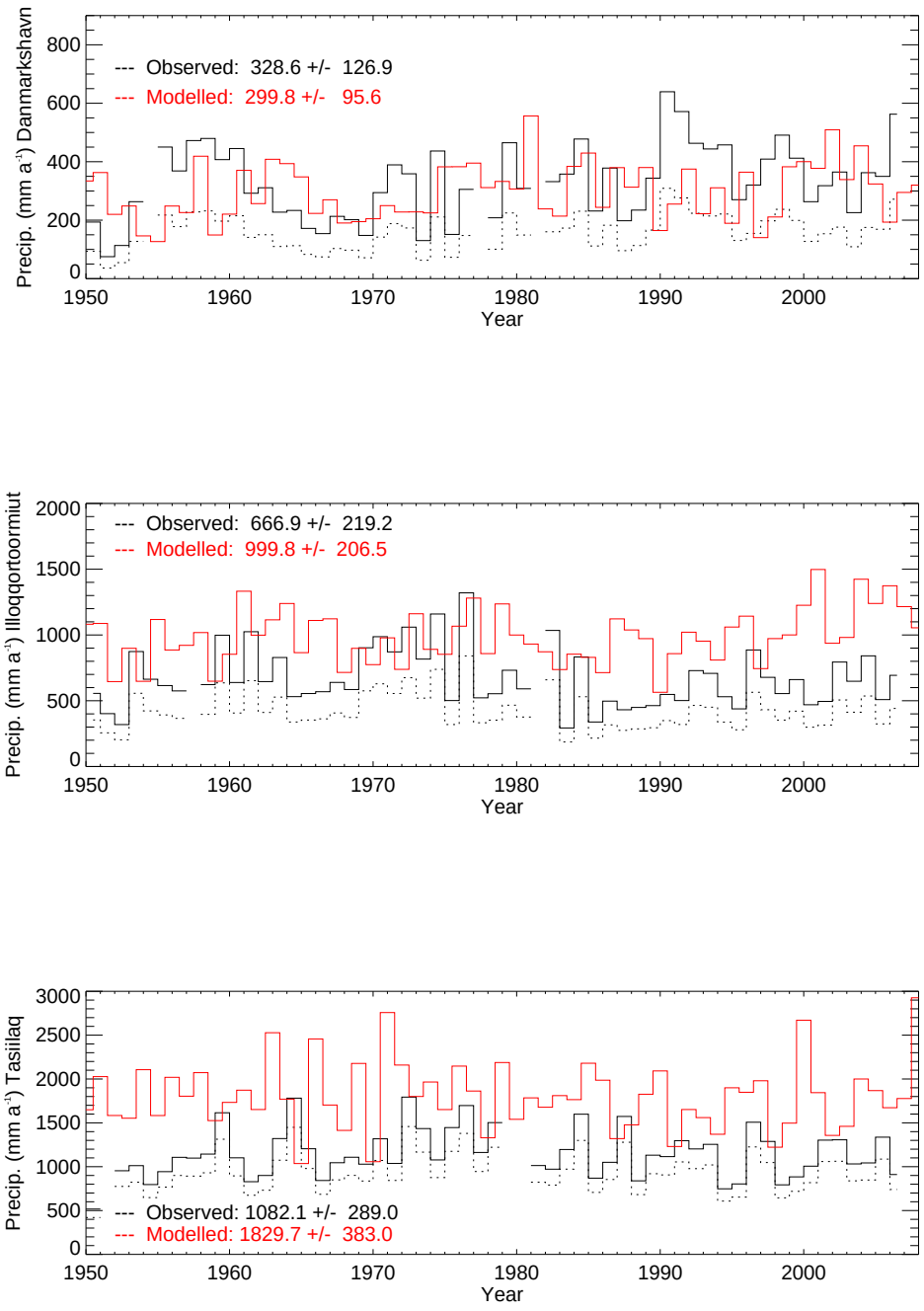

Figure 6.25: Mean annual precipitation from the DMI weather stations and the closest grid point from HIRHAM4 for the period 1950-2008. The mean value and standard deviation for this period is shown. Measurements are corrected with a factor (Table 4.1) for each location (correction for Illoqqortoormiut is from *Allerup et al.* (2000)). The uncorrected annual time series is shown with a dotted line.

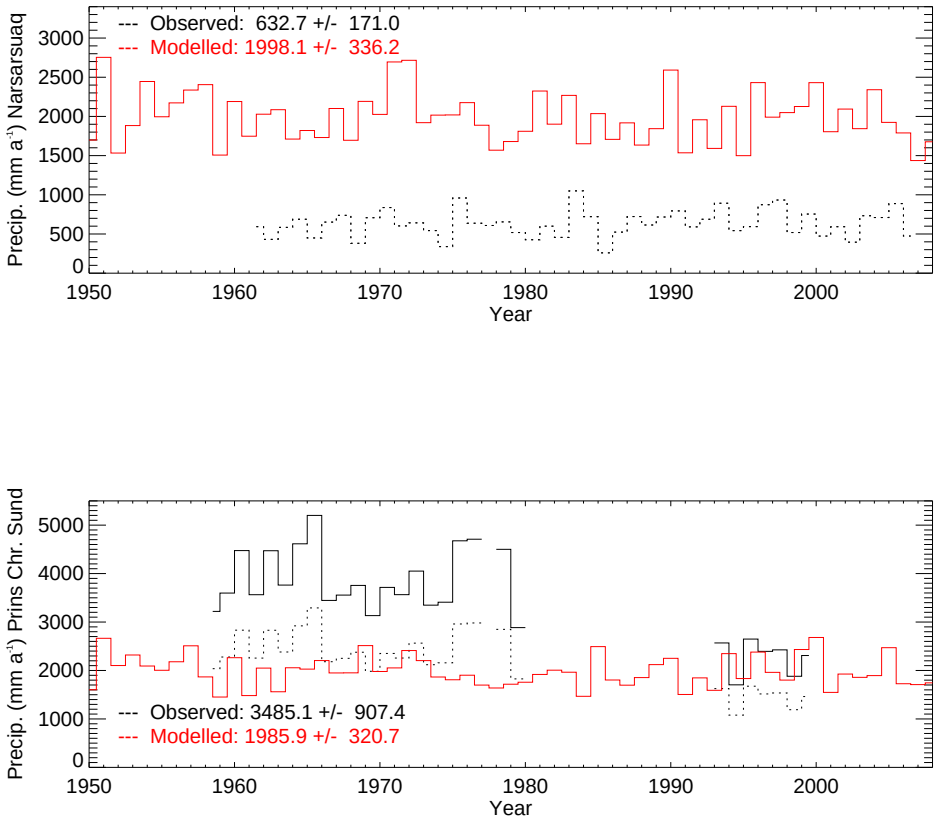

Figure 6.26: Mean annual precipitation from the DMI weather stations and the closest grid point from HIRHAM4 for the period 1950-2008. The mean value and standard deviation for this period is shown. Measurements are corrected with a factor (Table 4.1) for each location. The uncorrected annual time series is shown with a dotted line.

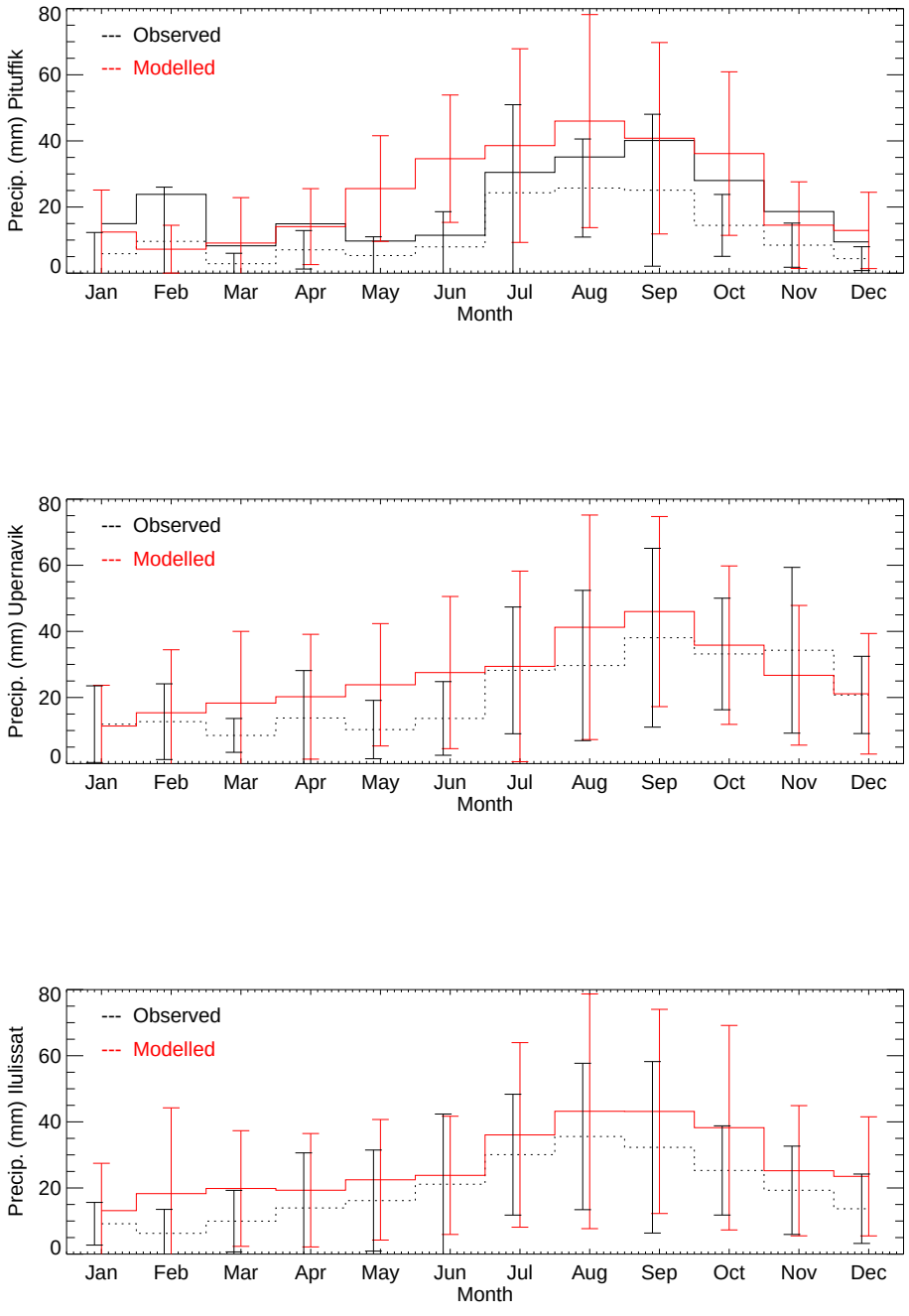

Figure 6.27: Monthly mean precipitation from the DMI weather stations and the closest grid point from HIRHAM4. The bars indicate the standard deviation of the 30 years time series.

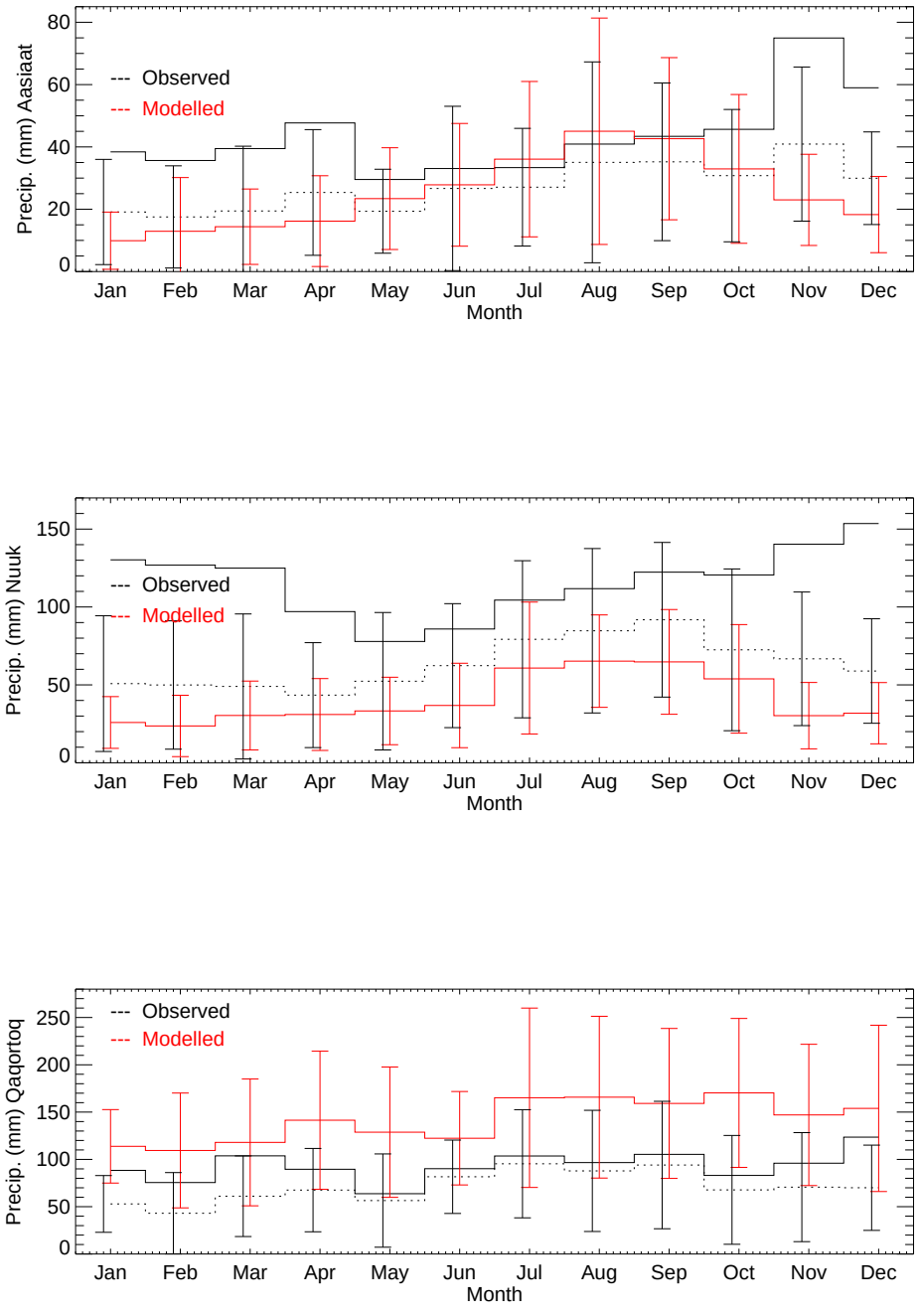

Figure 6.28: Monthly mean precipitation from the DMI weather stations and the closest grid point from HIRHAM4. The bars indicate the standard deviation of the 30 years time series.

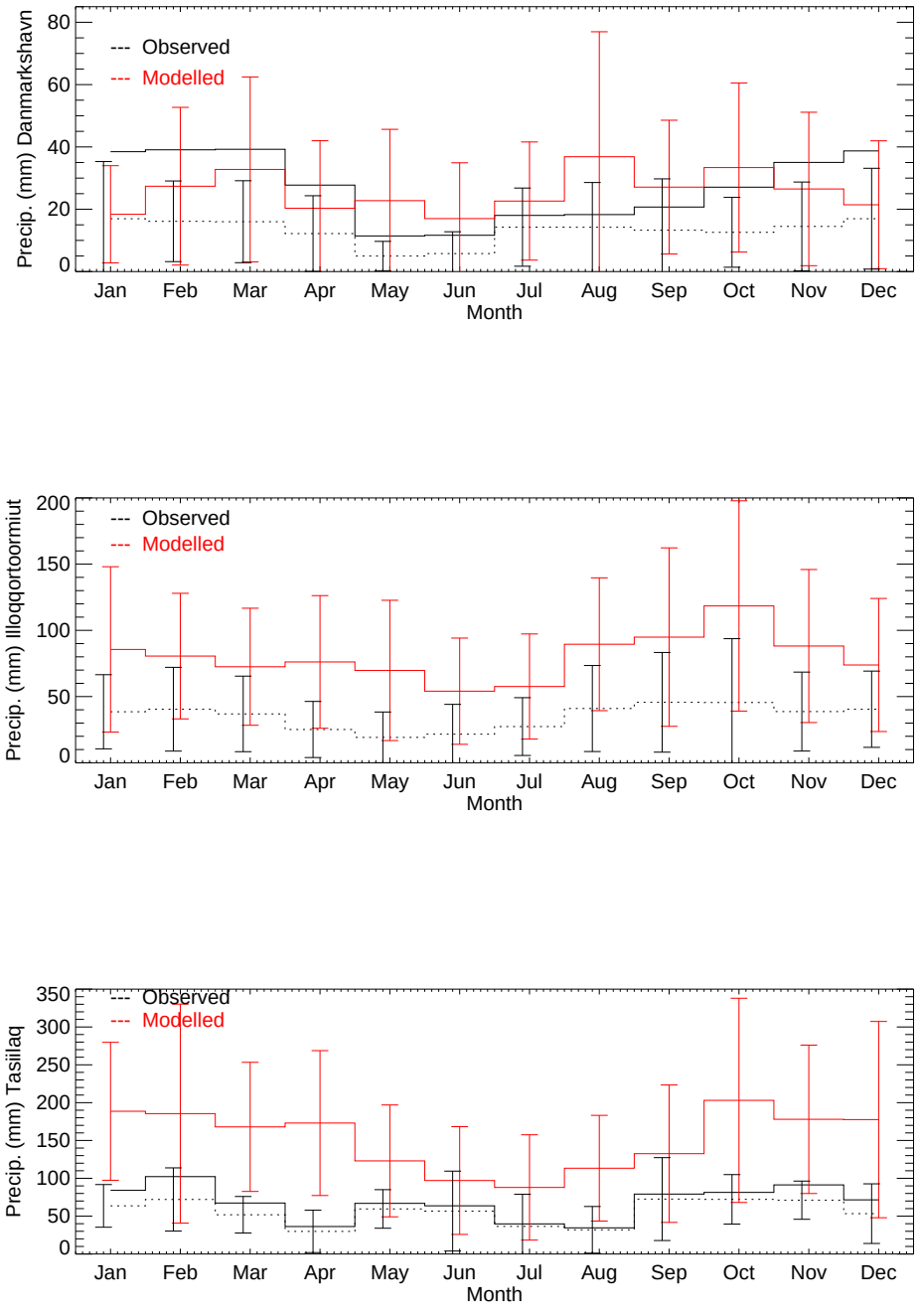

Figure 6.29: Monthly mean precipitation from the DMI weather stations and the closest grid point from HIRHAM4. The bars indicate the standard deviation of the 30 years time series.

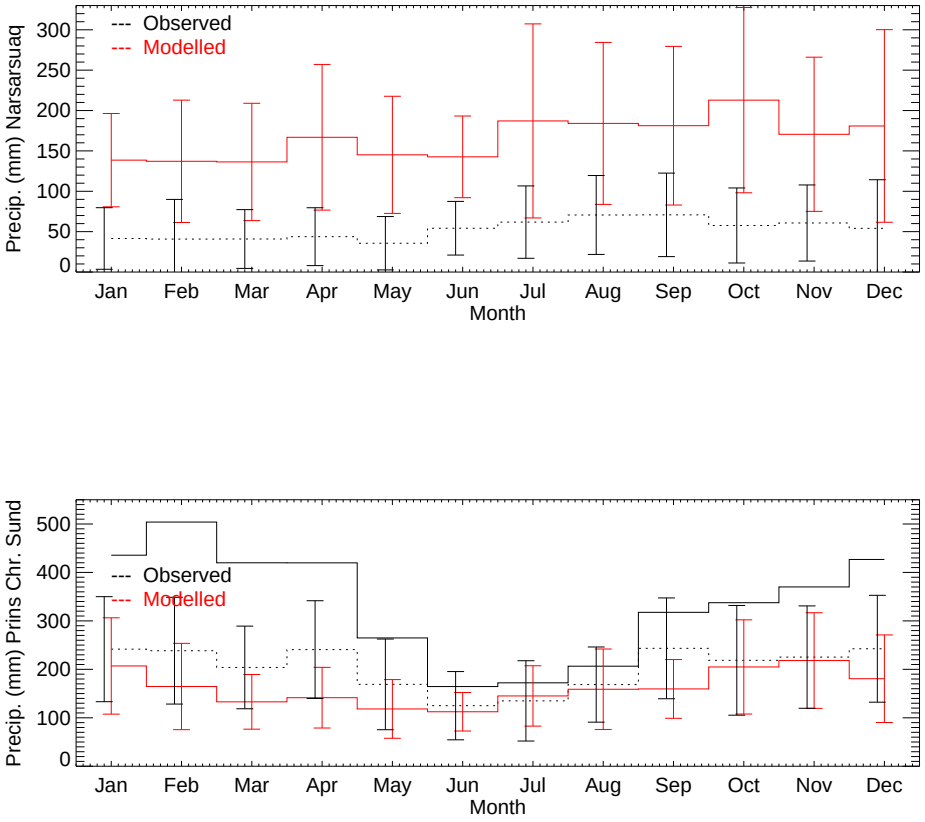

Figure 6.30: Monthly mean precipitation from the DMI weather stations and the closest grid point from HIRHAM4. The bars indicate the standard deviation of the 30 years time series.

6.3 Temperature distribution over ice sheet

To assess the temperature distribution of the RCM, the mean annual and mean July temperatures, averaged over the period 1961-1990 for the present day temperature distribution, are compared to the parameterisation that has been used to force a number of ice sheet models (*Ritz et al.*, 1997). The mean annual temperature, T_a, and the summer temperature, T_{summer}, are parameterised as a function of the surface elevation, H, and latitude, Φ,

$$\begin{aligned} T_a[^oC] &= 49.13 - 7.99210^{-3}\,\mathrm{H}\,[\mathrm{m}] - 0.7574\,\Phi\,[^o\mathrm{N}], \\ T_{summer}[^oC] &= 38.38 - 6.27710^{-3}\,\mathrm{H}\,[\mathrm{m}] - 0.3262\,\Phi\,[^o\mathrm{N}]. \end{aligned} \tag{6.1}$$

The lapse rates and variation of temperature with latitude were parameterised from maps of *Ohmura* (1987) and seasonal variation assumed to be a sine function with an amplitude of (T_{summer}-T_a). This parameterisation has been modified to include a temperature inversion on northern Greenland (*Huybrechts and de Wolde*, 1999), and has recently been updated to include longitude dependence and constrained with additional data on the ice sheet and on the coast (*Fausto et al.*, 2009). The temperature distribution for the mean annual and July temperature is shown in Figure 6.31 and the difference between this and the first parameterisation (*Ritz et al.*, 1997) is shown in Figure 6.32.

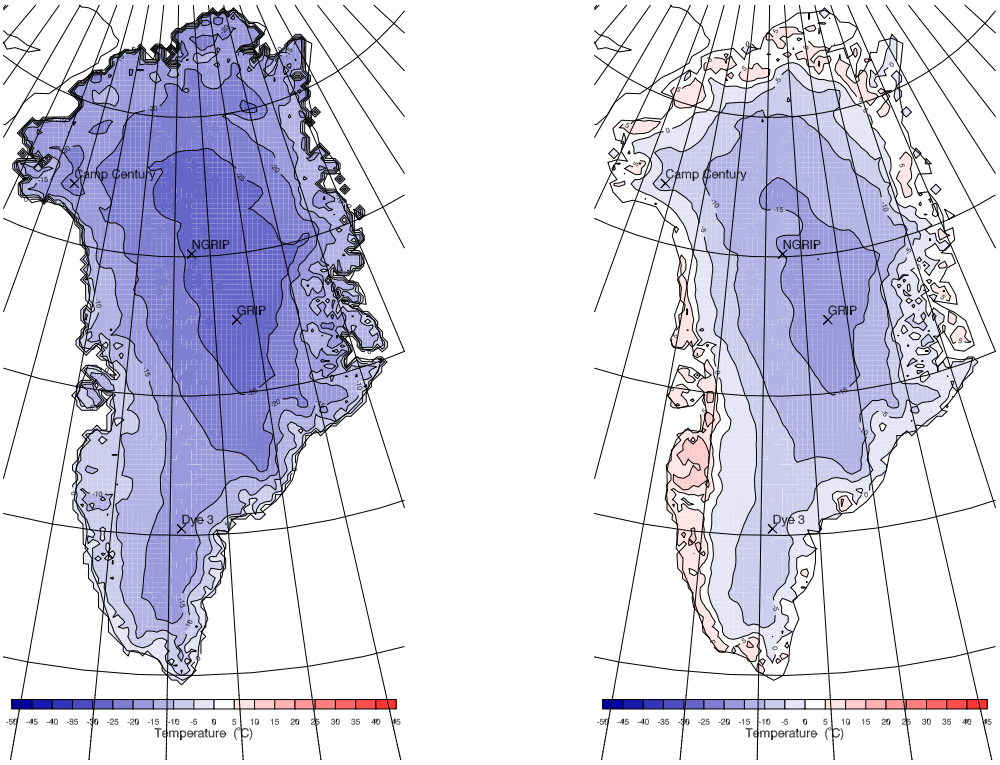

Figure 6.31: Mean annual (left) and July (right) temperature distributions for the Greenland ice sheet from RCM averaged over the period 1961-1990.

.

The mean annual RCM temperature is warmer on most part of the ice sheet than the parameterisation. The difference is about 5°C on the highest and central part of the ice cap. Coldest temperature in the RCM output is -28.17°C while it is -32.02°C in the parameterisation. The annual temperature for all the coastal areas is on the other hand colder and therefore is the temperature lapse rate in the RCM large than in the parameterisation.

The modification of the parameterisation (*Huybrechts and de Wolde*, 1999) acts to lower the temperature on the coast north of 60°N, resulting in colder temperature than the RCM output, so the RCM is between the two parameterisation in this area. The new present-day parameterisation, which is based on more data than the previous one, results in warmer temperature on the ice sheet and colder on the coast (*Fausto et al.*, 2009). The mean annual temperature of 1961-1990 from the RCM is therefore closer to the new parameterisation than the original one.

The July temperature distributions are also compared in Figure 6.32. The RCM output is colder than the parameterisation over the main ice cap, with coldest temperatures of -16.9°C compared to -13.44°C. In north Greenland the RCM is warmer, up to 5°C warmer around most of the coastal areas. The 0°C contour is at a higher elevation than in the parameterisation and the lapse rate therefore larger in the RCM. In the southern part of Greenland there is a difference between the west and east, in the west the RCM has temperatures up to 10°C in the area south of Disco Bay, while the temperatures in the parameterisation in the same area are only around 5°C. On the southern dome, there is a better match and the -5°C contour line is in a similar location. On the east coast, on the other hand, the RCM is colder. The RCM temperature on the coast is around 5°C but is warmer, up to 10°C, in the parameterisation. On the east coast, north of Illoqqortoormiut the temperatures are similar, around 0-5°C, with a few areas where the RCM is warmer. The new parameterisation

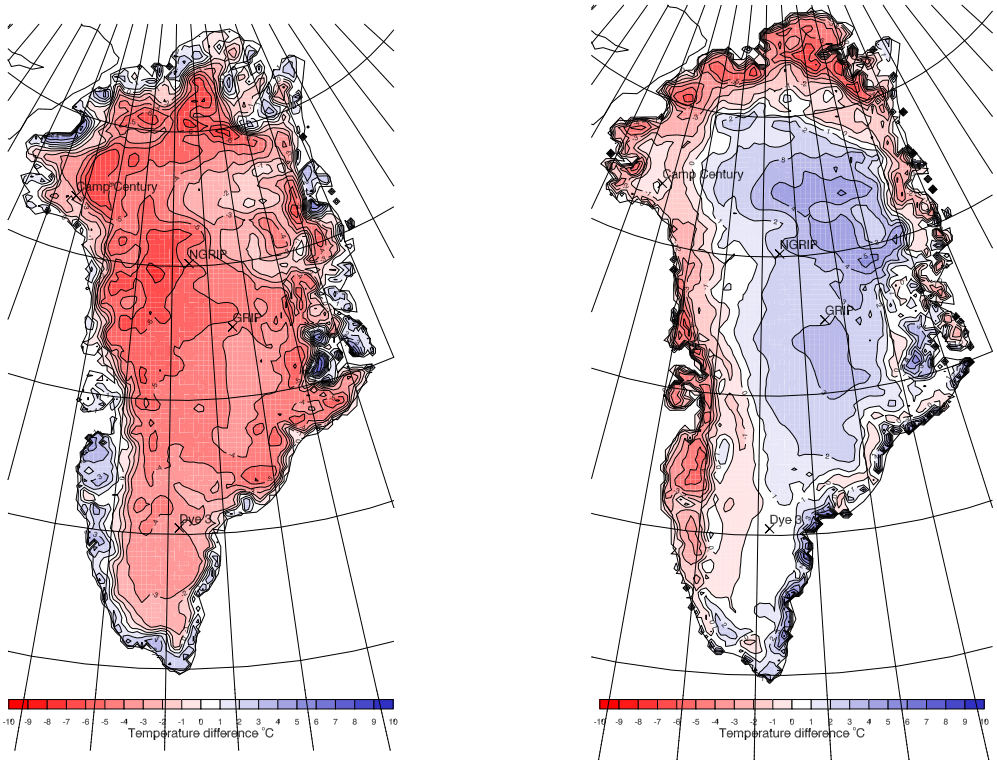

Figure 6.32: Difference of mean annual (left) and July (right) temperature distributions between the RCM output averaged over the period 1961–1990 and the parameterisation based on altitude and latitude that has been used to force ice sheet models (*Ritz et al.*, 1997).

.

(*Fausto et al.*, 2009) increases the temperature for July, which results in larger difference between the RCM July temperature and the new parameterisation than the older parameterisation, the difference is about 1-2°C over the ice sheet, but the pattern is similar to the one shown in Figure 6.32.

6.4 Precipitation, Evaporation and Snow fields

Precipitation is one of the most difficult components in the climate system to both model and measure, particularly over the large ice sheets, where measurements are scarce due to remoteness and solid precipitation measurements are subject to large uncertainties. Number of studies have shown, however, that the precipitation in reanalysis appears fairly reasonable (*Bromwich et al.*, 1993; *Genthon and Braun*, 1995; *Ohmura et al.*, 1996; *Hanna et al.*, 2001, 2006). It has been noted by *Genthon and Braun* (1995) that in coastal Greenland, the mean precipitation is generally overestimated by the model but inland and at high elevation the model accumulation is sometimes low compared to observations from ice cores. The resolution of the model also appears to have a large impact on the extreme values, as well as the location of high precipitation areas, due to the representation of topography at different resolution.

The 25 km resolution HIRHAM4 precipitation, evaporation and snow fields over Greenland are presented below and validated by comparing the snow pattern with available accumulation maps (*Ohmura and Reeh*, 1991; *Calanca et al.*, 2000; *Bales et al.*, 2001, 2009). The different precipitation estimates (model and maps) are also compared at the same locations as the AWS on the ice cap (GC-Net, *Steffen and Box* (2001)), even though precipitation data is not available there. Monthly mean values are presented to assess the seasonality in the model and finally the snow field from the

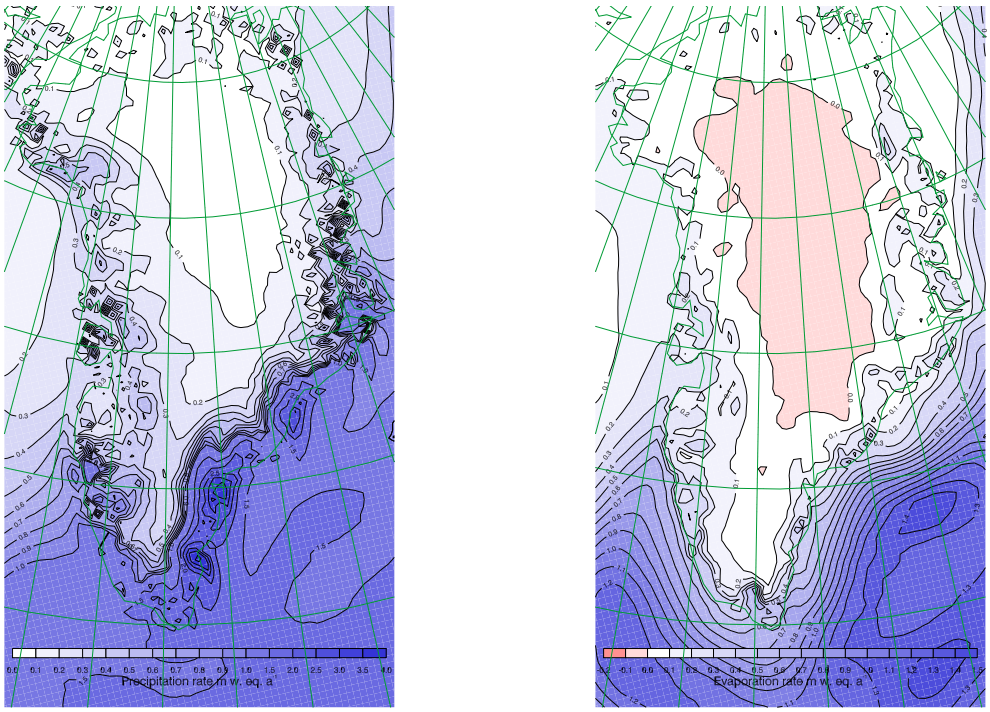

Figure 6.33: Mean annual precipitation (left) and evaporation (right) distributions for the Greenland ice sheet from HIRHAM4 averaged over the period 1961-1990.

.

model compared with the parameterisation (*Marsiat*, 1994) that has been used to separate snow from total precipitation in ice sheet modelling work until now (e.g. *Greve*, 2005).

6.4.1 Precipitation and Evaporation distributions

The mean annual precipitation and evaporation fields from HIRHAM4, averaged over the thirty year period 1961–1990, are shown in Figure 6.33. The large scale features of the precipitation, highest values at the southeast coast, high precipitation band along the western coastal slopes and dry areas over the main ice cap and northern slopes, are well presented in the model. The evaporation map shows small negative values over the main ice cap, indicating condensation, and relatively high positive values in the coastal areas and over the ocean south of Greenland. The combination of these fields, P-E, is compared to the accumulation map from (*Calanca et al.*, 2000) and the updated annual accumulation map based on ice core data and coastal meteorological data (*Bales et al.*, 2009) in Figure 6.34. Compared to the older estimate (*Bales et al.*, 2001), the updated accumulation map (*Bales et al.*, 2009) has 20–50% lower accumulation in the southwest, northwest and eastern regions and 20–50% higher accumulation in southeast and northeast regions. These updates are based on the same coastal data (DMI weather stations) as presented above.

The figure shows the ratio between the model and the map, areas where HIRHAM4 has higher P-E values are green and areas where HIRHAM4 has lower P-E values are blue. The RCM produces considerably higher P-E values than both estimates along the south coast and southeast, up to the area north of Illoqqortoormiut (Scoresby Sund). There are values above 2 m w.e. along the southeast coast, where the previous estimates have indicated up to 1 m w.e. values. This area is however not well constrained with measurements. In the updated PARCA map (*Bales et al.*, 2009) the precipitation was increased considerably (20–50%) when data from two coastal stations operated by DMI were added to the data base. This shift can be seen when comparing the two ratio-maps in

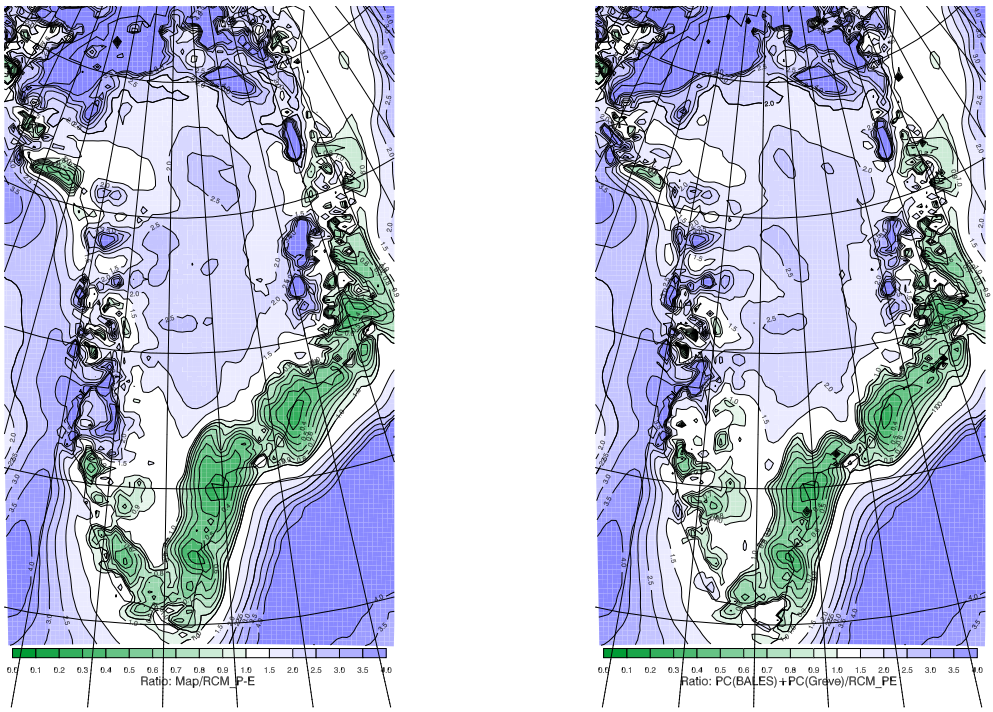

Figure 6.34: The ratio between the precipitation map of *Calanca et al.* (2000) (left) and the updated PARCA grid (*Bales et al.*, 2009) (right) and the P-E field from HIRHAM4 on 25 km grid averaged over the period 1961-1990.

Figure 6.34 the model is now close to the estimate on the southwest coast, but the general overestimation on the southeast coast and underestimation over the main ice sheet is still present, even when compared to the new accumulation map.

The model run with HIRHAM4 at a 25 km resolution shows the same characteristics as previous model runs with the same model at 50 km resolution (*Dethloff et al.*, 2002; *Kiilsholm et al.*, 2004). The increasing model resolution resolves the orographic features around the margins of the Greenland Ice Sheet, that control most of the coastal precipitation, at increasingly more detail. All areas with relatively high P-E values are associated with sloping terrain resulting in high precipitation values by orographic lifting. On the other hand, the areas with low accumulation rates over the main ice cap and the north and northeast slopes are simulated with lower than the ERA40 dataset (*Dethloff et al.*, 2002). The model run at 25 km resolution shows this as well, HIRHAM4 has a tendency to overestimate the Arctic desert conditions in the northern most parts and the western central plateau (*Kiilsholm et al.*, 2004) and the higher precipitation at the southeast coast in this model simulation is even more extreme than at 50 km resolution. This indicates that the model resolution at 25 km is starting to resolve the orographic features controlling the coastal precipitation, but the areas subject to the high precipitation on the steep slopes is overestimated, due to the still relatively large grid size.

Preliminary results done with the model at 5 km resolution (Lucas-Picher, personal communication, 2009) indicate that the areas with high precipitation at that high resolution are considerably smaller, resulting in smaller amount of total precipitation in these coastal areas. The orographic accumulation maximum over the northwestern coastal slopes that appears in both accumulation estimates (*Calanca et al.*, 2000; *Bales et al.*, 2009) is, however, not well captured in the RCM simulation. This has been noted for other modelled approaches (*Bromwich et al.*, 1993) and should be investigated further.

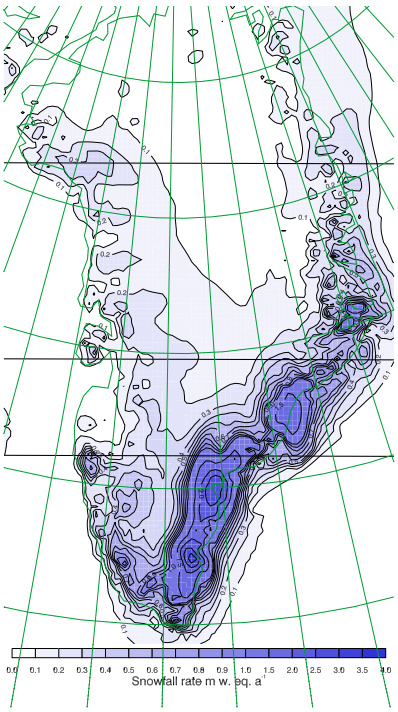

Figure 6.35: Mean annual snow from the RCM HIRHAM4 on 25 km grid averaged over the period 1961-1990. The three horizontal lines indicate the location of the cross sections shown in figures 6.50- 6.61.
.

6.4.2 Snow

The computation of snow fall in the HIRHAM4 model is a combination of sedimentation and cloud microphysics. The total snow flux is found by integrating a number of fluxes (including conversion rate from cloud ice to snow by aggregation of ice crystals, by super cooled cloud droplets colliding and coalescing with them (riming), accretion rate of ice crystals by snow, subtracting the sublimation of snow and snow melt within the cloud) over the whole atmospheric column (*Roeckner et al.*, 2003). The mean annual snow fall averaged over the period 1961–1990 is shown in Figure 6.35. The snow fall has the same large scale pattern as the precipitation, with highest snow fall on the south east coast and very dry over the main ice cap and the northern most part of Greenland.

In the formulation of the surface mass balance in the ice sheet model Sicopolis the snow is extracted from the precipitation based on temperature, with an empirical relation by *Marsiat* (1994). In this formulation there is no snow if the mean monthly temperature is above 7°C and all the precipitation falls as snow if the mean monthly temperature is below -10°C, the amount of snow relative to the precipitation changes linearly from 0 to 1 between 7°C and -10°C. This formulation has been used to convert the accumulation maps to precipitation and estimate the amount of snow for the long ice sheet model runs (*Greve*, 2005). The snow field output from the HIRHAM4 model makes it possible to evaluate this assumption and compare the amount of snow by the model with the parameterisation.

To assess the RCM output and the snow formulation that has been used in large scale ice sheet models, a comparison of the P, P-E and snow fields with the estimate from *Calanca et al.* (2000) is done at all the GC-Net locations (Figures 6.36- 6.42). Four things are observed in this comparison, (1) the maximum precipitation occurs during the summer months over the main ice cap and about a month later at the stations on the west coast, (2) the maximum P-E in the model is lower than the map over the main ice cap (NGRIP, Summit, Saddle), as already discussed above, the summer P-E is

about the same amount as in the estimate at the stations on the north side (GITS, Humboldt, Tunu-N, NASA_U and NASA_E) and the mean annual value is relatively close to the estimate on the western coast and south part of the ice cap (Swiss Camp, JAR stations and Crawford Point stations, Dye 2 and South Dome), (3) there is a minimum in P-E during the summer months in the southeast stations (KULU and NASA_SE) and (4) the timing of snow fall in the model and from the parameterisation (red and green solid lines) is well matched, but the amount of snow in the parameterisation is underestimated compared to the difference between the P (orange dotted line) and the snow fall computed in the HIRHAM4 model (blue line).

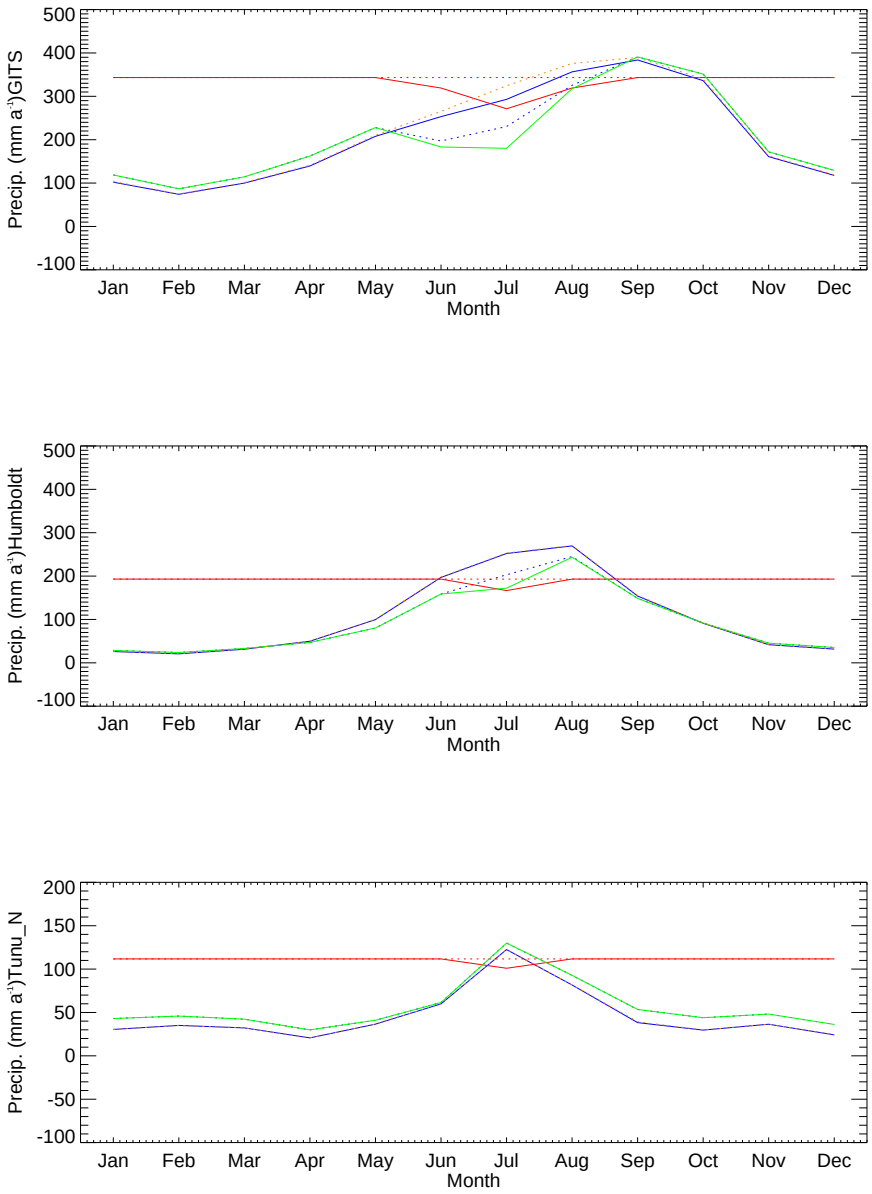

Figure 6.36: Yearly Precipitation, P-E and snow variation for the GC-Net stations GITS, Humboldt, and Tunu-N. The blue lines show P-E and snow from the HIRHAM4 model, orange line the Precipitation, and green line is the amount of snow computed from the P-E output from HIRHAM4 with the same conversion as has been used before. The red lines show the annual precipitation from (*Calanca et al.*, 2000) and the amount of snow computed with the snow conversion from *Marsiat* (1994).

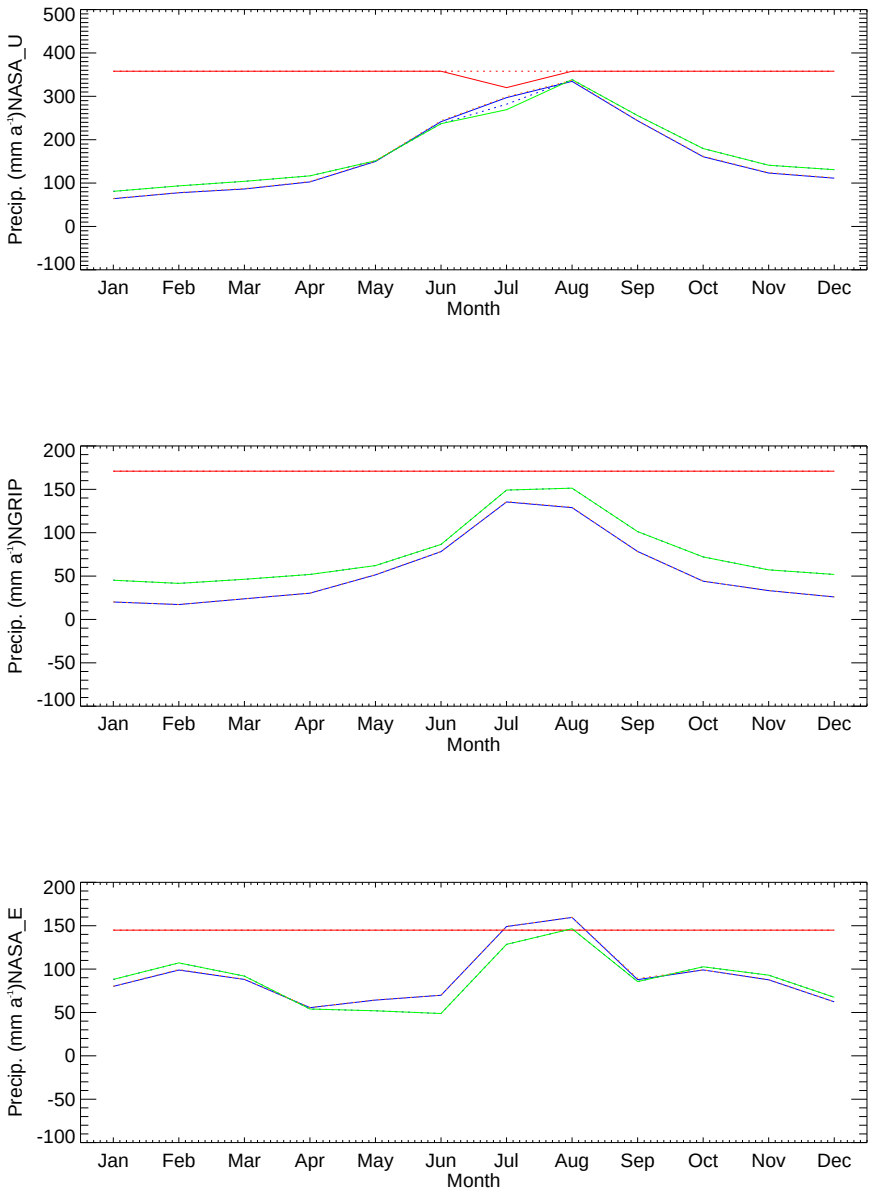

Figure 6.37: Yearly Precipitation, P-E and snow variation for the GC-Net stations NASA-U, North-GRIP, and NASA-E. The blue lines show P-E and snow from the HIRHAM4 model, orange line the Precipitation, and green line is the amount of snow computed from the P-E output from HIRHAM4 with the same conversion as has been used before. The red lines show the annual precipitation from (*Calanca et al.*, 2000) and the amount of snow computed with the snow conversion from *Marsiat* (1994).

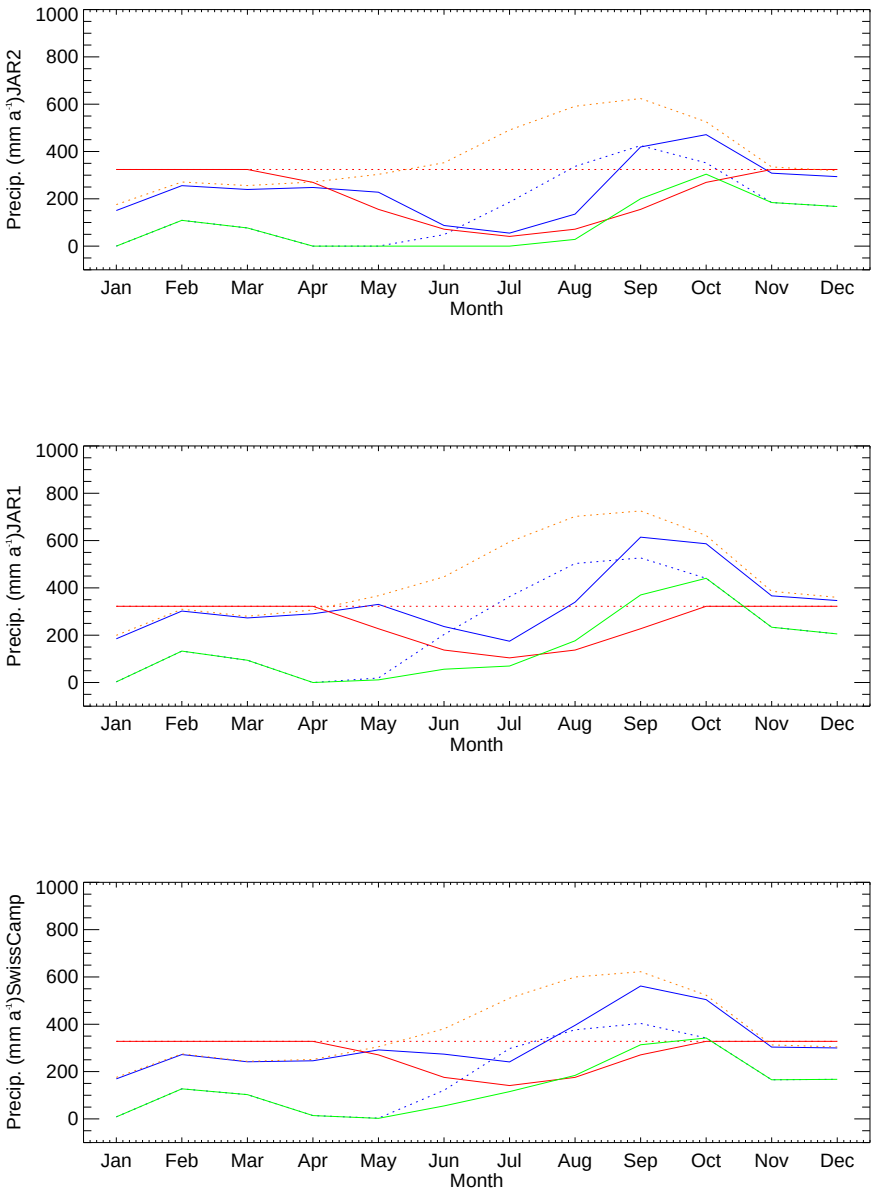

Figure 6.38: Yearly Precipitation, P-E and snow variation for the GC-Net stations JAR2, JAR2, and Swiss Camp. The blue lines show P-E and snow from the HIRHAM4 model, orange line the Precipitation, and green line is the amount of snow computed from the P-E output from HIRHAM4 with the same conversion as has been used before. The red lines show the annual precipitation from (*Calanca et al.*, 2000) and the amount of snow computed with the snow conversion from *Marsiat* (1994).

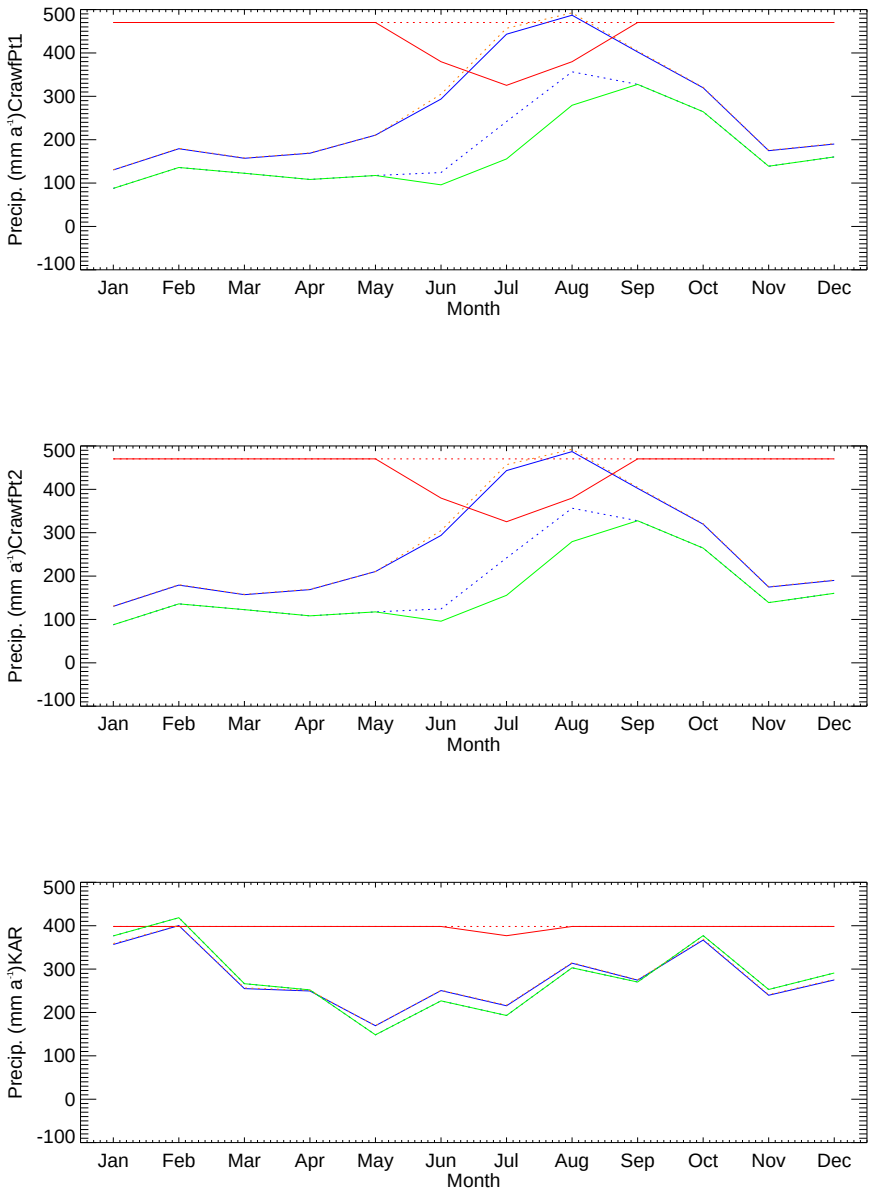

Figure 6.39: Yearly Precipitation, P-E and snow variation for the GC-Net stations Crawford Point 1, Crawford Point 2, and KAR. The blue lines show P-E and snow from the HIRHAM model, orange line the Precipitation, and green line is the amount of snow computed from the P-E output from HIRHAM4 with the same conversion as has been used before. The red lines show the annual precipitation from (*Calanca et al.*, 2000) and the amount of snow computed with the snow conversion from *Marsiat* (1994).

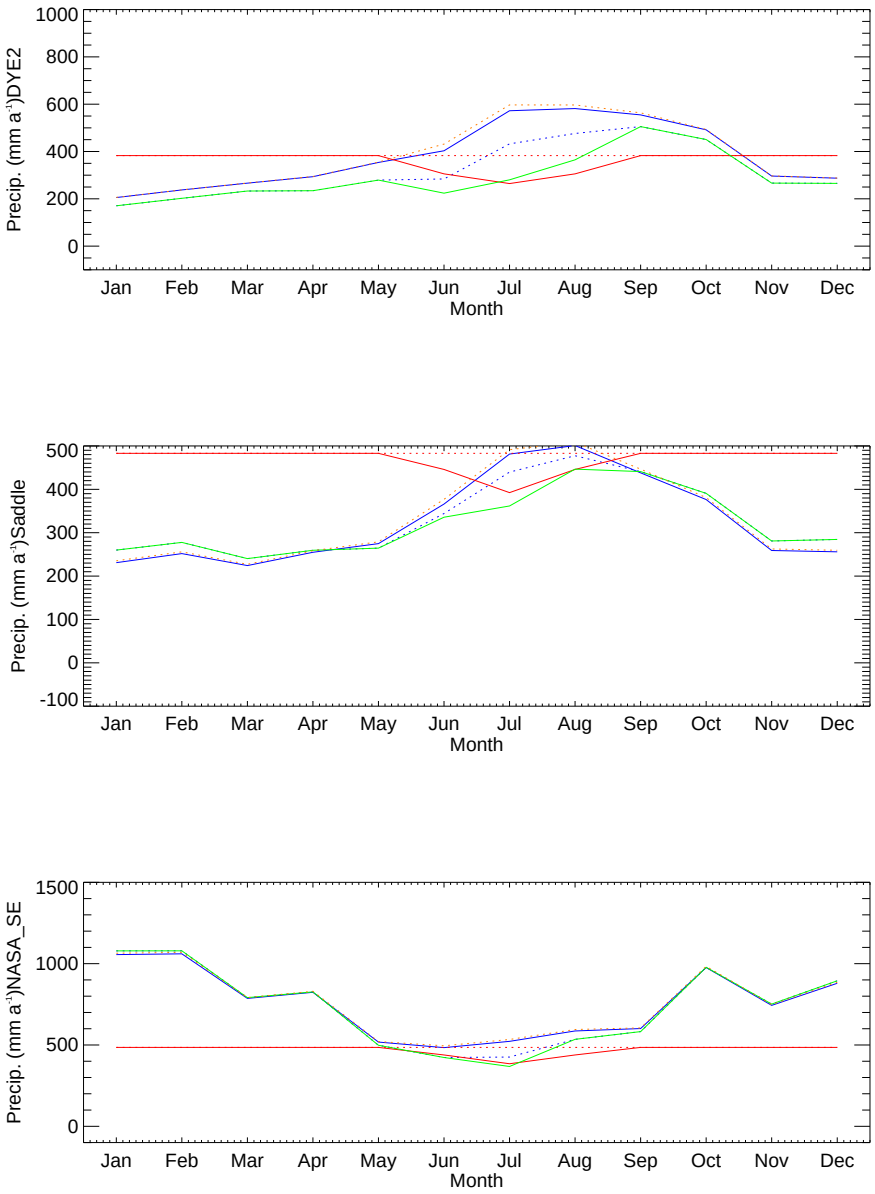

Figure 6.40: Yearly Precipitation, P-E and snow variation for the GC-Net stations Dye2, Saddle and NASA-SE. The blue lines show P-E and snow from the HIRHAM4 model, orange line the Precipitation, and green line is the amount of snow computed from the P-E output from HIRHAM4 with the same conversion as has been used before. The red lines show the annual precipitation from (*Calanca et al.*, 2000) and the amount of snow computed with the snow conversion from *Marsiat* (1994).

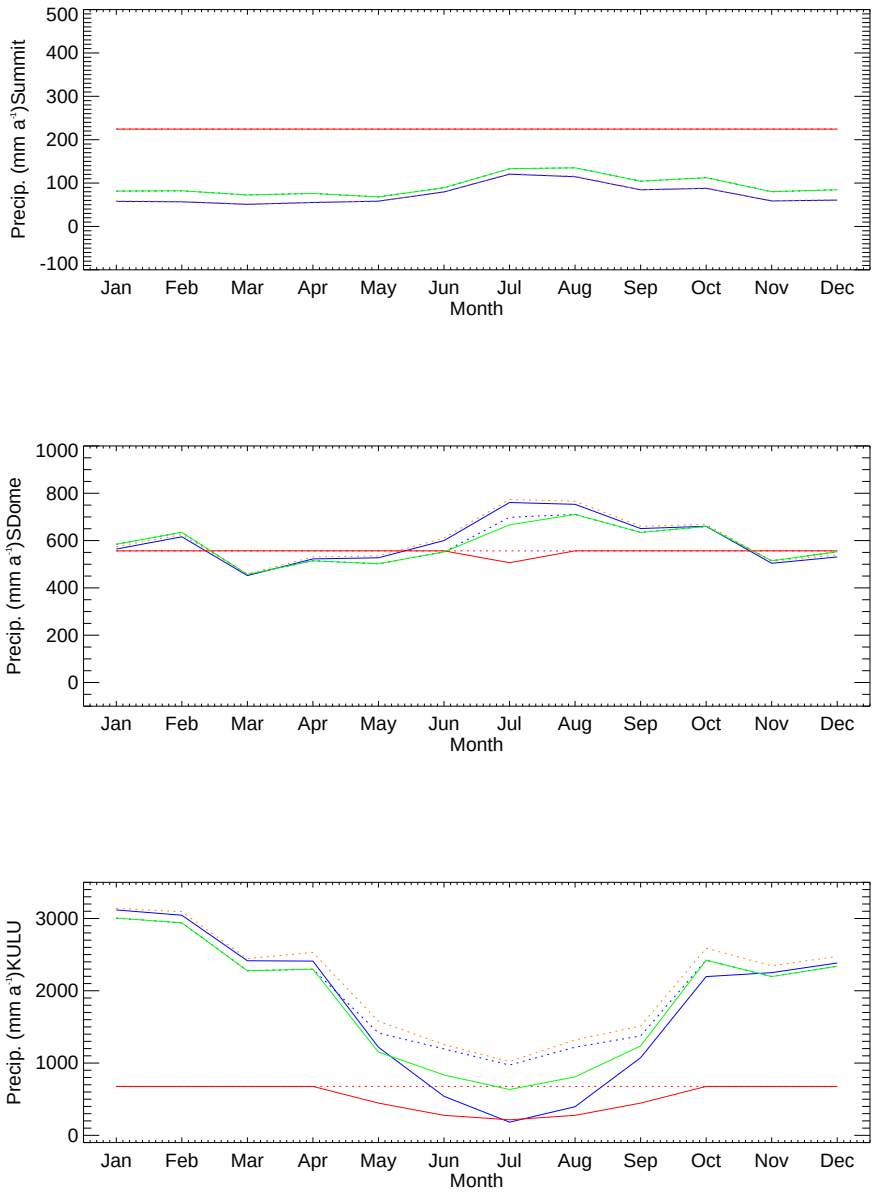

Figure 6.41: Yearly Precipitation, P-E and snow variation for the GC-Net stations Summit, South Dome and KULU. The blue lines show P-E and snow from the HIRHAM4 model, orange line the Precipitation, and green line is the amount of snow computed from the P-E output from HIRHAM4 with the same conversion as has been used before. The red lines show the annual precipitation from (*Calanca et al.*, 2000) and the amount of snow computed with the snow conversion from *Marsiat* (1994).

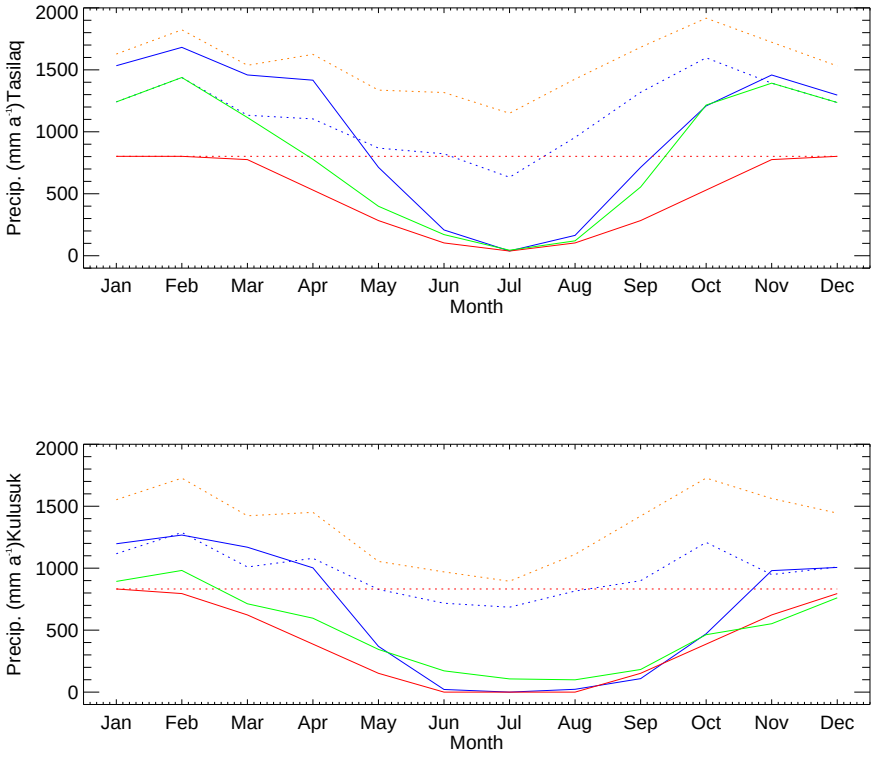

Figure 6.42: Yearly Precipitation, P-E and snow variation for the weather stations Tasiilaq and Kulusuk. The blue lines show P-E and snow from the HIRHAM4 model, orange line the Precipitation, and green line is the amount of snow computed from the P-E output from HIRHAM4 with the same conversion as has been used before. The red lines show the annual precipitation from (*Calanca et al.*, 2000) and the amount of snow computed with the snow conversion from *Marsiat* (1994).

This comparison reveals that the snow field appears to be computed without taking into account the amount of evaporation at each location and therefore, depending on the evaporation, the snow can be smaller or larger than the P-E. A look at three locations on the ice cap; NGRIP at the highest part of the ice cap, GITS on the north west part and Swiss Camp close to the equilibrium line on the west coast shows the different situation. At NGRIP, where it is cold throughout the year, the Evaporation is negative (condensation) and therefore P-E larger than the amount of snow. At GITS there is condensation during the winter, but in the summer months evaporation is computed in the model resulting in a snow field that is larger than the P-E amount. The third situation is at Swiss Camp, there is rather large amount of evaporation computed in the model resulting in P-E field that is considerably smaller than P. The snow field is nearly as large as the P during winter, but reduces relative to the P field in the summer indicating that part of the precipitation is falling as rain during summer. This results in snow field that is larger than the P-E most of the year, except during short period in the summer.

When applying these fields in the surface mass balance on the ice sheet the model will assume that the difference between P-E and snow at NGRIP and during winter at GITS is rain, which is unrealistic. It is therefore necessary to correct the snow field by adding the amount of condensation. During summer at GITS and Swiss Camp the Snow field is less than the precipitation, indicating that part of it is rain, but it is larger than the P-E, causing a problem in the surface mass balance model. Similar problem arises during winter at Swiss Camp when all the precipitation is snow, but it is

larger than the P-E, since there is this relatively large amount of evaporation computed in the model. A correction of the snow field is also necessary here and rather than assuming that all evaporation is snow it is decided that the amount of rain in the model (the difference between P and Snow) is maintained, but the snow is reduced so that the amount of rain is subtracted from the P-E field resulting in less snow.

There are therefore 4 corrections done to the snow field

1. Snow < Precipitation, but Snow > P-E => S = P-E - (P-S) this correction maintains the amount of rain indicated by P-S and subtracts that from P-E to get a snow amount relative to P-E. Then part of the evaporation is snow, part rain.
2. $S > P - E => S = P - E$ all the evaporation is snow and has to be removed from the snow field, this is valid for all areas
3. $P\&S < P - E => S = P - E$ In this area there is condensation (NGRIP) and this amount has to be added to the snow field
4. $P - E < 0$ or correction 1 has caused the $S < 0 => P - E = 0\&S = 0$ Negative P-E occurs over the ocean areas and some of the very driest areas of the ice cap in the north during winter, and during summer there are negative values along the west coast, in the northern most part of the ice cap and along the north eastern coast in April-July and only at small areas at the north eastern coast in August and September, these values, as well as the negative snow values that may have resulted after the first correction, are set to zero, to avoid problems in the surface mass balance model.

The results of this snow correction is shown in similar figures for the GC-Net locations in Figures 6.43- 6.49. The snow fields is now realistic and consistent with the amount of evaporation in the model and maintains the amount of rain (difference between the precipitation and the snow field in the model).

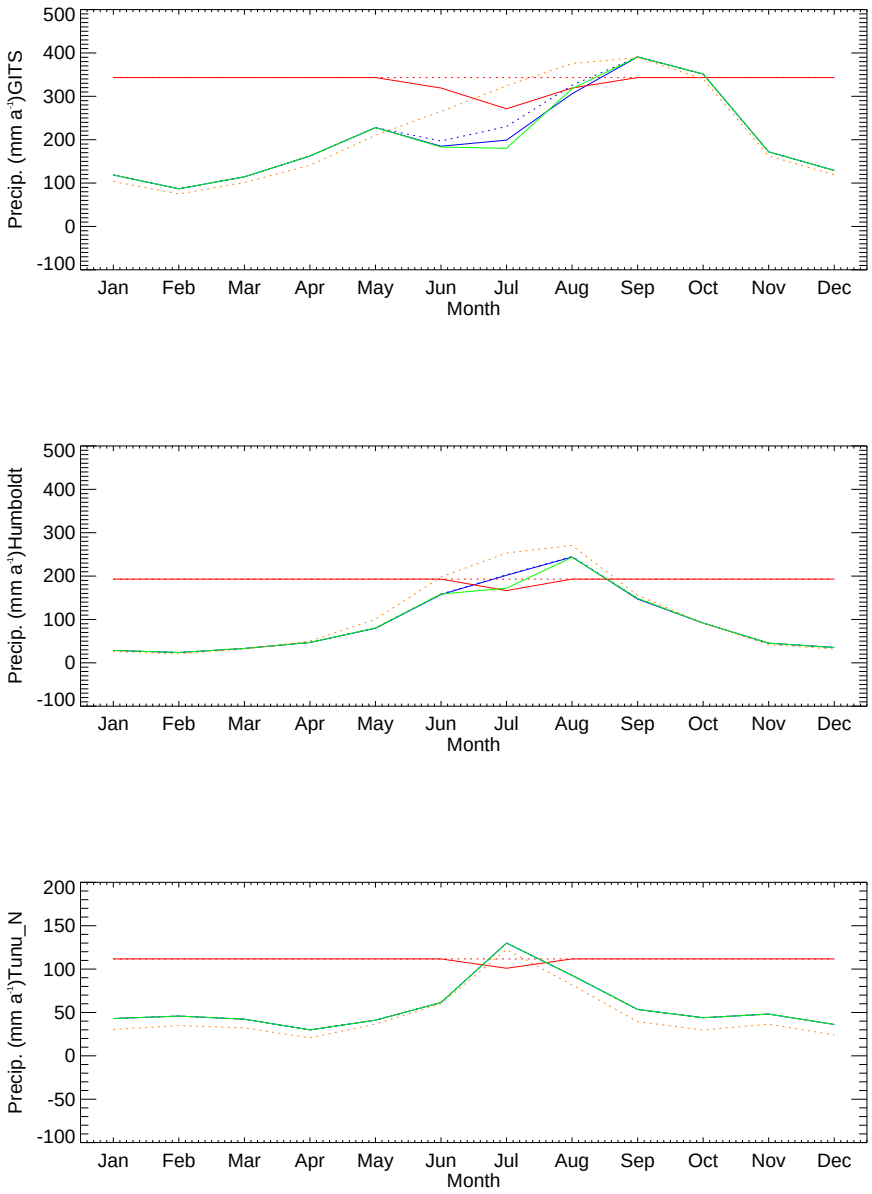

Figure 6.43: Yearly Precipitation, P-E and snow variation for the GC-Net stations GITS, Humboldt, and Tunu-N. The blue lines show P-E and corrected snow from the HIRHAM4 model, orange line the Precipitation, and green line is the amount of snow computed from the P-E output from HIRHAM4 with the same conversion as has been used before. The red lines show the annual precipitation from (*Calanca et al.*, 2000) and the amount of snow computed with the snow conversion from *Marsiat* (1994).

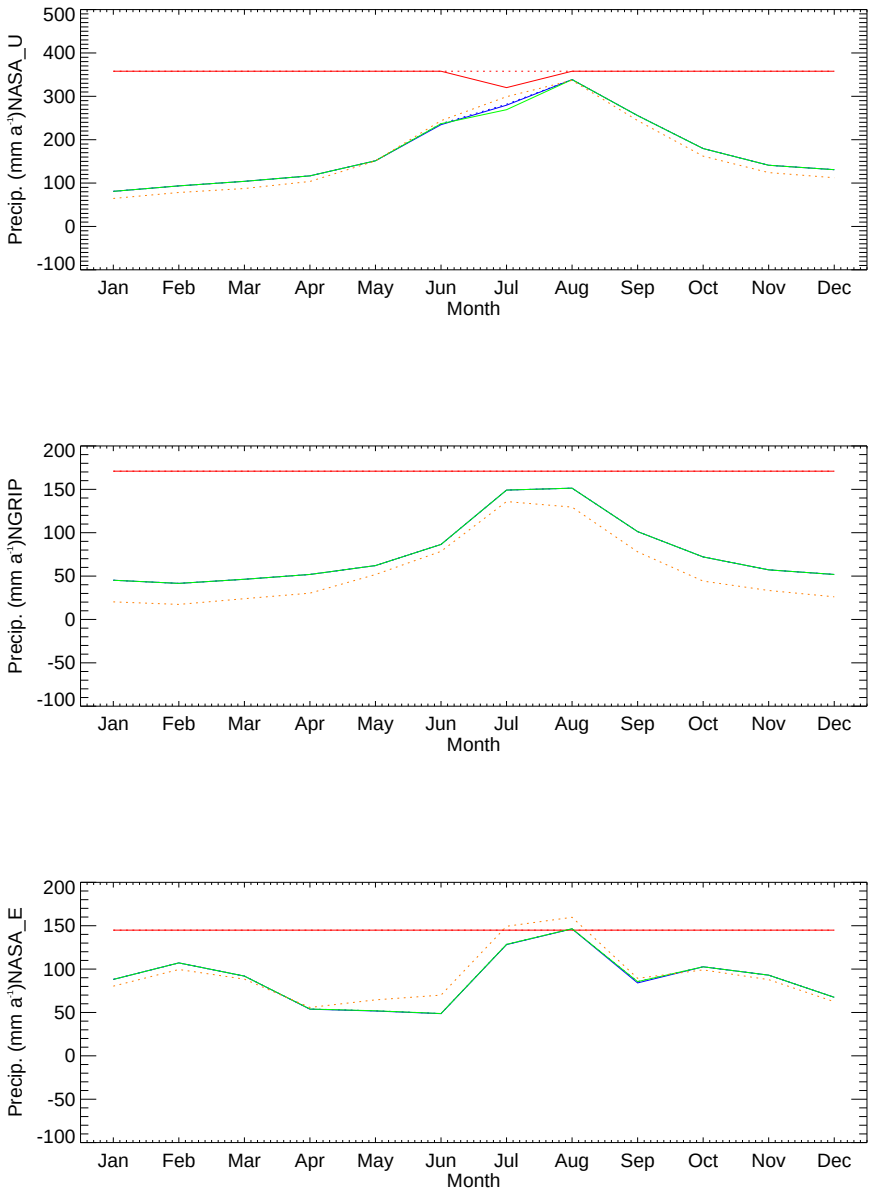

Figure 6.44: Yearly Precipitation, P-E and snow variation for the GC-Net stations NASA-U, North-GRIP, and NASA-E. The blue lines show P-E and corrected snow from the HIRHAM4 model, orange line the Precipitation, and green line is the amount of snow computed from the P-E output from HIRHAM4 with the same conversion as has been used before. The red lines show the annual precipitation from (*Calanca et al.*, 2000) and the amount of snow computed with the snow conversion from *Marsiat* (1994).

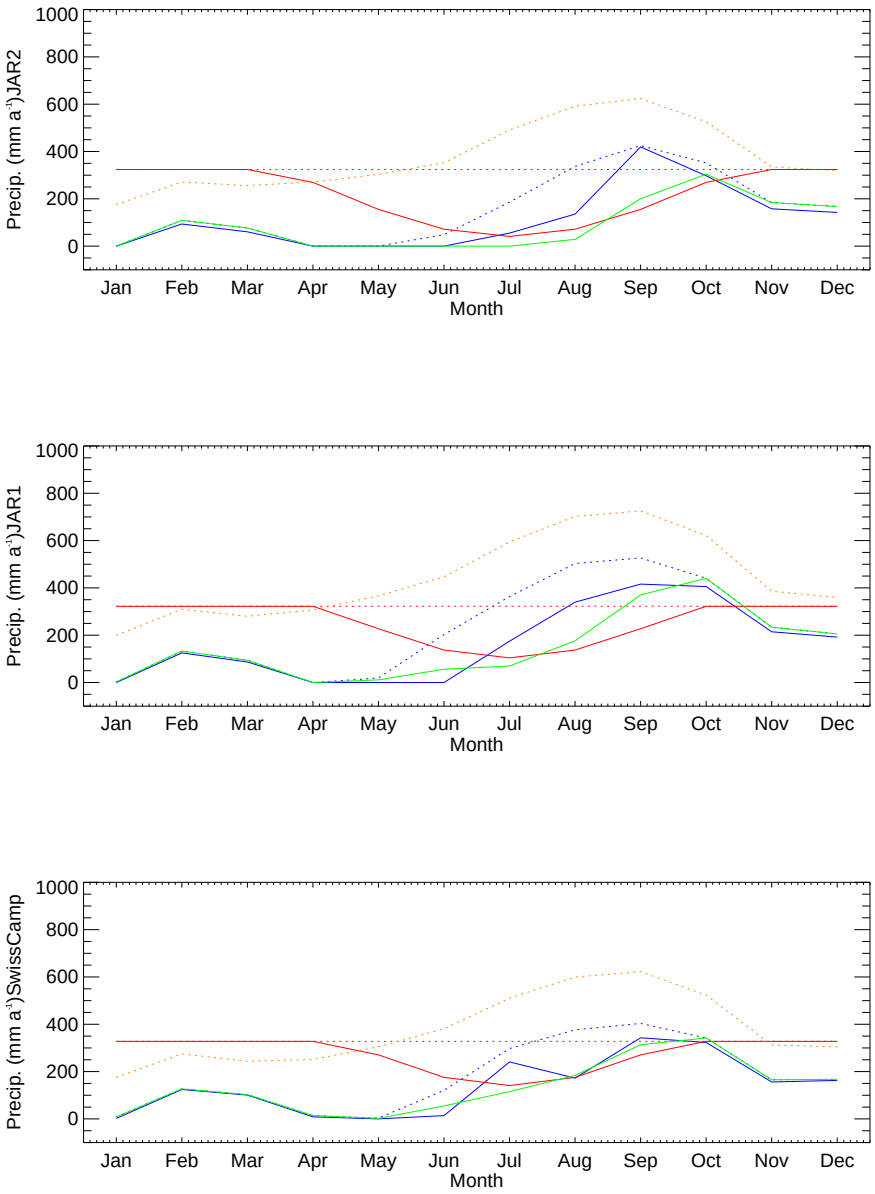

Figure 6.45: Yearly Precipitation, P-E and snow variation for the GC-Net stations JAR2, JAR2, and Swiss Camp. The blue lines show P-E and corrected snow from the HIRHAM4 model, orange line the Precipitation, and green line is the amount of snow computed from the P-E output from HIRHAM4 with the same conversion as has been used before. The red lines show the annual precipitation from (*Calanca et al.*, 2000) and the amount of snow computed with the snow conversion from *Marsiat* (1994).

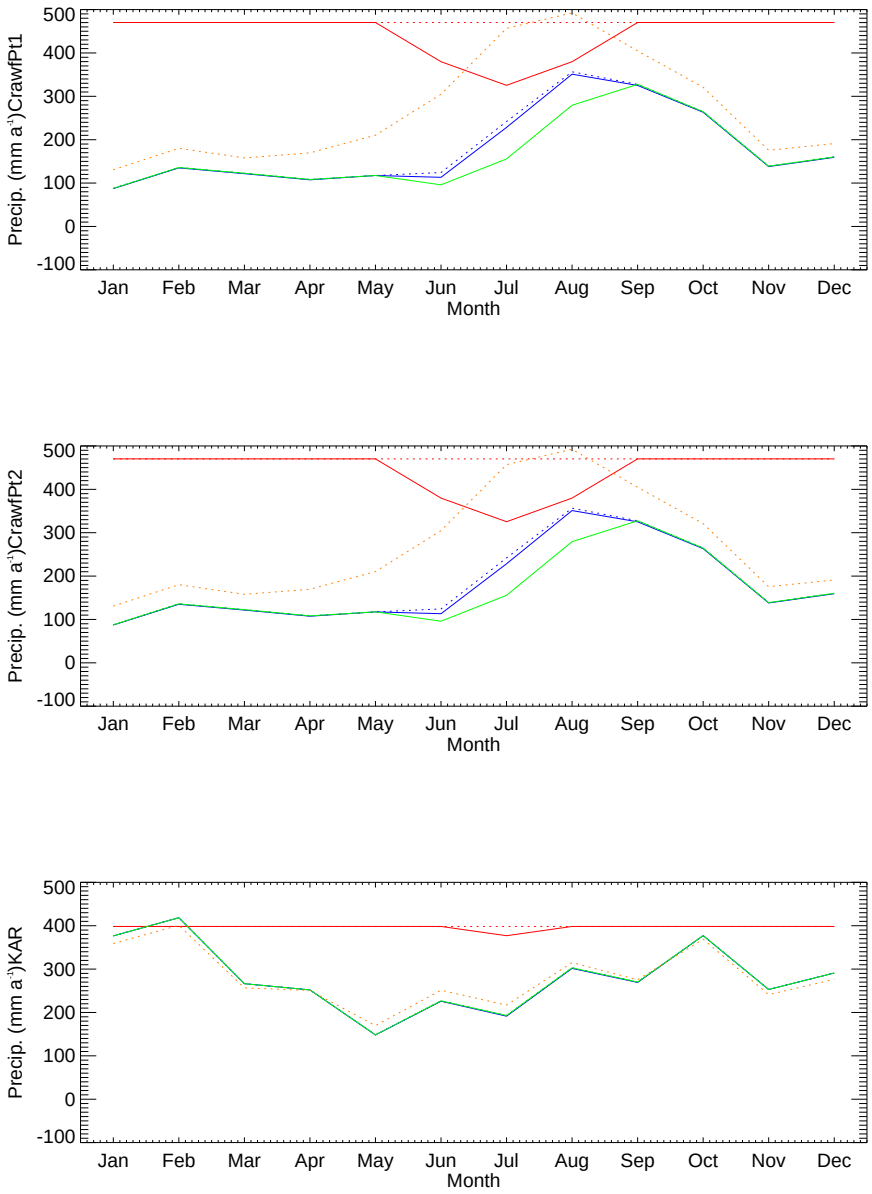

Figure 6.46: Yearly Precipitation, P-E and snow variation for the GC-Net stations Crawford Point 1, Crawford Point 2, and KAR. The blue lines show P-E and corrected snow from the HIRHAM4 model, orange line the Precipitation, and green line is the amount of snow computed from the P-E output from HIRHAM4 with the same conversion as has been used before. The red lines show the annual precipitation from (*Calanca et al.*, 2000) and the amount of snow computed with the snow conversion from *Marsiat* (1994).

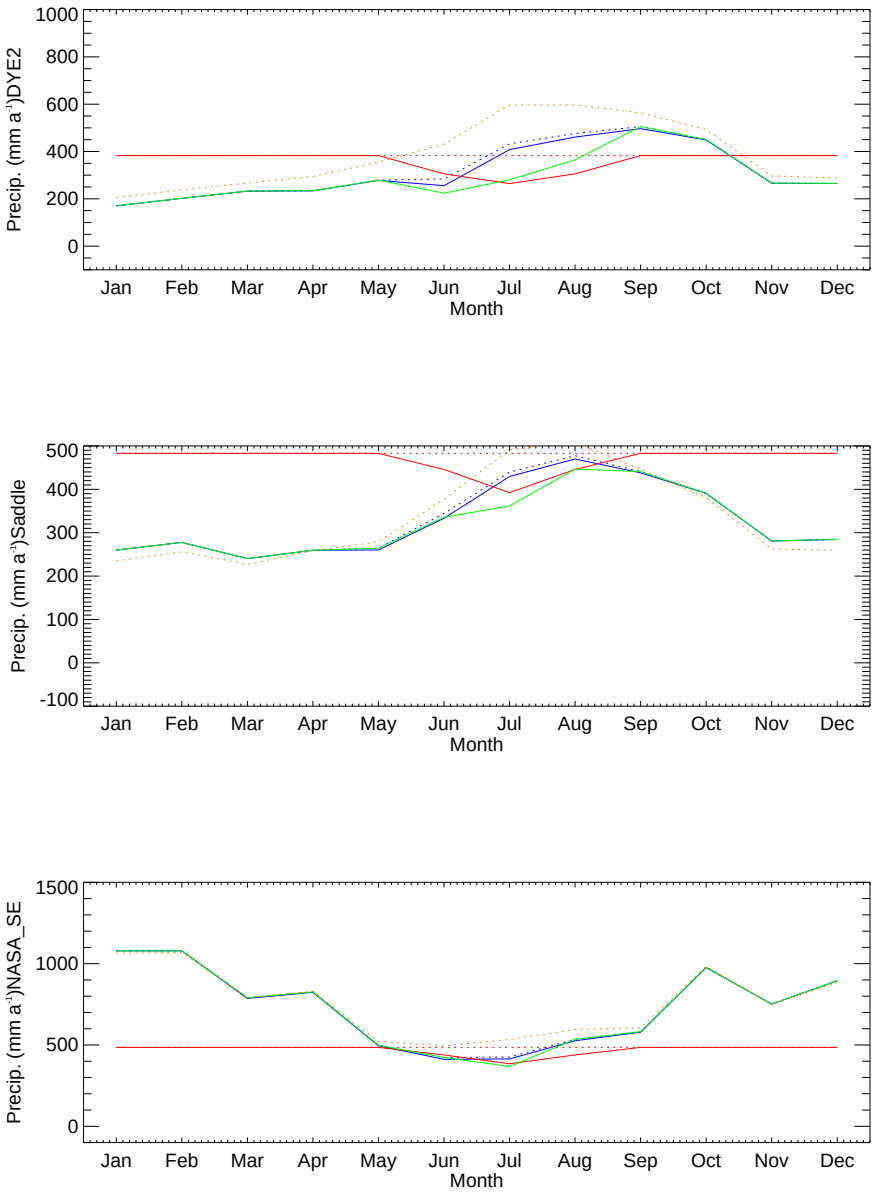

Figure 6.47: Yearly Precipitation, P-E and snow variation for the GC-Net stations Dye2, Saddle and NASA-SE. The blue lines show P-E and corrected snow from the HIRHAM4 model, orange line the Precipitation, and green line is the amount of snow computed from the P-E output from HIRHAM4 with the same conversion as has been used before. The red lines show the annual precipitation from (*Calanca et al.*, 2000) and the amount of snow computed with the snow conversion from *Marsiat* (1994).

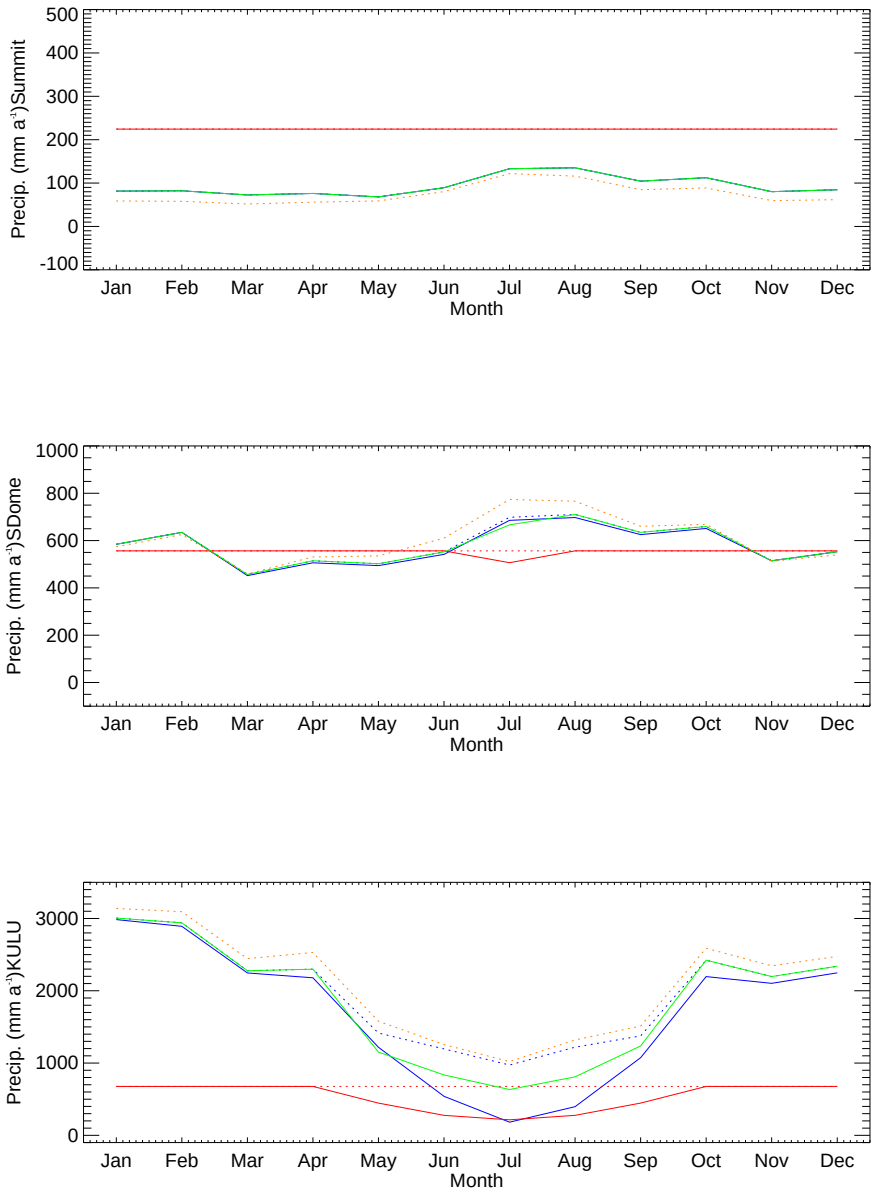

Figure 6.48: Yearly Precipitation, P-E and snow variation for the GC-Net stations Summit, South Dome and KULU. The blue lines show P-E and snow from the HIRHAM4 model, orange line the Precipitation, and green line is the amount of snow computed from the P-E output from HIRHAM4 with the same conversion as has been used before. The red lines show the annual precipitation from (*Calanca et al.*, 2000) and the amount of snow computed with the snow conversion from *Marsiat* (1994).

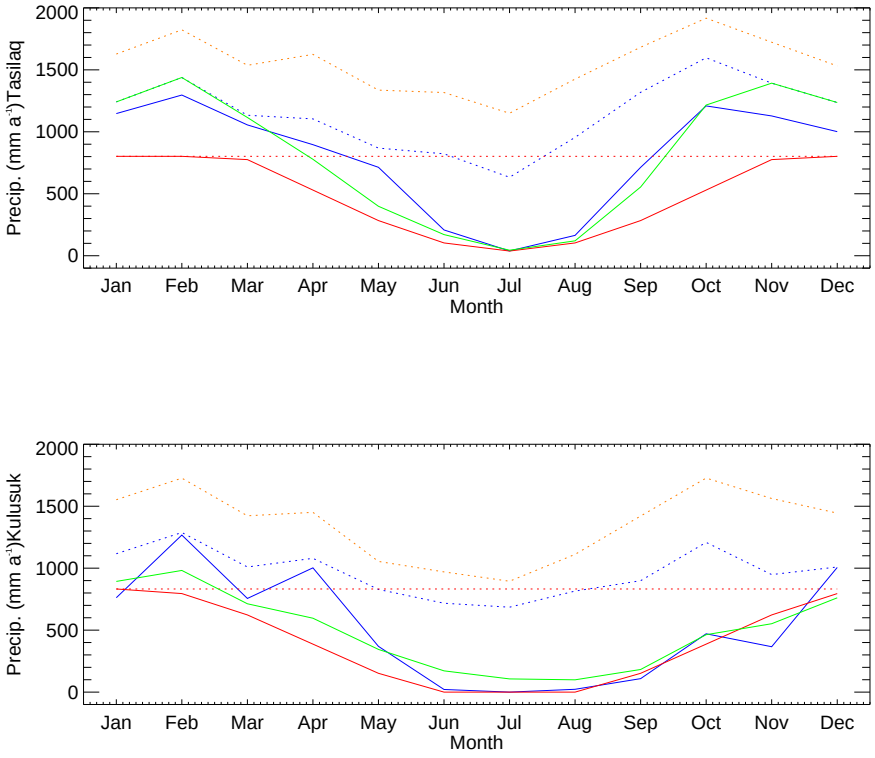

Figure 6.49: Yearly Precipitation, P-E and snow variation for the weather stations Tasiilaq and Kulusuk. The blue lines show P-E and corrected snow from the HIRHAM4 model, orange line the Precipitation, and green line is the amount of snow computed from the P-E output from HIRHAM4 with the same conversion as has been used before. The red lines show the annual precipitation from (*Calanca et al.*, 2000) and the amount of snow computed with the snow conversion from *Marsiat* (1994).

In Figures 6.50 - 6.61 a comparison of the monthly mean precipitation, P-E, corrected snow and the snow amount computed from P-E with the parameterisation along 3 cross sections of the Greenland ice sheet is shown. The mean annual precipitation, from the accumulation map from *Calanca et al.* (2000), and the parameterised snow are shown with red dotted and solid lines respectively. It is clear from these figures that the RCM exaggerates the orographic features of the P-E fields along the coastal areas of Greenland. There is less precipitation over the main ice cap, and in the north compared to the estimate, but it is varying difference over the year. The summer precipitation in HIRHAM4 is similar as the annual mean in the south and the difference is smaller in the cross sections further north. The amount of snow computed with the parameterisation (*Marsiat*, 1994) is generally smaller than the modelled amount.

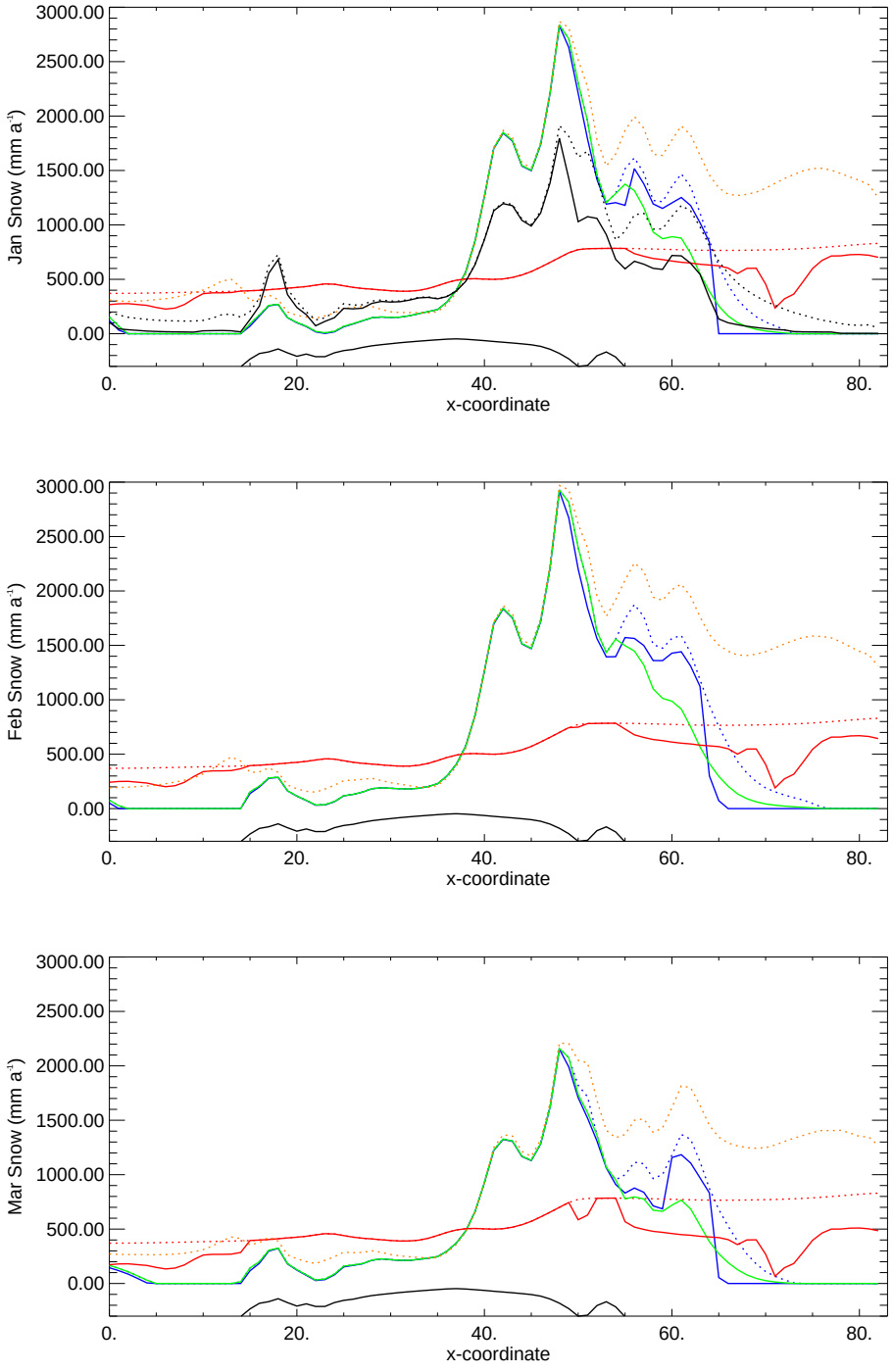

Figure 6.50: Comparison of the monthly mean precipitation and corrected snow over cross section 1 (furthest south). Solid lines show snowfall and dotted line precipitation or P-E. Red lines are the from the mean annual precipitation that has been used until now. Blue lines show the output from HIRHAM4 (P-E and snow), orange line the HIRHAM4 precipitation, and the green line is the amount of snow computed from the P-E output from HIRHAM4 with the same conversion as has been used before. The topography of the cross section is shown at the bottom of the figure. Black lines in the January figure show the mean annual HIRHAM4 P-E and snowfall.

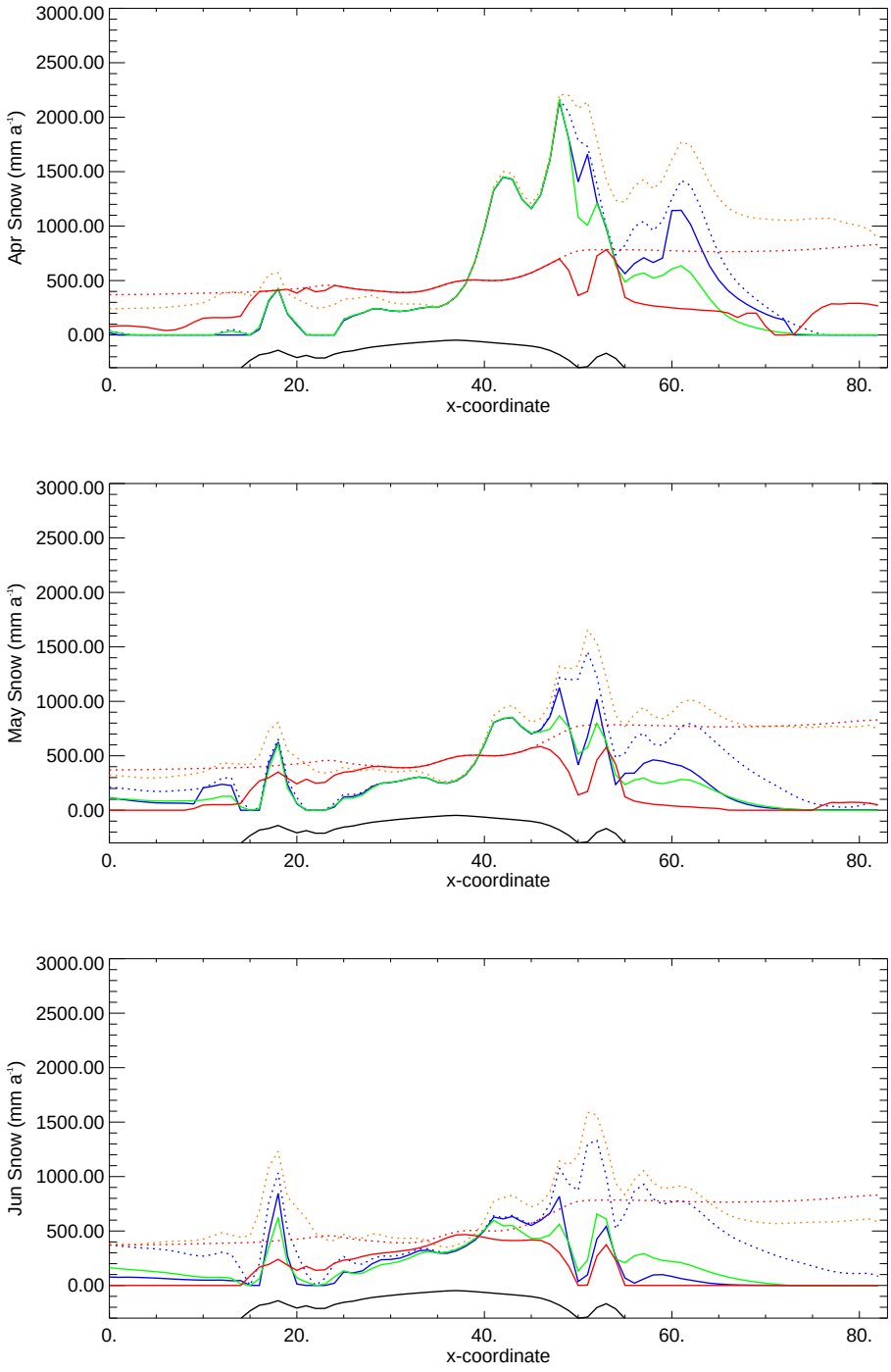

Figure 6.51: Comparison of the monthly mean precipitation and corrected snow over cross section 1 (furthest south). Solid lines show snowfall and dotted line precipitation or P-E. Red lines are the from the mean annual precipitation that has been used until now. Blue lines show the output from HIRHAM4 (P-E and snow), orange line the HIRHAM4 precipitation, and the green line is the amount of snow computed from the P-E output from HIRHAM4 with the same conversion as has been used before. The topography of the cross section is shown at the bottom of the figure.

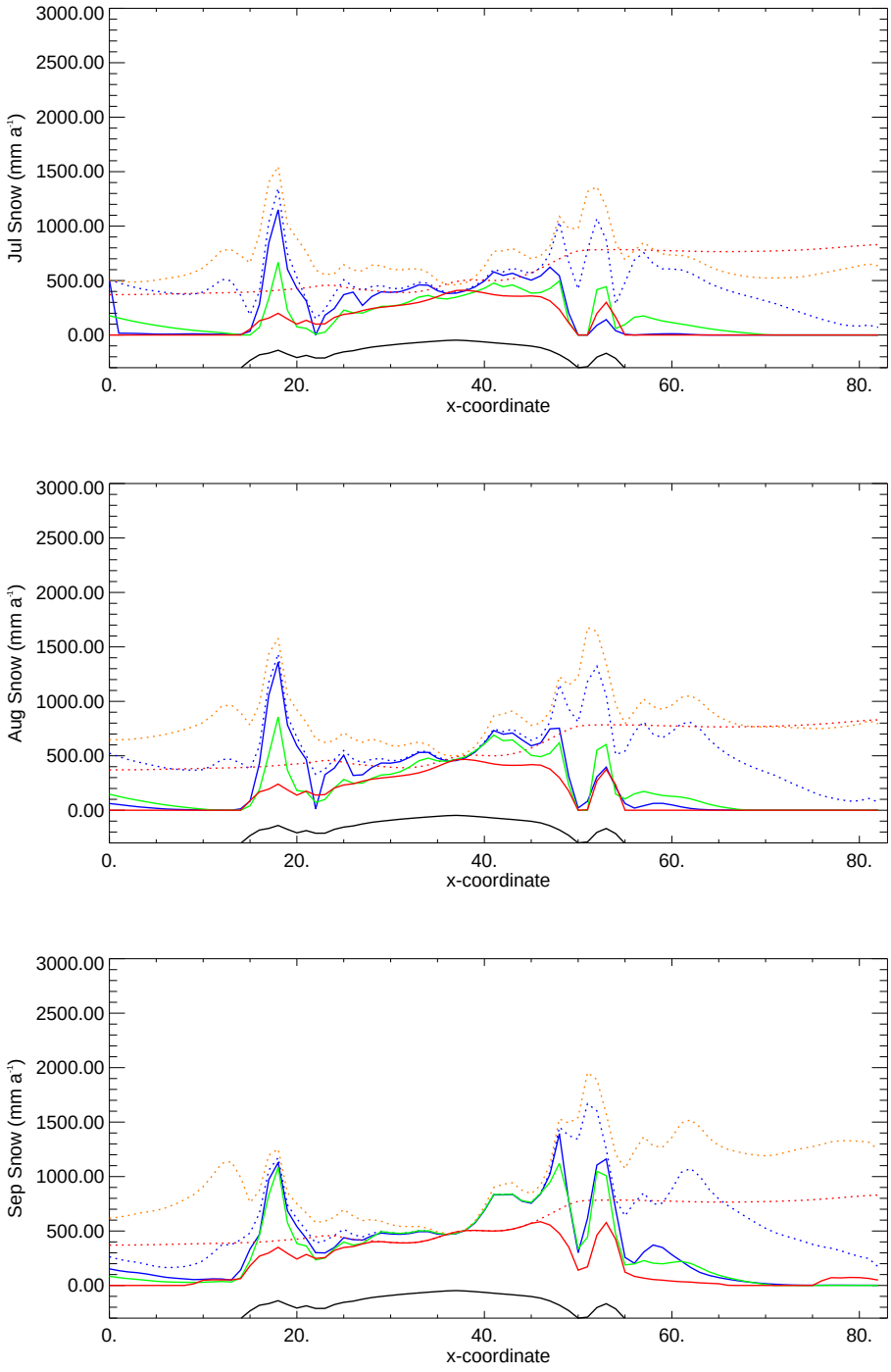

Figure 6.52: Comparison of the monthly mean precipitation and corrected snow over cross section 1 (furthest south). Solid lines show snowfall and dotted line precipitation or P-E. Red lines are the from the mean annual precipitation that has been used until now. Blue lines show the output from HIRHAM4 (P-E and snow), orange line the HIRHAM4 precipitation, and the green line is the amount of snow computed from the P-E output from HIRHAM4 with the same conversion as has been used before. The topography of the cross section is shown at the bottom of the figure.

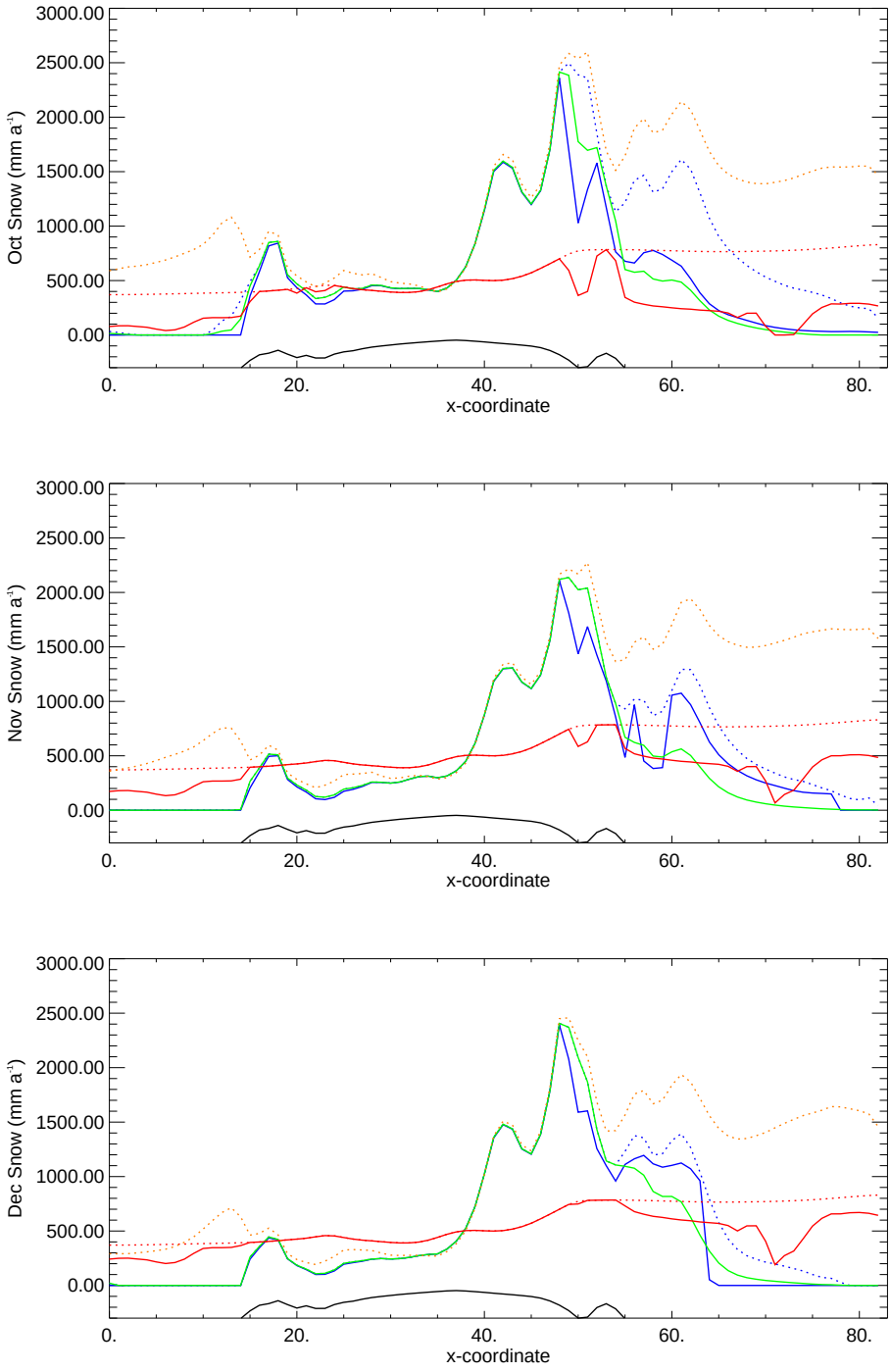

Figure 6.53: Comparison of the monthly mean precipitation and corrected snow over cross section 1 (furthest south). Solid lines show snowfall and dotted line precipitation or P-E. Red lines are the from the mean annual precipitation that has been used until now. Blue lines show the output from HIRHAM4 (P-E and snow), orange line the HIRHAM4 precipitation, and the green line is the amount of snow computed from the P-E output from HIRHAM4 with the same conversion as has been used before. The topography of the cross section is shown at the bottom of the figure.

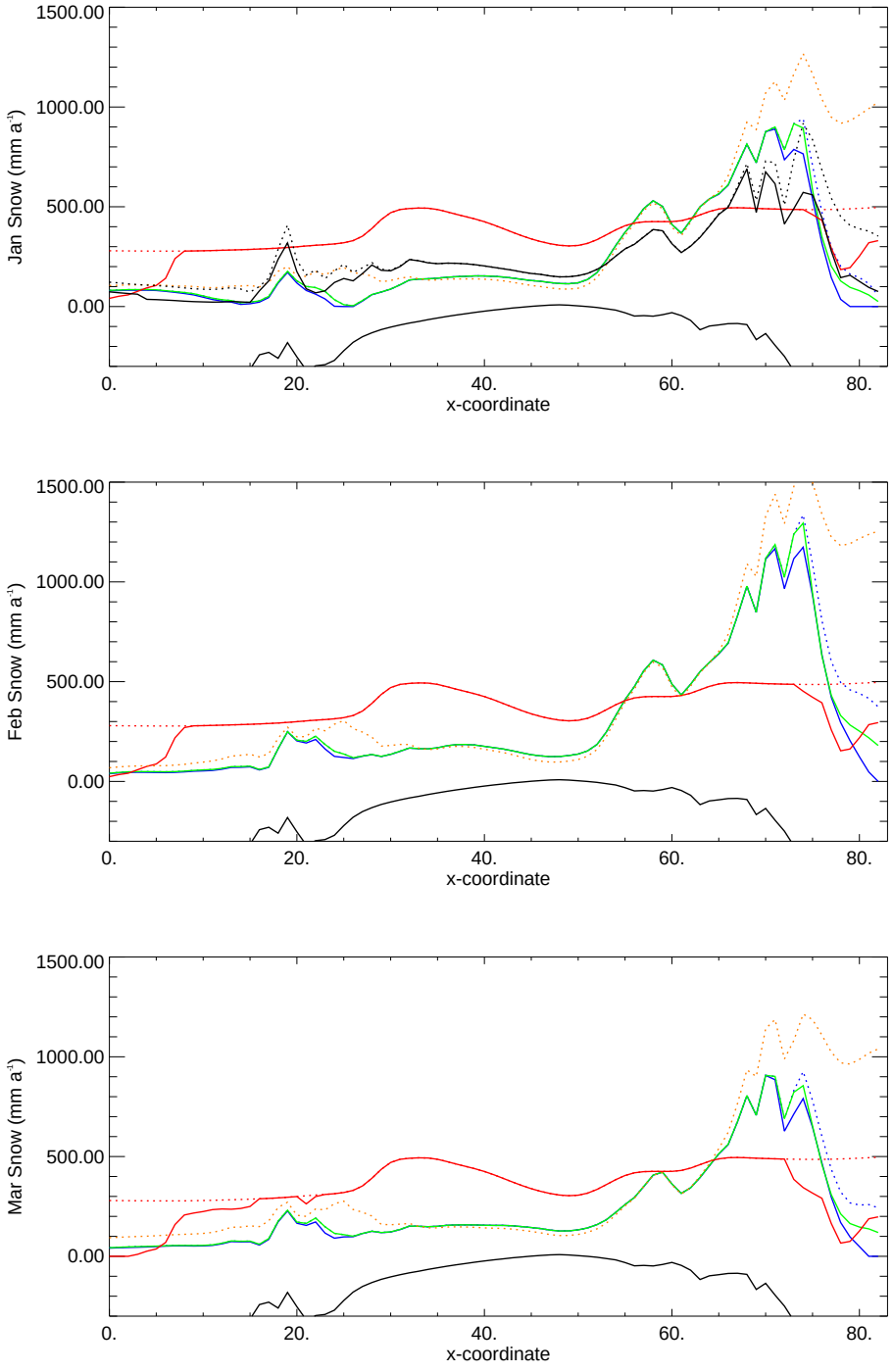

Figure 6.54: Comparison of the monthly mean precipitation and corrected snow over cross section 2 (middle). Solid lines show snowfall and dotted line precipitation or P-E. Red lines are the from the mean annual precipitation that has been used until now. Blue lines show the output from HIRHAM4 (P-E and snow), orange line the HIRHAM4 precipitation, and the green line is the amount of snow computed from the P-E output from HIRHAM4 with the same conversion as has been used before. The topography of the cross section is shown at the bottom of the figure. Black lines in the January figure show the mean annual HIRHAM4 P-E and snowfall.

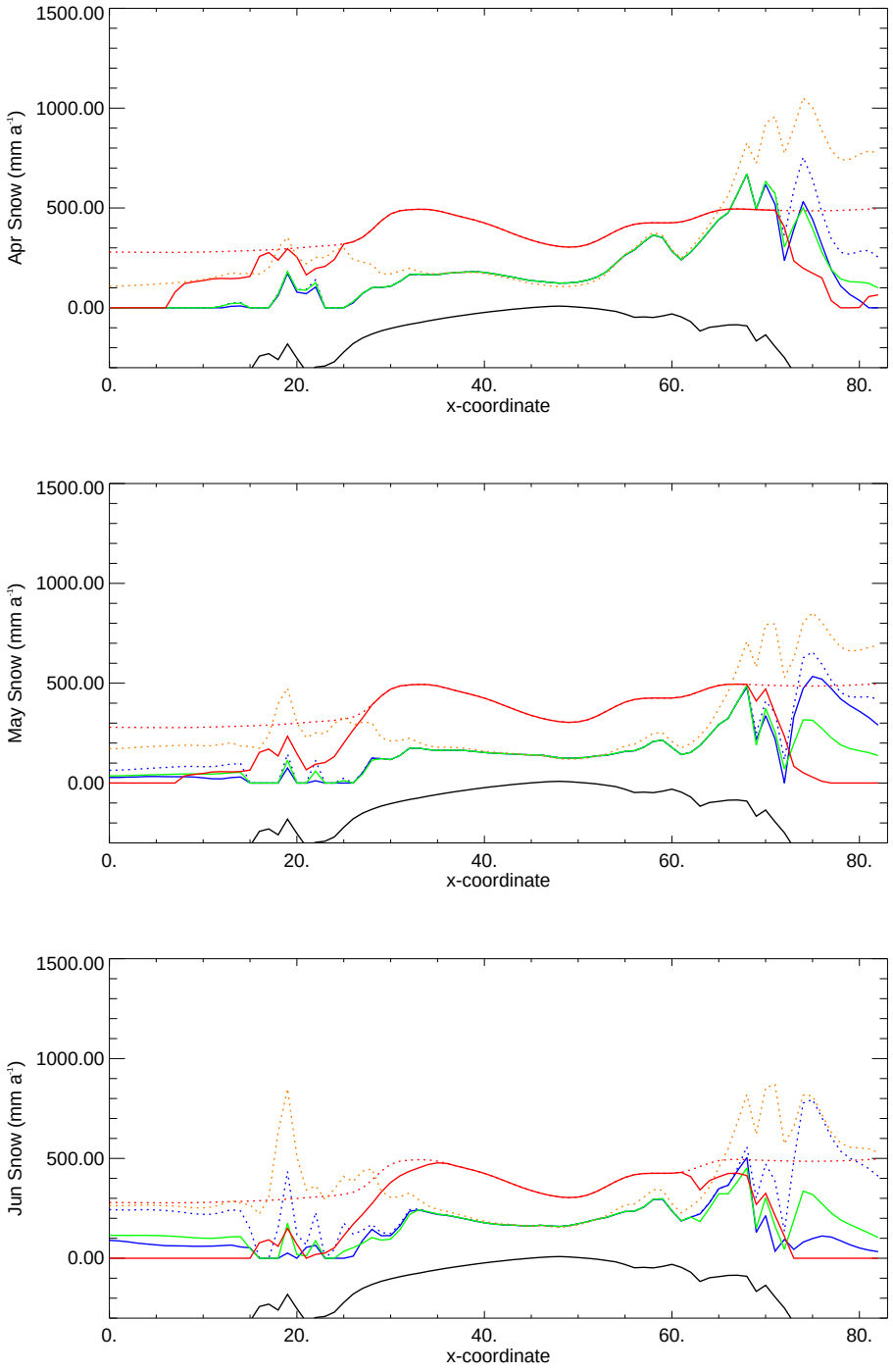

Figure 6.55: Comparison of the monthly mean precipitation and corrected snow over cross section 2 (middle). Solid lines show snowfall and dotted line precipitation or P-E. Red lines are the from the mean annual precipitation that has been used until now. Blue lines show the output from HIRHAM4 (P-E and snow), orange line the HIRHAM4 precipitation, and the green line is the amount of snow computed from the P-E output from HIRHAM4 with the same conversion as has been used before. The topography of the cross section is shown at the bottom of the figure.

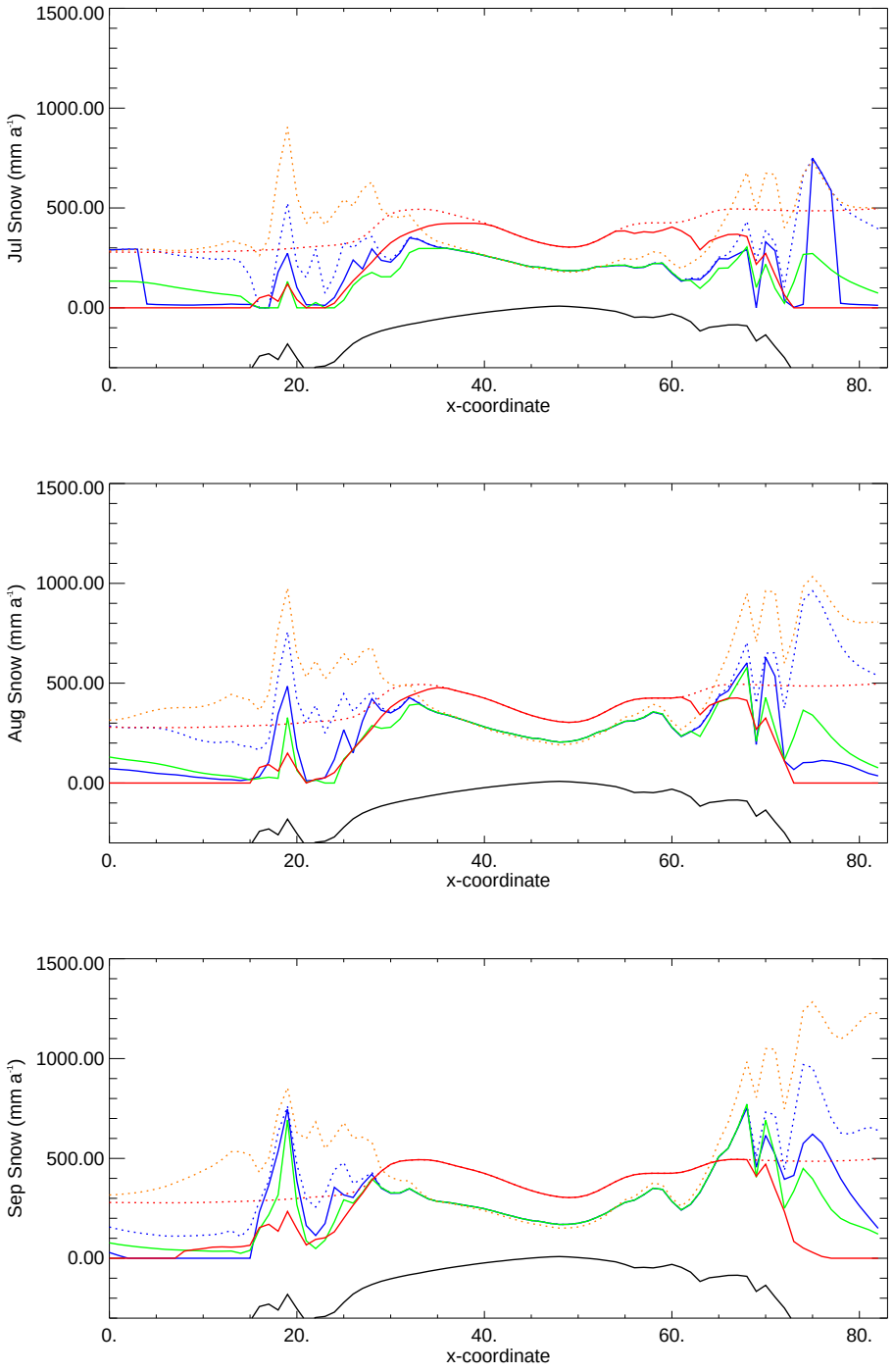

Figure 6.56: Comparison of the monthly mean precipitation and corrected snow over cross section 2 (middle). Solid lines show snowfall and dotted line precipitation or P-E. Red lines are the from the mean annual precipitation that has been used until now. Blue lines show the output from HIRHAM4 (P-E and snow), orange line the HIRHAM4 precipitation, and the green line is the amount of snow computed from the P-E output from HIRHAM4 with the same conversion as has been used before. The topography of the cross section is shown at the bottom of the figure.

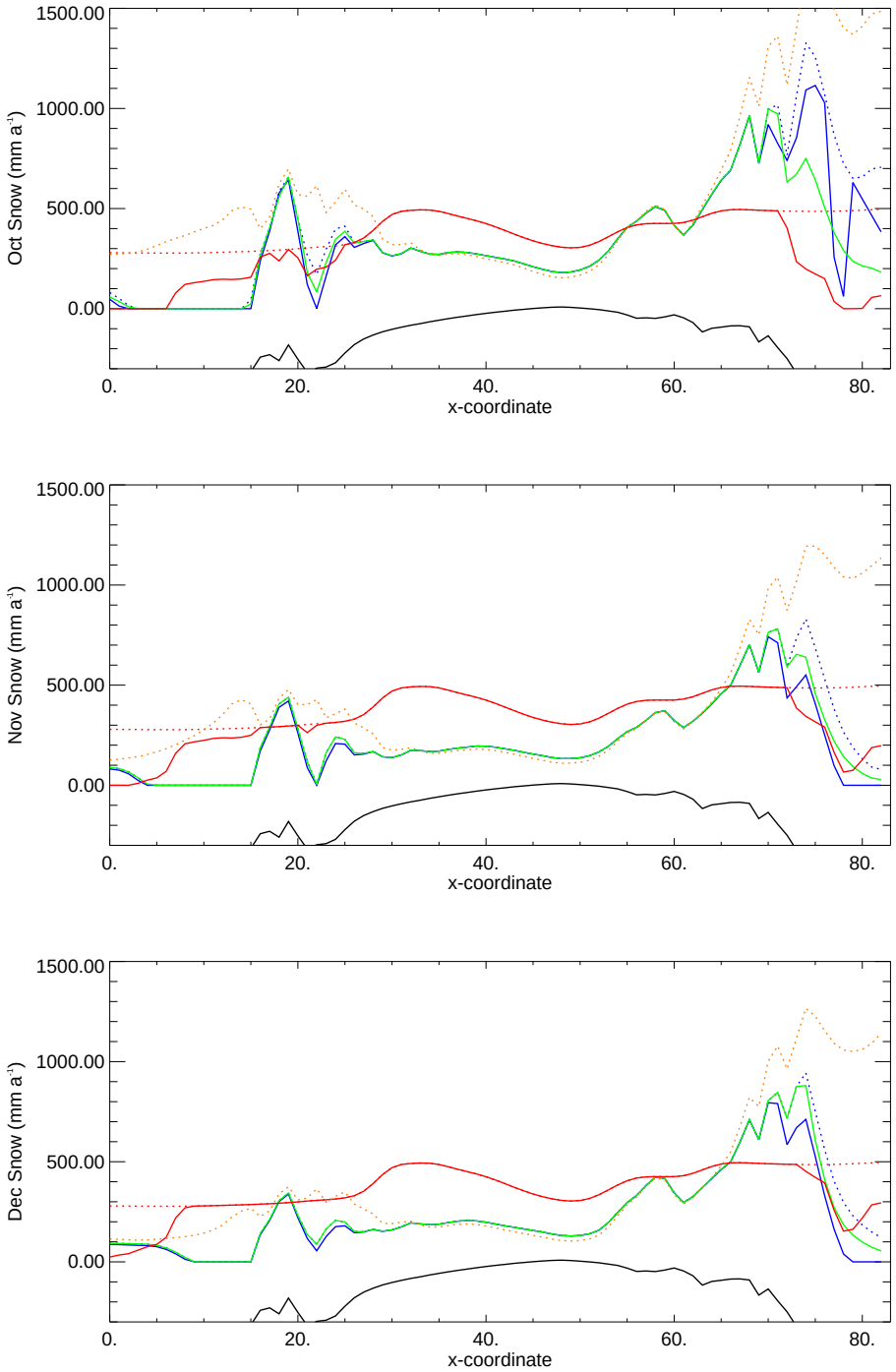

Figure 6.57: Comparison of the monthly mean precipitation and corrected snow over cross section 2 (middle). Solid lines show snowfall and dotted line precipitation or P-E. Red lines are the from the mean annual precipitation that has been used until now. Blue lines show the output from HIRHAM4 (P-E and snow), orange line the HIRHAM4 precipitation, and the green line is the amount of snow computed from the P-E output from HIRHAM4 with the same conversion as has been used before. The topography of the cross section is shown at the bottom of the figure.

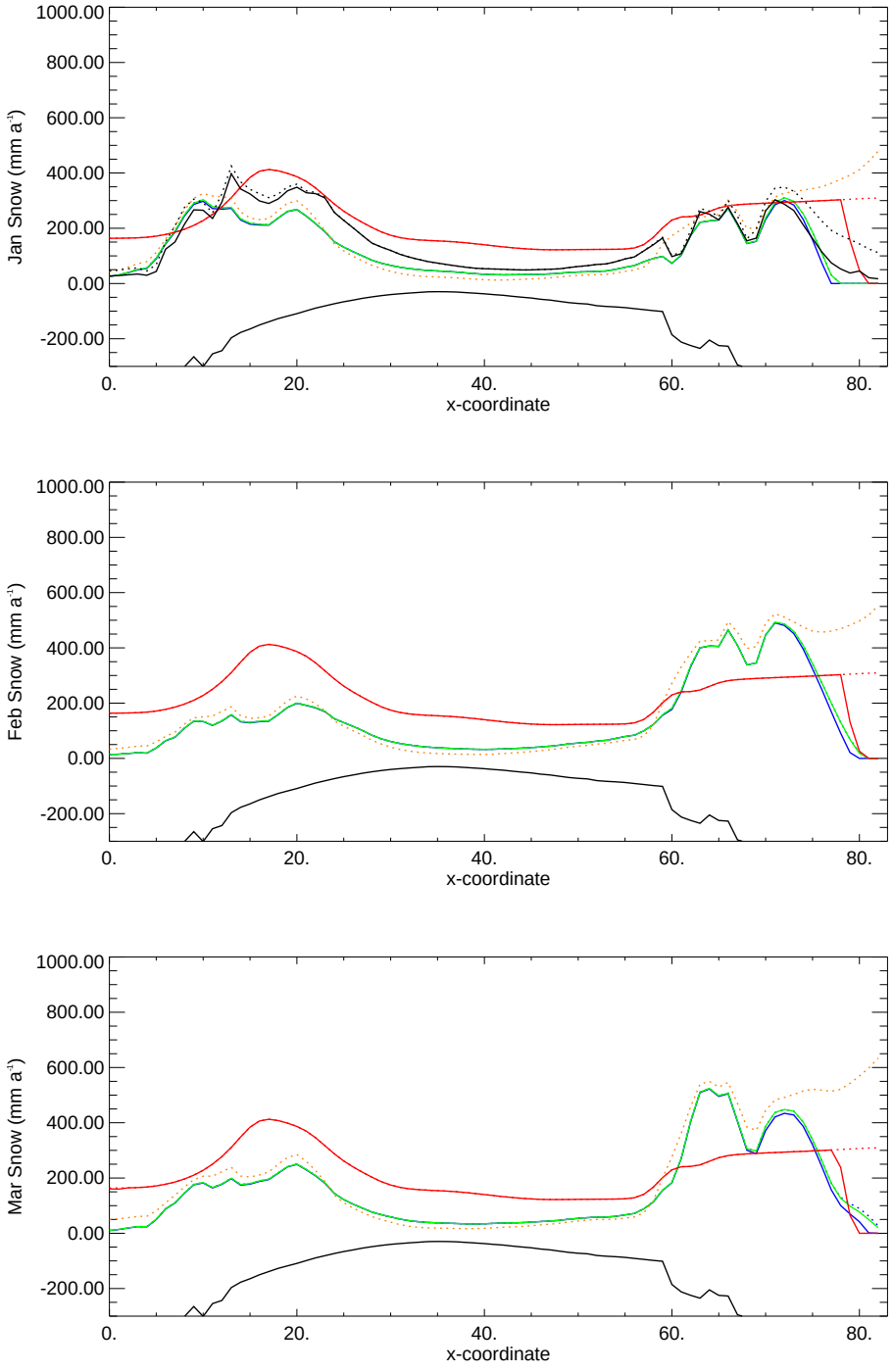

Figure 6.58: Comparison of the monthly mean precipitation and corrected snow over cross section 3 (furthest north). Solid lines show snowfall and dotted line precipitation or P-E. Red lines are the from the mean annual precipitation that has been used until now. Blue lines show the output from HIRHAM4 (P-E and snow), orange line the HIRHAM4 precipitation, and the green line is the amount of snow computed from the P-E output from HIRHAM4 with the same conversion as has been used before. The topography of the cross section is shown at the bottom of the figure. Black lines in the January figure show the mean annual HIRHAM4 P-E and snowfall.

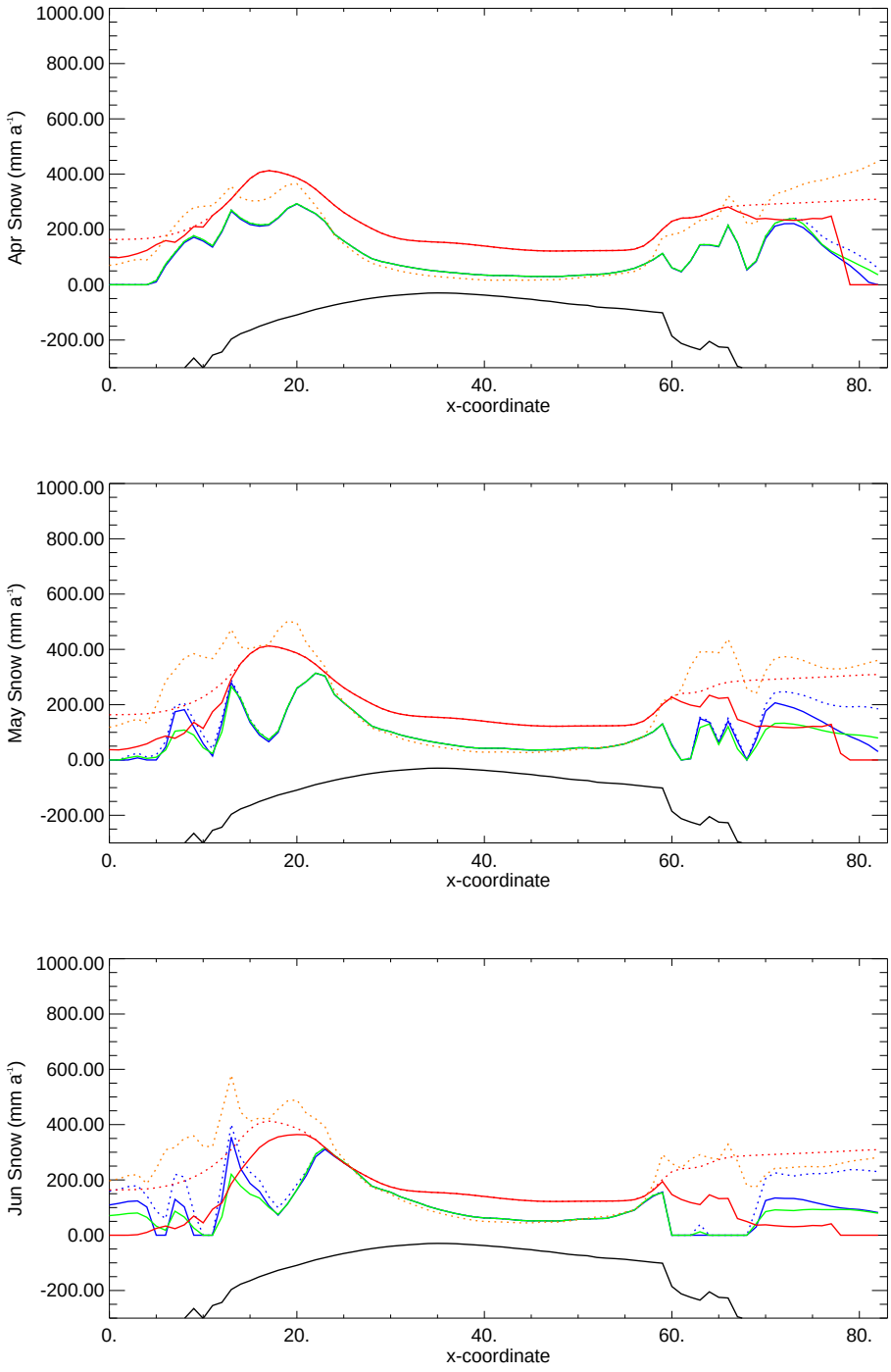

Figure 6.59: Comparison of the monthly mean precipitation and corrected snow over cross section 3 (furthest north). Solid lines show snowfall and dotted line precipitation or P-E. Red lines are the from the mean annual precipitation that has been used until now. Blue lines show the output from HIRHAM4 (P-E and snow), orange line the HIRHAM4 precipitation, and the green line is the amount of snow computed from the P-E output from HIRHAM4 with the same conversion as has been used before. The topography of the cross section is shown at the bottom of the figure.

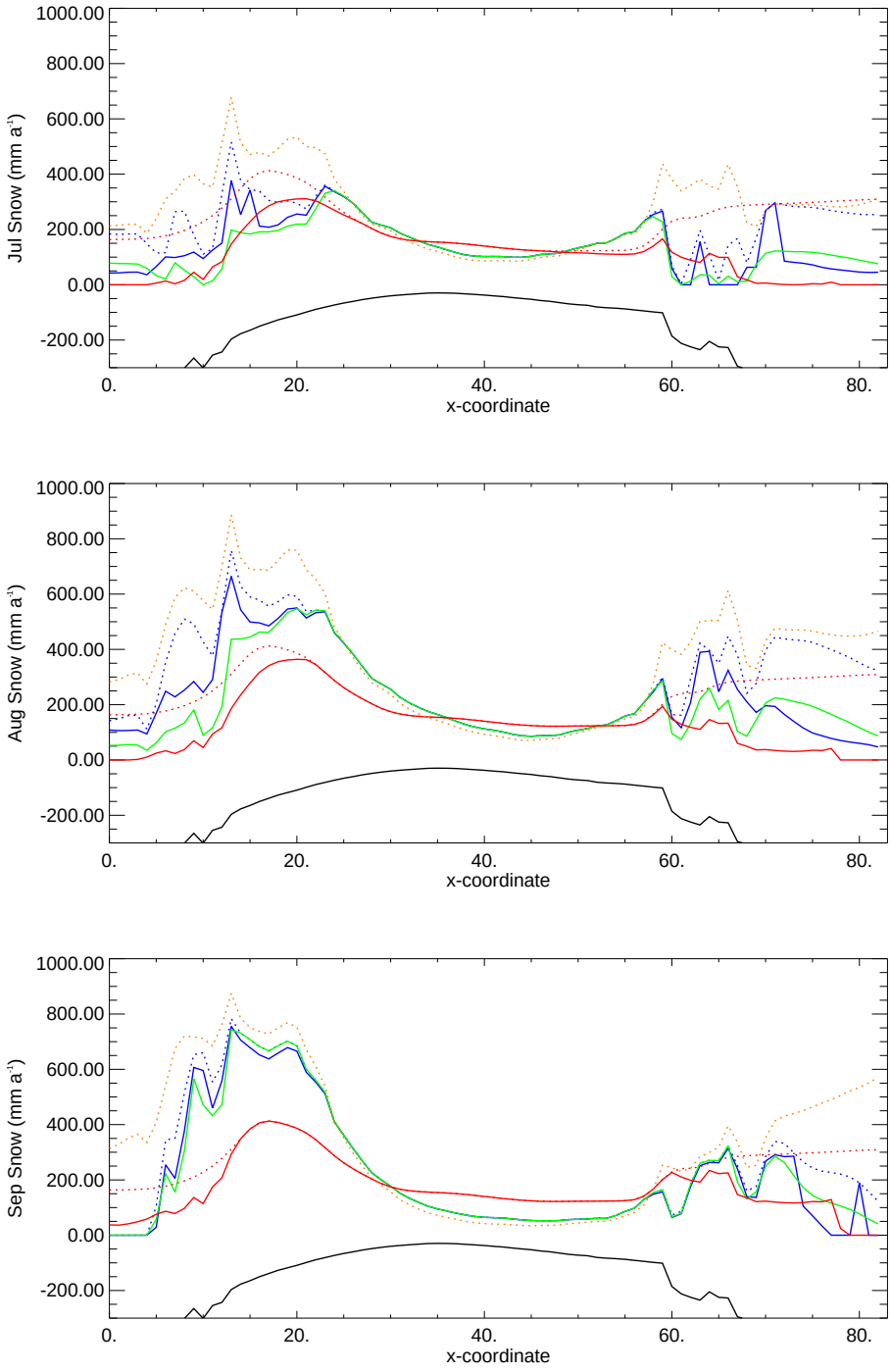

Figure 6.60: Comparison of the monthly mean precipitation and corrected snow over cross section 3 (furthest north). Solid lines show snowfall and dotted line precipitation or P-E. Red lines are the from the mean annual precipitation that has been used until now. Blue lines show the output from HIRHAM4 (P-E and snow), orange line the HIRHAM4 precipitation, and the green line is the amount of snow computed from the P-E output from HIRHAM4 with the same conversion as has been used before. The topography of the cross section is shown at the bottom of the figure.

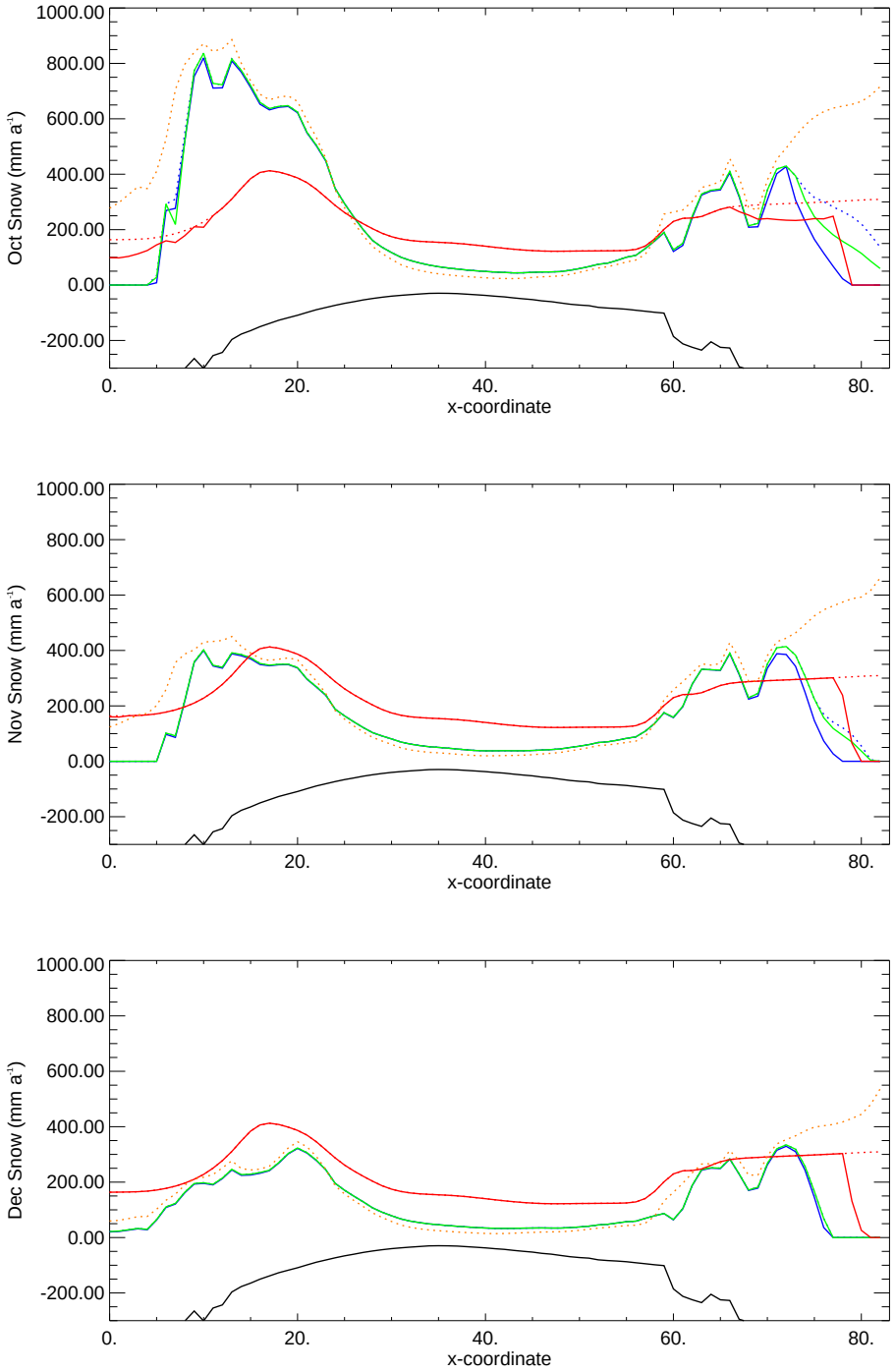

Figure 6.61: Comparison of the monthly mean precipitation and corrected snow over cross section 3 (furthest north). Solid lines show snowfall and dotted line precipitation or P-E. Red lines are the from the mean annual precipitation that has been used until now. Blue lines show the output from HIRHAM4 (P-E and snow), orange line the HIRHAM4 precipitation, and the green line is the amount of snow computed from the P-E output from HIRHAM4 with the same conversion as has been used before. The topography of the cross section is shown at the bottom of the figure.

7. Conclusion

RCM generated temperature, precipitation, evaporation and snow fields have been compared to available data from weather stations (DMI station on the coast and GC-Net AWS on the ice sheet), to a previously used temperature parameterisation (*Ritz et al.*, 1997) and to compilations of temperature and precipitation measurements (*Calanca et al.*, 2000; *Bales et al.*, 2001, 2009). HIRHAM4 simulates the large scale characteristics of the climate over the Greenland Ice Sheet well. The inter annual variability in both temperature and precipitation is very similar in the model and the observations. The seasonal variation in precipitation along the coast is well captured and the seasonal temperature variation is also well simulated with the coldest and warmest months at the right time. However, the temperature range over the ice sheet is smaller in the model compared to observations, the winter temperatures have up to 10°C warm bias, and in some places the summer temperatures is colder than observations. This temperature bias is likely a result of the small number of vertical levels in the boundary layer of the model, which does not properly generate the temperature inversion that is generally observed over the ice sheet, particularly the deep inversions that often form in winter. Increasing vertical layers in the high resolution model is likely to reduce this bias.

A new set of monthly and annual correction factors for precipitation measurements in Greenland are presented and these are used to correct the measurements. The correction of the precipitation increases the gauge-measured precipitation by 23-100% on a yearly basis. The monthly correction values are dependent on temperature and relative amount of snow. At the stations furthest north the magnitude of deficit can amount to more than half of the true precipitation in the winter months.

The RCM simulated snow fields appear not to take into account the amount of Evaporation (evaporation, sublimation and condensation) within the model. This results in unrealistic snow fields that were corrected in order to be able to apply these in ice sheet modelling study. The correction maintains the amount of rain in the simulated RCM climate.

The output fields of the 25 km resolution HIRHAM4 model simulation (*Stendel et al.*, 2008a,b) have been validated and assessed for applicability to use as forcing fields of an ice sheet model. In an ice sheet model study (*Aðalgeirsdóttir et al.*, 2009) these fields are used to force the ice sheet model SICPOLIS as the first steps towards a fully coupled climate-ice sheet model system that will be used to simulate the future evolution of the Greenland Ice Sheet in response to climate change and reduce the uncertainty in predictions of the contribution of the melting ice sheet to sea level rise.

References

Aðalgeirsdóttir, G., M. Stendel, J. H. Christensen, J. Cappelen, F. Vejen, H. A. Kjær, R. Muttrom, P. Lucas-Picher, and M. Drews (2009), Towards modelling the Greenland Ice Sheet with regional climate model generated forcing data, *in preparation*.

Allerup, P., H. Madsen, and F. Vejen (1997), A comprehensive model for correcting point precipitation, *Nordic Hydrology*, *28*, 1–20.

Allerup, P., H. Madsen, and F. Vejen (2000), Correction of observed precipitation in Greenland, in *XXI Nordic Hydrological Conference, Upsala, 26-30 June 2000*.

Bales, R. C., J. R. McConnell, E. Mosley-Thompson, and B. Csatho (2001), Accumulation over the Greenland ice sheet from historical and recent records, *Journal of Geophysical Research*, *106*(D24), 33,813–33,825.

Bales, R. C., Q. Guo, D. Shen, J. R. McConnell, G. Du, J. F. Burkhart, V. B. Spikes, E. Hanna, and J. Cappelen (2009), Annual accumulation for Greenland updated using ice core data developed during 2000-2006 and analysis of daily coastal meteorological data, *JGR*, *114*, doi:10.1029/2008JD011208.

Bromwich, D. H., F. M. Robasky, R. A. Keen, and J. F. Bolzan (1993), Modeled variation of precipitation over the Greenland Ice Sheet, *J. Climate*, *6*, 1253–1268.

Calanca, P., H. Gilgen, S. Ekholm, and A. Ohmura (2000), Gridded temperature and accumulation distributions for Greenland for use in cryospheric models, *Annals of Glaciology*, *31*, 118–120.

Cappelen, J., B. V. Jørgensen, E. V. Laursen, L. S. Stannius, and R. S. Thomsen (2001), The observed climate of Greenland, 1958–99 - with climatological standard normals, 1961–90, *Tech. Rep. 00–18*, Danish Meteorological Institute.

Cappelen, J., E. V. Laursen, P. V. Jørgensen, and C. Kern-Hansen (2008), DMI monthly climate data collection 1768-2007, Denmark, the Faroe Islands and Greenland, *Tech. Rep. 08–04*, Danish Meteorological Institute.

Christensen, J. H., O. B. Christensen, P. Lopez, E. van Meijgaard, and M. Botzet (1996), The HIRHAM4 Regional Atmospheric Climate Model, *Tech. Rep. 96–4*, Danish Meteorological Institute.

Dethloff, K., M. Schwager, J. H. Christensen, S. Kiilsholm, A. Rinke, W. Dorn, F. Jung-Rothenhäusler, H. Fischer, S. Kipfstuhl, and H. Miller (2002), Recent Greenland accumulation estimated from regional climate model simulations and ice core analysis, *J. Climate*, *15*, 2821–2832.

Fausto, R. S., A. P. Ahlstrøm, D. van As, C. E. Bøggild, and S. J. Johnsen (2009), A new present-day temperature parameterization for Greenland, *Journal of Glaciology*, *55*(189), 95–105.

Genthon, C., and A. Braun (1995), ECMWF analysis and predictions of the surface climate of Greenland and Antarctica, *J. Climate*, *8*, 2324–2332.

Greve, R. (2005), Relation of measured basal temperatures and the spatial distribution of the geothermal flux for the Greenland ice sheet, *Annals of Glaciology*, *42*, 424–342.

Hanna, E., P. Valdes, and J. McConnell (2001), Pattern and variations of snow accumulation over Greenland, 1979-98, from ECMWF analysis, and their verification, *J. Climate*, *14*, 3521–3535.

Hanna, E., J. McConnell, S. Das, J. Cappelen, and A. Stephens (2006), Observed and modeled Greenland ice sheet accumulation, 1958–2003, *J. Climate*, *19*, 344–358.

Huybrechts, P., and J. de Wolde (1999), The dynamic response of the Greenland and Antarctic ice sheets to multiple-century climatic warming, *J. Climate*, *12*(8), 2169–2188.

Källén, E. (1996), HIRLAM Documentation Manual, System 2.5., Swed. Meteorol. and Hydrol. Inst., Norrköping, 126 pp.

Kiilsholm, S., J. H. Christensen, K. Dethloff, and A. Rinke (2004), Net accumulation of the Greenland ice sheet: High resolution modeling of climate changes, *Geophysical Research Letters*, *30*(9, 1485), doi:10.1029/2002GL015742.

Marsiat, I. (1994), Simulation of the Northern hemisphere continental ice sheets over the last glacial-interglacial cycle: experiments with a latitude-longitude vertically integrated ice sheet model coupled to a zonally averaged climate model, *Palaeoclimates*, *1*, 59–98.

May, W. (2008), Climatic changes associated with a global "2^{o}C-stabilization" scenario simulated by the ECHAM5/MPI-OM coupled climate model, *Clim. Dyn.*, *31*, 283–313, doi:10.1007/s00382-007-0352-8.

Ohmura, A. (1987), New temperature distribution maps for Greenland, *Zeitschrift für Gletscherkunde und Glazialgeologie*, *23*(1), 1–45.

Ohmura, A., and N. Reeh (1991), New precipitation and accumulation maps for Greenland, *Journal of Glaciology*, *37*(125), 140–148.

Ohmura, A., M. Wild, and L. Bengtsson (1996), A possible change in mass balance of Greenland and Antarctic ice sheets in the coming century, *Journal of Climate*, *9*, 2124–2135.

Ritz, C., A. Fabre, and A. Letréguilly (1997), Sensitivity of a Greenland ice sheet model to ice flow and ablation parameters: Consequences for the evolution through the last climatic cycle, *Clim. Dyn.*, *13*, 11–24.

Roeckner, E., G. Bäuml, L. Bonaventura, R. Brokopf, M. Esch, M. Giorgetta, S. Hagemann, I. Kirchner, L. Kornblueh, E. Manzini, A. Rhodin, U. Schlese, U. Schulzweida, and A. Tompkins (2003), The atmospheric general circulation model ECHAM5. Part I: Model description, *Tech. Rep. 349*, Max Planck Institute for Meteorology, 127 pp.

Steffen, K., and J. Box (2001), Surface climatology of the Greenland ice sheet: Greenland climate network 1995-1999, *Journal of Geophysical Research*, *106*, 33,951–33,964.

Steffen, K., J. E. Box, and W. Abdalati (1996), Greenland climate network: GC-Net, US Army Cold Regions Research and Engineering (CRREL), CRREL monograph, trib. to M. Meier.

Stendel, M., J. Christensen, G. Aðalgeirsdóttir, N. Kliem, and M. Drews (2008a), Regional climate change for Greenland and surrounding seas, *Tech. Rep. 07–02*, Danish Meteorological Institute.

Stendel, M., J. Christensen, and D. Petersen (2008b), Arctic climate and climate change with a focus on Greenland, *In: H. Meltofte, T.R. Christensen, B. Elberling, M.C. Forchhammer and M. Rasch (eds.): High Arctic Ecosystem Dynamics in a Changing Climate. Ten years of monitoring and research at Zackenberg Research station, Norheast Greenland. Advances in Ecological Research. Advances in Ecological Research. Academic Press*, *40*, 13–43.

Uppala, S. M., et al. (2005), The ERA-40 re-analysis, *Quart. J. Roy. Met. Soc.*, *131*, 2961–3012.

Walsh, J. E., W. L. Chapman, V. Romanovsky, J. H. Christensen, and M. Stendel (2008), Global climate model performance over Alaska and Greenland, *J. Climate*, *21*, 6156–6174, doi:10.1175/2008JCLI2163.1.

Previous reports

Previous reports from the Danish Meteorological Institute can be found on:
http://www.dmi.dk/dmi/dmi-publikationer.htm